Hybrid Hydrogels based on RAFT mediated Poly(*N*-vinyl pyrrolidone)

by

Zaskia-Hillét Eksteen

Thesis submitted in partial fulfilment for the degree of

Master of Science (Polymer Science)

at

Stellenbosch University

Department of Chemistry and Polymer Science

Faculty of Science

Promoter: Prof. Bert Klumperman
Co-Promoter: Dr Deon Bezuidenhout

Date: December 2009

Declaration

I, the undersigned, hereby declare that the work contained in this thesis is my own original work and that I have not previously in its entirety or in part, submitted it at any university for a degree.

_____
Signature

_____
Name in full

_____/_____/_____
Date

Abstract

The goal of this study was to synthesize hybrid hydrogels via a chemical crosslinking mechanism through use of chain end functional poly(*N*-vinyl pyrrolidone) (PVP) with various topologies. The crosslinking chemistries should be benign in nature *i.e.* at physiological pH ranges and at 37 °C. The degradation products should be biologically tolerable and renal clearance should be possible (< 30 000 g/mol PVP).

PVP of various topologies, controlled molar mass and quantitative chain end functionality was obtained *via* Reversible Addition Fragmentation chain Transfer (RAFT) mediated polymerization (PDI = 1.1- 1.4).

The synthesized polymers were chain end functionalized to introduce thiol or aldehyde moieties. Thiol chain ends were obtained through post polymerization modification of xanthate functional PVP with either aminolysis or reduction. The aldehyde moiety was obtained by post polymerization modification of xanthate end functional PVP with sequential hydrolysis and thermolysis.

Thiol functional four arm star PVP was reacted with acrylate difunctional poly(ethylene glycol) (DIAC PEG) crosslinker under standard Michael addition conditions. In order to obtain thioether crosslinked hydrogels from tetra functional star PVP molecules it was found that a minimum thiol functionalization of 30% and a molar ratio of acrylate:thiol of 1:1.1 is required.

The Schiff base reaction was used to synthesize imine or secondary amine (after reduction) crosslinks with the lysine residues on either lysozyme or bovine serum albumin (BSA) or the primary amines of *bis*-(2-amino ethyl)amine). Hydrogels were obtained from aldehyde functionalized PVP molecules with a fraction of functional aldehyde chain ends of 0.88 for difunctional molecules and 0.50 for tetra functional star PVP molecules with lysozyme or BSA crosslinkers. The reaction rate was favoured by lowered pH (<6.0) and an optimum molar ratio of amine : aldehyde of 1:0.8.

Hydrogels were analyzed by equilibrium swelling calculations to determine the molar mass between crosslinks and the estimated pore size. In both crosslinking systems the properties of the formed hydrogels were seen to be affected by molar ratio used and by the topology of the crosslinking agent.

PVP BSA and PVP PEG hydrogels were tested for 24 h and 48 h cell viability by using H9C2 myoblast cells. A concentration range of 0.25×10^{-2} to 0.01 g/mL was studied. Cell mortality was tested by Trypan blue staining and results were verified with MTT assay. A very low cell death precentage (<37 %) was observed. Cells even appeared to experience a stimulatory effect after 48 h of exposure at low concentrations of PVP PEG hydrogel treatments.

The properties of the formed hydrogel could be tuned by the molar mass ratios of PVP and crosslinker. The functionality of the crosslinker directly affects the molar mass between crosslinks and thus indirectly the degradation profile.

It was concluded that PVP molecules with various topologies, well-defined molar masses and chain end functionality could be obtained via RAFT mediated polymerization. Obtained polymers were successfully modified and crosslinked to obtain hydrogels with stoichiometrically tuneable properties i.e. initial swelling ratio, degradation time, molar mass between crosslinks. The hydrogels had very positive cell viability results that would definitely justify further research into these materials as "tissue-mimetic" materials.

Opsomming

Die doel van die studie is om poli(*N*-viniel pirollidoon) (PVP) gebaseerde hibried hidrogelle te sintetiseer deur middel van kovalente kruisbindings met toepaslike kruisverbinder molekules. Die chemiese reaksies betrokke in die vorming van hierdie kovalente kruisbindings moet gematig van aard wees, by fisiologiese pH en by 37 °C plaasvind. Die degradasieprodukte van die hibried-hidrogel moet biologies verdraagsaam en ook uitskeibaar deur die endokrinologiese sisteem wees.

PVP van verskillende topologieë, beheerde molêre massa en kwantitatiewe kettingendfunksionaliteit is berei deur 'n omkeerbare addisie-fragmentasie-kettingoordrag (OAFO)-beheerde polimerisasieproses (PDI = 1.1-1.4).

Xantaat-kettingend-PVP is aangepas na thiol of aldehied kettingendfunksies. Thiol-endfunksies is verkry deur middel van 'n aminolisasie-reaksie. Xantaat kettingend-PVP is stapsgewys gemodifiseer deur hidroliese en verhittingstappe om die aldehied ketting-endfunksionaliteit te bekom.

Thiol ketting-endfunksionele vier-armige ster-PVP is kovalent gebind aan difunksionele poly(etileen glikol) deur middel van die Michael-addisiereaksie. PVP PEG hidrogelle het slegs gevorm met vier-armige ster-PVP molekules wat oor 'n minimum van 30 % thiol-funksionaliteit beskik het en 'n optimale molêre massa verhouding van 1:1.1 vir ankrilaat to thiol.

Die Schiff-basisreaksie is gebruik om hidrogel te sintetiseer wat met imiene of amiene (na redusering) kovalente bindings gekruisbind is. In hierdie sisteme het hidrogel slegs gevorm as die aldehied-PVP molekules oor 'n fraksie funksionele kettingend-waarde van 0.88 vir dialdehied-PVP molekules en 0.5 vir vier armige ster-PVP molekules beskik het.

Die reaksie snelheid van die Schiff-basis kovalente bindings is bevoordeel deur die pH te verlaag (≤ 6.0) en 'n gunstige molêre massa verhouding van 1:0.8 vir die nukleofiel teen oor die akseptor molekule is waargeneem.

Ewewigswel berekeninge is gebruik om die molêre massa tussen kruisbindings en die gemiddelde benaderde porieë binne die drie-dimensionele interne struktuur van die hydrogel te bepaal.

Die seltoksisiteit van PVP-BSA en PVP-PEG hidrogelle is oor 24 h en 48 h in die teenwoordigheid van H9c2 mioblast-selle getoets. Die hydrogel behandelings is uitgevoer in 'n konsentrasie reeks van 0.25×10^{-2} tot 0.01 g/mL. Selmortaliteit is getoets deur 'n Trypan-blou verkleuringstudie. Hierdie resultate is ondersteun deur MTT sel-lewensvatbaarheidstoetse. 'n Lae selmortaliteit (≤ 37 %) is waargeneem en, opspraakwekkend, het van die selle na 48 h verhoogde vitaliteit getoon in die teenwoordigheid van lae konsentrasies PVP-PEG hidrogelle.

Dit is bevind dat hidrogel eienskappe deur stoichiometriese molêre massa verhoudings asook die keuse in die topologie van kruisverbinder beïnvloed word. Hierdie eienskappe het 'n direkte effek op die degradasieprofiel van die gevormde hidrogel.

Samevattend dus is PVP molekules met 'n variasie van topologieë, spesifieke molêre massas en kettingfunksionalitete deur middel van OAFO-gemedieerde polimerisasies gesintetiseer. Xantaatkettingendfunksionele PVP-molekules kon suksesvol omgeskakel word na die kettingendfunksionaliteit van ons keuse om 'n hibried-hidrogel met stoichiometries-manupileerbare eienskappe te sintetiseer. Die positiewe sel-lewensvatbaarbheidstudie resultate staaf verdere ondersoeke in hierdie PVP-gebaseerde hibried hidrogelmateriaal as 'n weefsel nabootsingsmateriaal.

Acknowledgements

I thank my parents and brother for their unwavering love and support in all my endeavours. Our family is small and broken, but I wouldn't swap it for anything in the world.

I thank Bert Klumperman for being such an inspiring laidback promoter, no one could ask for a more approachable boss. Also I thank him for sacrificing so much of himself to be here for us so far away from his family and home. I thank Gwen Pound-Lana for laying the ground work for this project and editing this thesis so completely.

I thank the analysts and researchers of the University of Stellenbosch: Mark Thomas for teaching me the intricacies of the cell culture laboratory and for his time. Elsa Malherbe and Jaco Brand I thank you for running all my NMR experiments with such sincere dedication. Ben Loos thank you for the excellent Fluorescence Microscopy imaging and tutelage on the essence of fluorescence imaging.

I thank friends and co-workers: Rueben Pfukwa for his assistance with organic synthesis and the interpretation of analytical results. I thank Lebohang Hlalele for running the Spartan calculations required in the kinetics chapter. I thank Erinda Cooper and Elsa du Plessis for helping me edit my Afrikaans opsomming and having patience with my atrocious spelling. I would like to thank Khotso Mpitso for being the best laboratory mate in the world, for protecting my lab ware from thieves and for never telling me to put the music down. I thank my friends for the copious amounts of coffee we consumed together on the wall outside Polymer Science.

I thank Dr Mallon for teaching me the finer details of polymer analysis and for infecting me with his love for polymer science.

I thank Niels Akeroyd, for sharing his vast knowledge of organic synthesis, for his sometimes brutal criticism, for being my best friend and for loving me.

List of Figures

List of Schemes

Abbreviations

PVP	poly(vinyl pyrrolidone)
FRP	free radical polymerization
AIBN	azobis(iso butyronitrile)
DEP	dead end polymerization
ATRP	atom transfer radical polymerization
NMP	nitroxide mediated polymerization
CTA	chain transfer agent
RAFT	reversible addition fragmentation chain transfer polymerization
MADIX	macromolecular design via the interchange of xanthates
$R^{\cdot}$	leaving group radical
PDI	poly dispersity index
NVP	*N* vinyl pyrrolidone
UV	ultra violet light spectroscopy
LRP	living radical polymerization
M_n	number average molar mass
TERP	telluride-mediated polymerization
DMAP	4-dimethyl amino pyridine
DCM	dichloromethane
$NaCNBH_3$	sodium cyano borohydride
NMR	nuclear magnetic resonance
H NMR	proton nuclear magnetic resonance
C NMR	carbon nuclear magnetic resonance
TMS	tetramethylsilane
SEC	size exclusion chromatography
HFIP	hexafluoroisopropanol
DMF	dimethylformamide
DMAc	dimethylacetamide
PMMA	poly(methyl methacrylate)
BHT	butylated hydroxytoluene
MS	mass spectrometry

X_D	xanthate RAFT agent difunctional
X_L	xanthate RAFT agent linear
X_T	xanthate RAFT agent tetra functional
X_M	xanthate RAFT agent multi functional
%Conv	percentage conversion of the polymerization
%Unsat	percentage chain end unsaturation
$M_{n\ exp}$	number average molar mass experimentally derived
TEA	tetra functional acrylate crosslinker
DIAC PEG	diacrylate poly(ethylene glycol)
LYS	lysine residue
HSQC	heteronuclear single quantum correlation
pKa	acid dissociation constant
RT	room temperature
MTT	3-(4,5-dimethylthiazol-2-yl)-2,5-diphenyltetrazoliumbromide
DMAP	*4*-dimethyl amino pyridine
BP	benzophenone initiated photopolymerization
RP	Rhodamine B initiated photopolymerization
FP	free radical photopolymerization
PVP-BSA	hybrid hydrogel consisting of PVP and BSA
PVP-LYSINE	hybrid material consisting of PVP and poly(lysine)
PVP-PEG	hybrid hydrogel consisting of PVP and DIAC PEG
PVP SH	thiol end functional PVP
PVPALD	aldehyde end functional PVP
IR	infrared spectroscopy
SEM	scanning electron microscope
HPLC	high performance liquid chromatography
HPLC MS	HPLC coupled to MS
L1_A1_M1	linear polymer 1, aminolysis 1, Michael addition 1
L1_H1_S1	linear polymer 1, hydrolysis 1, Schiff base reaction 1
GHPLC	gradient profile HPLC
ELSD	evaporative light scattering detector

MALDI-ToF spectroscopy	matrix assisted laser desorption ionization time of flight mass
DTT	*D-L*-dithiothreitol
THF	tetrahydrofuran
$NaBH_4$	sodiumborohydride
PBS	phosphate buffer saline solution
IM	*in situ* michael addition reaction

Table of Contents

1. The Plan

The aim of this work was to synthesise hybrid hydrogels or "tissue-mimetic" materials *via* a chemical cross-linking system by using end functionalized poly(*N*-vinyl pyrrolidone) (PVP). The formed hybrid hydrogel should have tuneable characteristics, e.g. gel time, degradation time or percentage swelling.

The crosslinking mechanism itself should be physiologically safe i.e. non toxic crosslinking chemicals, reaction at physiological pH (close to 7.4) and at 37°C. We selected two reaction mechanisms that complied with all these requirements, i.e. Schiff base formation and Michael addition reactions.

The planned strategy was to control the topology of the PVP macromolecules, to control their molar masses and chain end functionalities. These requirements were met by the use of Reversible Addition Fragmentation chain Transfer (RAFT) mediated polymerization.

PVP with a reactive thiocarbonyl thio chain-end can be obtained and quantitative chain end modification can be achieved through hydrolysis or aminolysis to yield an aldehyde or a thiol, respectively, to be used in covalent bond formation.

Covalent bond formation would then be used to form well defined chemically crosslinked hybrid hydrogels with stoichiometrically tuneable physical characteristics.

2. Historical

2.1 Hydrogels are "tissue-mimetic" materials

Hydrogels can be defined as "tissue-mimetic" because of their soft consistency and large propensity to store water. They can also be defined as three dimensional, hydrophilic, polymeric structures capable of imbibing large amounts of water or biological fluids[1, 2]. Since the introduction of hydrogels[3] as soft contact lenses in the 1960s they have found a broad range of pharmaceutical and biomedical applications[4]. A major component of contact lenses is poly(*N*-vinyl pyrrolidone) (PVP), hence the interest in this material for biological hydrogels.

Applications of hydrogels include matrices for the controlled release of various molecules, e.g. pharmaceutical proteins, for the encapsulation of living cells and as tissue scaffolds[5]. Hydrogels have been used for these and other applications due to their biocompatibility with the human body as they resemble living tissues. These tissue mimicking characteristics are due to the high water content and soft consistency of hydrogels[6].

2.2 Hydrogel formation

Three dimensional networks result in the insolubility of hydrogels in aqueous media. The crosslinks may be covalent, electrostatic, hydrophobic or dipole-dipole in character [2].

Hybrid hydrogels are defined as hydrogels that are composed of at least two components from distinct classes of molecules, for example water-soluble synthetic polymers crosslinked with molecules of biological origin[7]. These biomolecules can be used as tunable links in the hydrogel to introduce degradability into the three-dimensional structure[7, 8].

To obtain covalently bonded, chemically linked, hybrid hydrogels between polymers and specific molecules, polymer molecules with multiple functional star topologies with specific chain end moieties are required.

2.3 Free radical Polymerization

In free radical polymerization (FRP), initiating radicals are generated by thermally or photo chemically induced homolysis of a radical initiator. Typically used initiators are azo compounds, such as azobis(iso butyronitrile) (AIBN) or peroxide initiators, such as benzoyl peroxide.

The initiator radicals add to the monomer to produce the propagating radicals. Propagation is the chain building stage whereby the polymer chain grows by repetitive addition of monomer.

Chain growth is terminated *via* bimolecular reactions either by coupling of radicals or by disproportionation between radicals. Propagation is a first order reaction with regards to the radical concentrations, whilst termination is a second order reaction. A number of other chain breaking reactions can take place simultaneously, *e.g.* chain transfer reactions to monomer and/or to the solvent[9].

A significant drawback of free radical polymerization with respect to the aim of this study is the poor control over the molar mass distributions and the chain transfer reactions to monomer and/or to solvent. These chain transfer reactions are always present, resulting in poor control over the chain end functionality which in turn limits post polymerization functionalization. This situation was slightly improved by dead end polymerization (DEP) procedures[10], but not sufficiently for our purposes.

2.4 Living Polymerization

The term living was first used in 1956 to describe living anionic polymerizations[11]. Recently, living radical polymerizations have been achieved by ensuring that only a small fraction of the total population of chains undergoes bimolecular termination. The lifetime of the growing chains in living polymers is significantly prolonged through the introduction of a dormant state for the propagating species. This behaviour can be created through two distinct modes of reaction for the propagating radicals by either reversible termination or reversible transfer. Fast initiation is important, but more importantly, an equilibrium between the propagating radical and a dormant species should be present. An appropriate equilibrium constant determines the living character of these reaction systems. The introduction of the dormant state for living polymers increases the average lifetime of living polymers (active and dormant) by up to four orders of magnitude. As a consequence all chains grow almost simultaneously at the same rate throughout the polymerization until all monomer is consumed.

Two distinct modes of deactivation for the propagating radicals:

1. Reversible deactivation with a stable radical or reversible end capping. The initiator undergoes homolytic bond cleavage to produce one reactive (transient) and one stable (persistent) free radical. The transient radicals quickly initiate the polymerization but the persistent radicals are too stable to initiate poymerization[12]. Techniques that fall into this class are atom transfer radical polymerization (ATRP) and nitroxide mediated polymerization (NMP) (scheme 2.1).

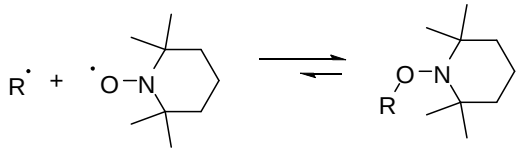

Scheme 2-1 Nitroxide mediated reversible end capping mechanism

2. Degenerative transfer or reversible degenerative chain transfer is characterized in that two polymer chains are required for the change from dormant to active species to occur. Activation occurs via a bimolecular radical transfer between a dormant and an active species. Polymer formation occurs by an overall insertion of monomer units in the chain transfer agent (CTA). The molar mass of the CTA increases between two activation to deactivation steps. Apart from reactions involving the initial CTA, the transition between active and dormant chains results in thermodynamically identical equilibrium. Techniques that fall into this class are reversible addition fragmentation chain transfer polymerization (RAFT) and iodine mediated living radical polymerization.

2.4.1 RAFT mediated polymerization

The RAFT process was patented in 1998 by Le *et al.*[13] In the RAFT process, the CTA is a thiocarbonyl thio species (scheme 2.2). It must be noted though that when using xanthate as CTA the group at Rhodia coined the name macromolecular design via the interchange of xanthates (MADIX)[14], however the mechanism is the same as that of RAFT. The RAFT technique is considered to be highly effective because:

- Desired molecular weights can be targeted,
- Narrow molar mass distributions can be obtained (PDI <1.2)
- Chain end functionality is controlled and can be tuned through the choice of the RAFT agent

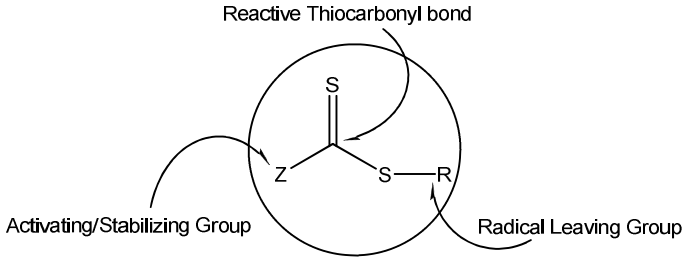

Scheme 2-2 General structure of a RAFT agent [15].

2.4.2 RAFT Mechanism

The generally accepted mechanism of the RAFT mediated polymerization was proposed by the CSIRO group[16] (scheme 2.3). Polymerization in this technique is initiated by a free radical initiator such as AIBN (similar to FRP). After one to a few monomer additions, the propagating radicals add to the CTA producing an intermediate radical. The fragmentation of the intermediate radical results in the release of the leaving group radical R·. R·, the leaving group radical can undergo on of two transitions, i.e. either reinitiating the polymerization or releasing the incoming propagating radical. The main equilibrium exists between the dormant species end-capped with the CTA and the active species that in turn can undergo propagation. Proof for the proposed mechanism was given by the identification of the intermediate thioketal radical by ESR spectroscopy[17].

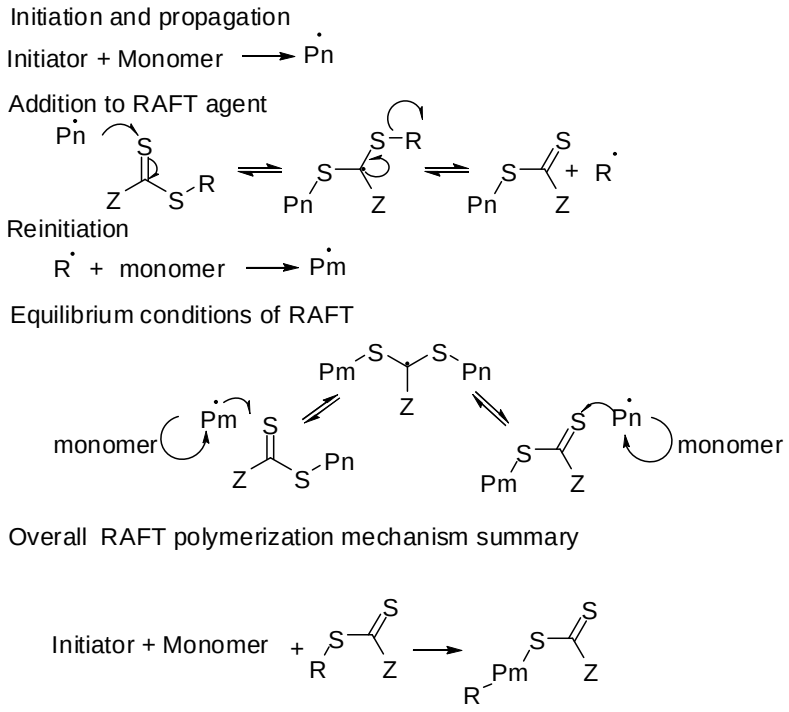

Scheme 2-3 The generally accepted RAFT mechanism

2.4.3 RAFT stars

To obtain chemically crosslinked hybrid hydrogels a polymer molecule with multiple arms of well defined molar mass and chain end functionality is required. Polymer stars can be defined as macromolecules with three or more arms that are attached to a central core. We opted to use the RAFT technique to obtain these molecules.

In the RAFT star polymerization technique the core of the star can be introduced via the functionalization of either the R or the Z substituent on the RAFT agent.

In the Z-group approach, the polymeric arms are detached from the core while they grow and are reattached to the core through a chain transfer reaction. If bimolecular termination via coupling occurs it will be between the arms and not between the stars, which is highly undesirable for post polymerization modification reactions.

In the R-group approach, the polymeric arms grow away from the core, but stay attached to it. Results similar to those from ATRP and NMP are obtained with PDI's ranging from 1.1 to 1.4. In the R-group approach, coupling predominantly occurs between stars, which in the opinion of the author was the lesser of the two evils and could be reduced to below the detection limit in size exclusion chromatography by limiting the polymerization conversion.

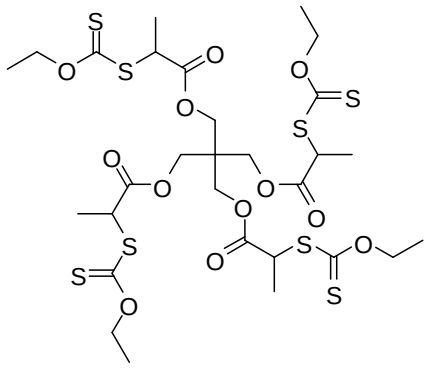

Scheme 2-4 R-group approach compound[18]

2.5 Chain end modification

Polymers prepared via RAFT mediated polymerizations are end-capped with a thiocarbonyl thio functional group. Methods are known that can be used to convert this end-group into a thiol functionality such as aminolysis[19, 20] or reduction[21]. The end-capping species can also be removed completely via thermolysis which results in unsaturated chain ends[22-24], radical coupling[25] or radical reduction[26]. It has also been shown an *O*-ethyl xanthate moiety on a PVP chain end can be removed and transformed into an aldehyde functionality[27] through sequential hydrolysis and heating steps.

2.6 Poly(*N*-vinyl pyrrolidone) (PVP)

PVP is obtained by the polymerization of *N*-vinyl pyrrolidone (NVP). NVP contains a polar cyclic amide that has a resonance structure (scheme 2.5). This resonance structure accounts for the inherent polar characteristics of this monomer. This polarity is retained in the polymerized form. Upon polymerization, a polymer with polar side groups on a relatively apolar hydrocarbon main chain is formed. Therefore PVP is a highly water soluble polymer that is also soluble in various organic solvents[28].

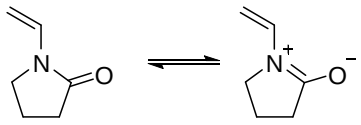

Scheme 2-5 Resonance structures of N-vinyl pyrrolidone

2.6.1 FRP of NVP

In the earliest records of PVP synthesis, NVP is heated in ethanol solutions with H_2O_2 or benzoylperoxide[29]. The synthesis was first reported by Fikentscher *et al.* in 1943[30].

The polymerization was carried out in aqueous solution with H_2O_2, ammonia and traces of heavy metal ions.

The two methods for free radical polymerization of PVP currently used in industry are solution polymerization in water or organic solvents and suspension polymerisation.

a) Solution polymerization: in solution, side reactions are possible if the radicals react with the solvent used. Various organic solvents have been used since the conception of this polymerization, the most common polymerization system being aqueous ethanol solutions as a solvent, AIBN as an initiator and H_2O_2 as a chain transfer agent to control the molecular weight achieved. The chain end in this type of polymerization is characteristically derived from the solvent molecule[31].

b) Suspension polymerization: special techniques are required in this method due to the high water solubility of NVP. Copolymerization of 80% acrylamide and 20% NVP can be conducted in a mixture containing at least 40% *tert*-butanol in water containing electrolytes such as KCl, NH_4Cl, Na_2SO_4, NaCl, NH_4OH etc. Initiators used in this type of polymerizations are typically ammonium persulfate, potassium persulfate, H_2O_2 or AIBN [31].

2. Cationic polymerization: theoretically this polymerization technique can be viable. Until now it has been shown in the literature that only oligomers are produced, thus this method is not favourable if high molecular weight polymer is needed [31, 32].

3. Radiation solid state polymerization: in a 1955 patent[33] the UV induced polymerization of NVP was described. Polymerization of liquid monomer is commonly induced by the γ-radiation at their melting points. A number of sensitizers are used in this field such as $ZnCl_2$, air or anthrachinone and metal perfluoroalkane sulfonates[31].

2.6.2 Living radical polymerization of NVP

As discussed in section 2.1.6.1 the shortcomings of FRP as a route for obtaining quantitative end functional PVP prompted the research into LRP methods. The monomer is very reactive and has a propensity to participate in side reactions e.g. disproportionation, chain transfer, dimerization and the formation of hydration products[34].

2.6.2.1 NMP

This method produced polymers with large polydispersity indexes[35] in the range of 1.8-2.0.

2.6.2.2 ATRP

Matyjaszewski and coworkers reported the polymerization of NVP with ATRP under copper catalyzed conditions with M_n of 2000 g/mol and reasonable control[36] (PDI 1.5). Lu *et al*[37] reported the copper catalyzed ATRP of NVP, with good control over the molar mass distribution (PDI 1.2-1.4).

2.6.2.3 Organostibine mediated LRP

The promotion of living radical polymerization of NVP in the presence of organostibines was shown by Ray *et al*[38]. Excellent control over the molar mass distribution (PDI 1.07-1.3) was obtained. A very slight decrease in the degree of control was observed with increasing conversion (PDI <1.4), due to the formation of an organostibine PVP derivative that is incapable of regenerating a propagating radical, essentially acting as a dead polymer.

2.6.2.4 TERP

Yusa *et al.*[39] showed that the polymerization of NVP can very successfully be mediated by organo telluride transfer agents. Excellent control over the molar mass distribution (PDI ≤ 1.1) was observed.

2.6.2.5 RAFT mediated polymerization

RAFT mediated polymerization of NVP has been performed using various CTAs. Dithiobenzoates[40] provided poor control over the molar mass distribution (PDI 1.6-1.9). Trithiocarbonates[35] (PDI 1.5-2.3), dithiocarbamates[41, 42] (PDI 1.3- 1.4) produced PVP with slightly improved control compared to ditiobenzoates, but xanthates[40, 43] outperformed both of these with good control over the molar mass distributions (PDI 1.2-1.3).

Through previous work in our group[44] it was elucidated that the initialization behaviour of the xanthate CTA used during the RAFT polymerization of NVP is determined by the nature of the R group. Simultaneously it must be added that the structure of the R group determines the degree of control effected by the RAFT agent during polymerization.

2.6.2.6 PVP biological application

PVP has been used in biological applications as far back as World War II as a blood plasma expander[45]. Some applications of PVP currently under investigation include the surface modification of polyurethane catheters[46], vitreous fluid replacement[47], haemodialysis membranes, as solubilising agent for intravenous medicine, e.g. oxytetracycline intravenous antibiotic[3], thin films used as wound dressing materials to stop bleeding and prevent infection[3], fluorescence marker in the diagnosis of bladder cancer [48] and as a local antiseptic, bactericidal, fungicidal and virucidal agent[31] (PVP-iodine complexes).

2.6.2.7 PVP hydrogels

PVP hydrogels have been proposed as wound dressing hydrogels[49] and are used as a major component of soft contact lenses[3]. PVP hydrogels also proved to be biocompatible and indirectly stimulate the growth of fibroblasts[50].

PVP hydrogels have been successfully synthesized via gamma irradiation[51] or free radical polymerization in the presence of an appropriate cross-linker[52, 53]. The applicability of these PVP hydrogels for in tissue biological applications is limited however by the $30x10^3$ g/mol upper limit (synthetic limitations in terms of molar masses obtained and large PDI values) for successful renal clearance[28] and by non-quantitative chain end modification. At higher molar masses PVP cannot be degraded by the renal system resulting in an unfavourable subcutaneous build up.

2.7 Crosslinking strategies

Physically crosslinked hydrogels are hydrophilic networks comprised of an amorphous hydrophilic polymer phase held together by highly ordered aggregates of polymer chain segments arising from secondary molecular forces and other intermolecular forces. Physically crosslinked polymers are of interest because they are well suited for biological applications[5] and require only external stimuli and no extra chemicals to crosslink. Once formed these hydrogels need external stimuli such as a change in pH or temperature in order to degrade.

Chemically crosslinked hydrogels are more versatile and stable than physically crosslinked hydrogels, but the crosslinking agents are often teratogenic, toxic and carcinogenic. The major drawback of chemically crosslinked hydrogels is thus the toxicity of the crosslinking agents. For applications in biological systems it is necessary that the degradation products of the hydrogel be harmless to its environment to ensure biocompatibility of the hydrogel at all stages of its use[5]. In this project the chemical crosslinking method is investigated for aldehyde and thiol

endfunctionalized PVP without the presence of toxic chemical crosslinking agents (scheme 2-6).

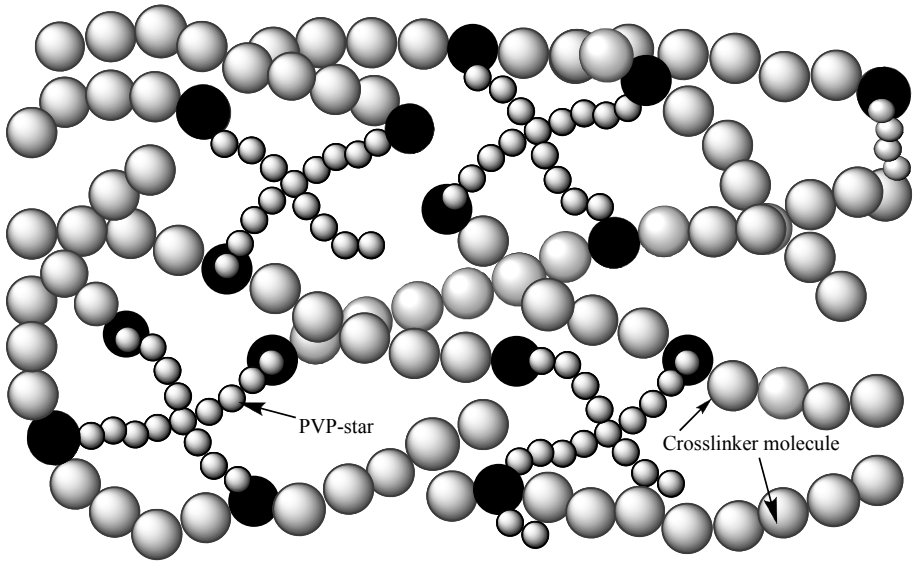

Scheme 2-6: Schematic representation of a chemically crosslinked PVP hydrogel

2.7.1 Michael addition

The Michael addition, named after Arthur Michael, is a straightforward reaction between nucleophiles and activated olefins or alkynes in which the nucleophile adds across a carbon-carbon multiple bond[54]. Michael type addition systems via the addition of thiol functionalized PVP to acrylate functionalized cross-linkers are promising because of the following characteristics:

- The absence of free thiols in the blood limits the chance of unexpected reactions
- No catalysts
- No UV irradiation
- Significantly faster degradation time of Michael addition systems compared to free radically cross-linked acrylic networks
- Conditions are mild enough to provide a protein friendly environment (no deactivation via denaturation of proteins)

Metters *et al.*[55] showed the biodegradability of these thio-acrylate (thioether crosslinked) networks via slow hydrolysis of ester bonds adjacent to the sulphide linkages. The degradation profile was shown to be tuneable in the order of days to weeks depending on the stoichiometric molar ratios used during crosslinking. Hubbell *et al.*[55] also showed that by varying the length of the alkyl spacer between the ester and the sulphide moieties the hydrolysis rate of these systems could be controlled.

The multiplicity or number of cross-linking arms has a direct effect on the system. The molar mass of the arms affects the cross link density and this in turn affects the diffusion of smaller molecules through the system. Increasing the number of cross-linking arms has a direct effect on the release properties of the hydrogel, *i.e.* the protein release rate from hydrogel networks decreases with increased crosslink density[56].

2.7.2 Schiff base formation

The formation of a Schiff base between an aldehyde and primary amine has been used to synthesize hydrogels[57] before but not to synthesize PVP hydrogels. From the article by Pound *et al.*[58] it was deduced that this method should result in a hydrogel if a multifunctional aldehyde PVP was used.

References:

1. Peppas, N. A.; Bures, P.; Leobandung, W.; Ichikawa, H., Hydrogels in pharmacceutical formulations. . *Eur. J. Pharm. Biopharm.* **2000,** 50, 27-46.
2. Sperling, L. H., *Introduction to Physical Polymer Science*. 4th ed.; John Wiley & Sons, Inc.: New Jersey, 2006.
3. Meltzer, Y. L., *Water-soluble resins and polymers: technology and applications* Noyes Data Corp Park Ridge, N.J 1976.
4. Van Tomme, S. R.; Storm, G.; Hennink, W. E., *In situ* gelling hydrogels for pharmaceutical and biomedical applications. *Int. J. Pharm.* **2008,** 355, 1-18.
5. Geever, L. M.; Devine, D. M.; Nugent, M. J. D.; Kennedy, J. E.; Lyons, J. G.; Higginbotham, C. L., The synthesis, characterisation, phase behaviour and swelling of temperature sensitive physically crosslinked poly(1-vinyl-2-pyrrolidinone)/poly(N-isopropylacrylamide) hydrogels. *Eur. Polym. J.* **2005,** 42, 69-80.
6. Devine, D. M.; Higginbotham, C. L., The synthesis of a physically crosslinked NVP based hydrogel. *Polymer* **2003,** 44, 7851-7860.
7. Ulbrich, K.; Strohalm, J.; Kopeček , J., Polymers containing enzymatically degradable bonds. VI.Hydrophilic gels cleavable by chymotrypsin. *Biomaterials* **1982,** 3, 150-154.
8. Kopeček, J., Smart and genetically engineered biomaterials and drug delivery systems. *Eur. J. Pharm. Sci.* **2003,** 20, 1-16.
9. Pfukwa, R. Synthesis and Characterization of Telechelic Hydroxyl Functional Poly(N-vinylpyrrolidone). University of Stellenbosch, Stellenbosch, 2008.
10. Cho, I.; Kim, J., Synthesis of telechelic vinyl polymers by a two-component iniferter. *Polymer* **1999,** 40, 1577-1580.
11. Szwarc, M.; Levy, M.; Milkovich, R., Polymerization initiated by electron transfer to monomer. A new method of formation of block copolymers. *J. Am. Chem. Soc.* **1956,** 78, 2656-7.
12. Odian, G., *Principles of polymerization*. 4th ed.; Wiley Interscience, A John Wiley & Sons, Inc. : 2004; p 314-330.

13. Le, T. P.; Moad, G.; Rizzardo, E.; Thang, S. H. Polymerization with living characteristics. WO98/01478, 1998.

14. Rhodia Chimie, i.; Corpart, P.; Charmot, D.; Biadatti, T.; Zard, S. Z.; Michelet, D. WO. 9858974, 1998.

15. Matyjaszewski, K.; Davis, T. P., *Handbook of Radical Polymerization*. John Wiley and Sons, Inc: 2002.

16. Chong, B. Y. K.; Le, T. P. T.; Moad, G.; Rizzardo, E.; Thang, S. H., A More Versatile Route to Block Copolymers and Other Polymers of Complex Architecture by Living Radical Polymerization: The RAFT Process. *Macromolecules* **1999,** 32, 2071-2074.

17. Hawthorne, D. G.; Moad, G.; Rizzardo, E.; Thang, S. H., Living Radical Polymerization with Reversible Addition-Fragmentation Chain Transfer (RAFT): Direct ESR Observation of Intermediate Radicals. *Macromolecules* **1999,** 32, 5457-5459.

18. Kavimandan, N. J.; Losi, E.; Wilson, J. J.; Brodbelt, J. S.; Peppas, N. A., Synthesis and Characterization of Insulin-Transferrin Conjugates. *Bioconjugate Chem.* **2006,** 17, 1376-1385.

19. Chan, M. F.; Garst, M. E., Oxidative S-dealkylation of tert-butyl aryl sulfides: a novel route to 3-substituted-3H-1,2-benzodithioles. *Chem. Commun.* **1991,** 7, 540-541.

20. Lima, V.; Jiang, X.; Brokken-Zijp, J.; Schoenmakers, P. J.; Klumperman, B.; Van der Linde, R., Synthesis and Characterization of Telechelic Polymethacrylates via RAFT Polymerization. *J. Polym. Sci., Part A: Polym. Chem* **2005,** 43, 959–973.

21. Sumerlin, B. S.; Lowe, A. B.; Stroud, P. A.; Zhang, P.; Urban, M. W.; McCormick, C. L., Modification of Gold Surfaces with Water-Soluble (Co)polymers Prepared via Aqueous Reversible Addition-Fragmentation Chain Transfer (RAFT) Polymerization. *Langmuir* **2003,** 19, 5559-5562.

22. Tournier, L.; Zard, S. Z., A direct approach to [alpha]-hydroxy and [alpha]-chloro trifluoromethyl derivatives. *Tetrahedron Lett.* **2005,** 46, 455-459.

23. Gagosz, F.; Zard, S. Z., A direct approach to alpha-trifluoromethylamines. *Org. Lett.* **2003,** 5, 2655-7.

24. Chong, B.; Moad, G.; Rizzardo, E.; Skidmore, M.; Thang, S. H., Thermolysis of RAFT-Synthesized Poly(Methyl Methacrylate). *Aust. J. Chem.* **2006,** 59, 755-762.

25. Perrier, S.; Takolpuckdee, P.; Mars, C. A., Reversible Addition-Fragmentation Chain Transfer Polymerization: End Group Modification for Functionalized Polymers and Chain Transfer Agent Recovery. *Macromolecules* **2005,** 38, 2033-2036.

26. Destarac, M.; Kalai, C.; Petit, L.; Wilczewska, A. Z.; Mignani, G.; Zard, S. Z., Radical reduction as a means for complete desulfuration of madix polymers. *Polymer Preprints* **2005,** 46, 372-373.

27. Pound, G. Reversible Addition Fragmentation Chain Transfer (RAFT) Mediated Polymerization of *N*-Vinylpyrrolidone. Phd, University of Stellenbosch, Stellebosch, 2007.

28. Kirsh, Y. E., *Water Soluble Poly-N-Vinylamides: Synthesis and Physicochemical Properties*. Wiley, Chichester, UK: 1998; p 233.

29. Reppe, W.; Schuster, C. Polymeric n-vinyl lactams and process of producing same. 1941.

30. Fikentscher, H.; Herrle, K., *Modern Plastics* **1943,** 23, 157-163.

31. Kricheldorf, H. R.; Nuyken, O.; Swift, G., *Handbook of polymer synthesis* 2nd ed.; Marcel Dekker New York 2005; p 121-127.

32. Madl, A.; Spange, S., On the Importance of the Amide-Bonded Hydrogen Atom in the Cationically Induced Oligomerization of N-Vinylamides. *Macromolecules* **2000,** 33, 5325-5335.

33. Polymerisation of N-vinyl-lactams. Brit Pat 725674, 1955.

34. Pound, G.; Eksteen, Z.; Pfukwa, R.; McKenzie, J. M.; Lange, R. F. M.; Klumperman, B., Unexpected reactions associated with the xanthate-mediated polymerization of N-vinylpyrrolidone. *J. Polym. Sci., Part A: Polym. Chem.* **2008,** 46, 6575-6593.

35. Bilalis, P.; Pitsikalis, M.; Hadjichristidis, N., Controlled Nitroxide-Mediated and Reversible Addition–Fragmentation Chain Transfer Polymerization of N-Vinylpyrrolidone: Synthesis of Block Copolymers with Styrene and 2-Vinylpyridine. *J. Polym. Sci., Part A: Polym. Chem* **2006,** 44, 659-665.

36. Coessens, V.; Pintauer, T.; Matyjaszewski, K., Functional Polymers by Atom Transfer Radical Polymerization. *Progr. Polym. Sci.* **2001,** 26, 337-377.

37. Lu, X.; Gong, S.; Meng, L.; Li, C.; Yang, S.; Zhang, L., Controllable synthesis of poly(N-vinylpyrrolidone) and its block copolymers by atom transfer radical polymerization. *Polymer* **2007,** 48, 2835-2842.

38. Ray, B.; Kotani, M.; Yamago, S., Highly Controlled Synthesis of Poly(*N*-vinylpyrrolidone) and Its Block Copolymers by Organostibine-Mediated Living Radical Polymerization. *Macromolecules* **2006,** 39, 5259-5265.

39. Yusa, S.-i.; Yamago, S.; Sugahara, M.; Morikawa, S.; Yamamoto, T.; Morishima, Y., Thermo-Responsive Diblock Copolymers of Poly(N-isopropylacrylamide) and Poly(N-vinyl-2-pyrroridone) Synthesized via Organotellurium-Mediated Controlled Radical Polymerization (TERP). *Macromolecules* **2007,** 40, 5907-5915.

40. Wan, D.; Satoh, K.; Kamigaito, M.; Okamoto, Y., Xanthate-Mediated Radical Polymerization of *N*-Vinylpyrrolidone in Fluoroalcohols for Simultaneous Control of Molecular Weight and Tacticity. *Macromolecules* **2005,** 38, 10397-10405.

41. Devasia, R.; Bindu, R. L.; Borsali, R.; Mougin, N.; Gnanou, Y., *Macromol. Symp.* **2005,** 229, 8-17.

42. Moad, G.; Rizzardo, E.; Thang, S. H., Living Radical Polymerization by the RAFT Process. *Aust. J. Chem.* **2005,** 58, 379-410.

43. Postma, A.; Davis, T. P.; Li, G.; Moad, G.; O'Shea, M. S., RAFT Polymerization with Phthalimidomethyl Trithiocarbonates or Xanthates. On the Origin of Bimodal Molecular Weight Distributions in Living Radical Polymerization. *Macromolecules* **2006,** 39, 5307-5318.

44. Pound, G.; McLeary, J. B.; McKenzie, J. M.; Lange, R. F. M.; Klumperman, B., In-Situ NMR Spectroscopy for Probing the Efficiency of RAFT/MADIX Agents. *Macromolecules* **2006,** 39, 7796 - 7797.

45. Robinson, B. V.; Sullivan, F. M.; Borzelleca, J. F.; Schwartz, S. L., *PVP:a critical review of kinetics and toxicology of polyvinylpyrrolidone (Povidone)*. Lewis Publishers: 1990.

46. Francois, P.; Vaudaux, P.; Nurdin, N.; Mathieu, H. J.; Descouts, P.; Lew, D. P., Physical and biological effects of a surface coating procedure on polyurethane catheters. *Biomaterials* **1996,** 17, 667-676.

47. Ye Hong, T. V. C., Sarojini Vijayasekaran, Weiyong Shen, Xia Lou, Paul D. Dalton,, Biodegradation *in vitro* and retention in the rabbit eye of crosslinked poly(1-vinyl-2-pyrrolidinone) hydrogel as a vitreous substitute. *J. Biomed. Mater. Res.* **1998,** 39, 650-659.

48. Chin, W. W. L.; Lau, W. K. O.; Bhuvaneswari, R.; Heng, P. W. S.; Olivo, M., Chlorin e6-polyvinylpyrrolidone as a fluorescent marker for fluorescence diagnosis of human bladder cancer implanted on the chick chorioallantoic membrane model. *Cancer Letters* **2007,** 245, 127-133.

49. Lugão, A. B.; Rogero, S. O.; Malmonge, S. M., Rheological behaviour of irradiated wound dressing poly(vinyl pyrrolidone) hydrogels. *Radiat. Phys. Chem.* **2002,** 63, 543-546.

50. Smith, L. E.; Rimmer, S.; MacNeil, S., Examination of the effects of poly(N-vinylpyrrolidinone) hydrogels in direct and indirect contact with cells. *Biomaterials* **2006,** 27, 2806-2812.

51. Kaplan, H.; Guner, A., Swelling Behavior of Poly(N-vinyl-2-pyrrolidone) and Poly(N-vinyl-2-pyrrolidone)/$K_2S_2O_8$ Hydrogels in Urea Solutions. *Adv. Polym. Tech.* **2000,** 19, 210-217.

52. Shalaby, W. S. W.; Park, K., Biochemical and Mechanical Characterization of Enzyme-Digestible Hydrogels. *Pharm. Res.* **1990,** 7, 816-823.

53. Jiao, Y.; Liu, Z.; Ding, S.; Li, L.; Zhou, C., Preparation of biodegradable crosslinking agents and application in PVP hydrogel. *J. Appl. Polym. Sci.* **2006,** 101, 1515-1521.

54. Mather, B. D.; Viswanathan, K.; Miller, K. M.; Long, T. E., Michael addition reactions in macromolecular design for emerging technologies. *Prog. Polym. Sci.* **2006**, 487-531.

55. Metters, A.; Hubbell, J., Network Formation and Degradation Behavior of Hydrogels Formed by Michael-Type Addition Reactions. *Biomacromolecules* **2005,** 6, 290-301.

56. Elbert , D. L.; Pratt, A. B.; Lutolf, M. P.; Halstenberg, S.; Hubbell, J. A., Protein delivery from materials formed by self-selective conjugate addition reactions. *J. Controlled Release* **2001,** 76, 11–25.

57. Balakrishnan, B.; Jayakrishnan, A., Self-cross-linking biopolymers as injectable in situ forming biodegradable scaffolds. *Biomaterials* **2005,** 26, 3941-3951.

58. Pound, G.; McKenzie, J. M.; Lange, R. F. M.; Klumperman, B., Polymer–protein conjugates from x-aldehyde endfunctional poly(N-vinylpyrrolidone) synthesised via xanthate-mediated living radical polymerisation. *Chem. Commun* **2008**, 3193-3195.

3. Synthesis & Analysis

In this chapter the synthesis of RAFT agents, polymerization using synthesized RAFT agents and the synthesis of crosslinking agents for Michael addition reactions are discussed.

3.1 Reagents

N-bromo succinimide (99 %, Sigma Aldrich), triethylamine (≥98 %, Fluka), *4*-dimethyl amino pyridine (for synthesis, Merck) (DMAP), hydroquinone (99%, Sigma Aldrich), *1,2,4,5*-tetramethyl benzene (99 %, Sigma Aldrich), deuterated solvent C_6D_6 (99.5 %, Cambridge Isotope Laboratories, Inc.), deuterated solvent D_2O (99.99%, Isotec), deuterated chloroform $CDCl_3$ (99.6 %, Sigma Aldrich), ethylene glycol (99%, Sigma Aldrich), acryloyl chloride (95 %, Sigma Aldrich), benzene (>99.9% HPLC grade, Sigma Aldrich); maleimide (99%, Sigma Aldrich) 2-bromopropionyl bromide (97 %, Fluka) pentaerythritol (for synthesis, Merck), $Na_2(CO_3)$ (NT laboratory supplies Ltd.), dichloromethane (DCM) (99 %, Saarchem), tetrahydrofuran (THF) (99 %, Saarchem), potassium-*o*-ethyl dithiocarbonate (96 %, Fluka), HCl (32%,) formalin (37 %, Merck), sodium chloride (reagent grade, R&S Enterprises), $MgSO_4$ (reagent, Saarchem), pyridine (99.5%, Saarchem), pentane (general, KIMIX), $NaCNBH_3$ (≥95.0 %, Fluka). Cavasol W7 cyclodextrin (reagent grade, Wacker) was dried under reduced pressure overnight in the presence of phosphorous pentoxide. All chemicals were used as received except *N*-vinylpyrrolidinone (>=99 %, Sigma Aldrich) which was distilled under reduced pressure at 64˚C and AIBN which was recrystallized from ethanol (std, KIMIX), poly(ethylene glycol) 1500 g/mol (reagent grade, Fluka)

3.2 Analysis

Nuclear magnetic resonance (NMR) spectroscopy

^{1}H NMR and ^{13}C NMR spectra were acquired in $CDCl_3$ with a Varian VXR-Unity (400MHz) spectrometer (unless specified otherwise). All chemical shifts are reported in parts per million (ppm) with tetramethylsilane (TMS) as a reference.

Size-exclusion chromatography (SEC)

The HFIP system: SEC set up consisted of a Shimadzu Lc-10AD pump, an eluent degasser (Alltech Elite), a gradient pump (Shimadzu, LC-10AD), a Spark Holland, MIDAS injector with an injection volume of 50 μL, a column oven (Spark Holland, Mistral) at 40 °C, a triple detector array in series: Waters 2487 dual wavelength UV detector (320), Viscotek 270 light scattering (RALLS/LALLS) and Viscometry (in series) and a Waters 2414 Differential Refractive Index (DRI) detector (35 °C). Mixed C columns a two-column set (PSS, PFG Linear XL 7 lm, 8 mm _ 300 mm, separation window 102–106 g/mol) using HFIP (Biosolve, AR-grade) with 0.02 mol/L KTFA added (potassium trifluoro acetate, 3.0 g/L, Fluka) as solvent at a flow rate of 0.8 mL/min. The calculated molar masses were based on a calibration curve for poly(methyl methacrylate) standards (molar mass range 650 to 1.5 $x10^4$ g/mol) of low polydispersity (Polymer Laboratories) in HFIP.

The DMF/DMAc system (Stellenbosch): The DMF SEC setup consisted of a Waters Alliance apparatus, Polymer Laboratories mixed D columns, and a dual wavelength UV detector (Waters, 2487) and a differential refractive-index detector (DRI) (Waters, 2414) in series. The injection volume was 100 μL, and the solvent was DMF with 0.02 M LiCl at a flow rate of 0.7 mL/min. The calculated molar masses were based on a calibration curve for poly(methyl methacrylate) standards (PMMA) standards (molar mass range: 850 to 3.5×10^5 g/mol) of low polydispersity (Polymer Laboratories). Data acquisition and processing were performed with Waters Breeze

software. The analysis with DMAc as a solvent was performed on the same system as DMF, the solvent was stabilized with 0.05% w/v BHT and 0.03% w/v LiCl[1], flow rate of 1.0 mL/min. A calibration curve was constructed with linear PMMA standards 850 to 3.5×10^5 g/mol of low polydispersity (Polymer Laboratories).

Mass spectrometry (MS)

MS was carried out on a Waters micromass Q-TOF Ultima API mass spectrometer with the following settings: sample introduction: 0.3 mL/min Waters Alliance 2690; injection: 10 μL; source: ESI+; MS settings: capillary voltage: 3.5 kV, cone voltage: 15, RF1: 40, source: 100 °C, desolvation temp: 400 °C, desolvation gas: 500 L/h, cone gas: 50 L/h.

3.3 RAFT agent synthesis

3.3.1 Monofunctional xanthates

3.3.1.1 S*-2-cyanopropan-2-yl* O*-ethyl carbonodithioate (X_{L1})*

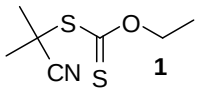

Figure 3-1 Chemical structure of X_{L1}

This RAFT agent (figure 3-1) was obtained via a method described in the literature[2,3].

3.3.1.2 Synthesis of S*-1-cyanoethyl O-ethyl carbonodithioate (X_{L2})*

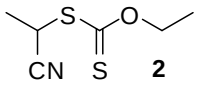

Figure 3-2: Chemical structure of X_{L2}

Method:

2-Bromopropionitrile (1.55 g, 1.20×10^{-2} mol) and potassium-o-ethyl dithiocarbonate (2.04 g, 1.30×10^{-2} mol) were dissolved in THF (30 mL) and stirred overnight at room

temperature. The product was extracted with 3 × 50 mL of diethyl ether and dried over anhydrous $MgSO_4$. This dried organic solution was then concentrated under reduced pressure. The product (figure 3-2) was purified by silica chromatography using pure pentane as eluent.

^{1}H-NMR δ: 1.45 (t, C<u>H</u>$_3$-CH$_2$, 3H), 1.70 (d, C<u>H</u>$_3$-CH, 3H), 4.70 (q, C<u>H</u>$_2$-O, 2H), 4.45 (q, C<u>H</u>-CN, 1H)

3.3.2 Difunctional Xanthate

3.3.2.1 Synthesis of difunctional Xanthate X_{D1}

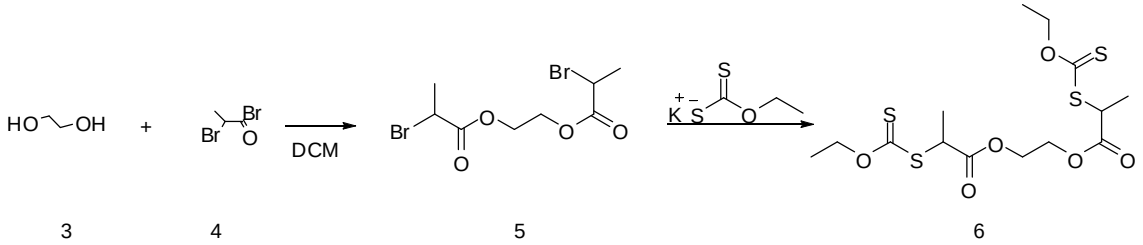

Scheme 3-1: Stages 1&2 of the synthesis of the difunctional RAFT agent.

Method: Stage 1

Ethylene glycol (2.49 g, 4.0×10^{-2} mol), pyridine (7.60 g, 9.6×10^{-2} mol) and dichloromethane (40 mL) were placed in a 100 mL three neck round bottom flask fitted with a condenser. The setup was then placed in an ice bath. *2*-Bromopropionyl bromide (10 mL, 9.6×10^{-2} mol) was added drop wise under stirring. After addition of *2*-bromopropionyl bromide, the mixture was allowed to stir overnight. After stopping the reaction, a white precipitate was removed by filtration and the filtrate was washed with 100 mL diethyl ether in 20 mL volume fractions. The combined ether fractions were then washed with 1M HCl (5×50 mL); 10% NaCl (5×50 mL) and finally with distilled water (3×50 mL). The organic layer was then dried with anhydrous $MgSO_4$ overnight. In the morning the $MgSO_4$ was removed via filtration and the product was concentrated under reduced pressure on the rotavap to yield product **5** (scheme 3-1).

Method: Stage 2

Product **5** (11.66 g, 3.8×10^{-2} mol) and 60 mL THF were added to a 100 mL round bottom flask, then the potassium-o-ethylditiocarbonate (11.55 g, 9.2×10^{-2} mol) was added and the round bottom flask was stoppered. This closed system was allowed to stir for 16 hours at room temperature. The following day the reaction mixture was dissolved in 200 mL distilled water. Product **6** was extracted with 3×100 mL diethyl ether and dried over anhydrous $MgSO_4$. The $MgSO_4$ was filtered off after two hours and product **6** was concentrated under reduced pressure by rotavap.

Thin layer chromatography (TLC) of product **6** in pentane justified purification by silica column chromatography using pentane as eluent initially. The polarity gradient of the column was increased by the systematic addition of ethyl acetate (1:0 to 0:1). The suspected product fractions separated into two yellow bands with increased polarity of the eluent mixture. The two fractions were kept separate, concentrated by rotavap and analyzed by ^{1}H NMR spectroscopy.

After ^{1}H NMR analysis of both bands it was apparent that further purification was required. The product was filtered over a 5 cm column of silica with diethyl ether. The yellow band was collected and concentrated under reduced pressure at 38 °C by rotavap. Product **6** was vacuum dried overnight.

^{1}H NMR δ: 4.61 (q, CH_3-C$\underline{H}_2$-, 4H), 4.38 (q, C$\underline{H}$-S, 2H), 4.34 (s, CH_2-CH_2-O, 4H), 1.56 (d, C$\underline{H}_3$-CH-S, 6H), 1.39 (t, C$\underline{H}_3$-CH_2-, 6H)

^{13}C NMR δ: 211.80 (C(O)O), 171.12 (C(S)S), 70.31 (CH_3-CH_2), 63.01 (CH-S), 47.01 (CH_2-CH_2O), 16.77 (CH_3-CH-S), 13.70 (CH_3-CH_2)

A purity of 93.3 % was determined by ^{1}H NMR spectroscopy. The structure was confirmed via Heteronuclear Single Quantum Correlation (HSQC) a 2D ^{1}H-^{13}C NMR spectroscopy (see figure 3-3)

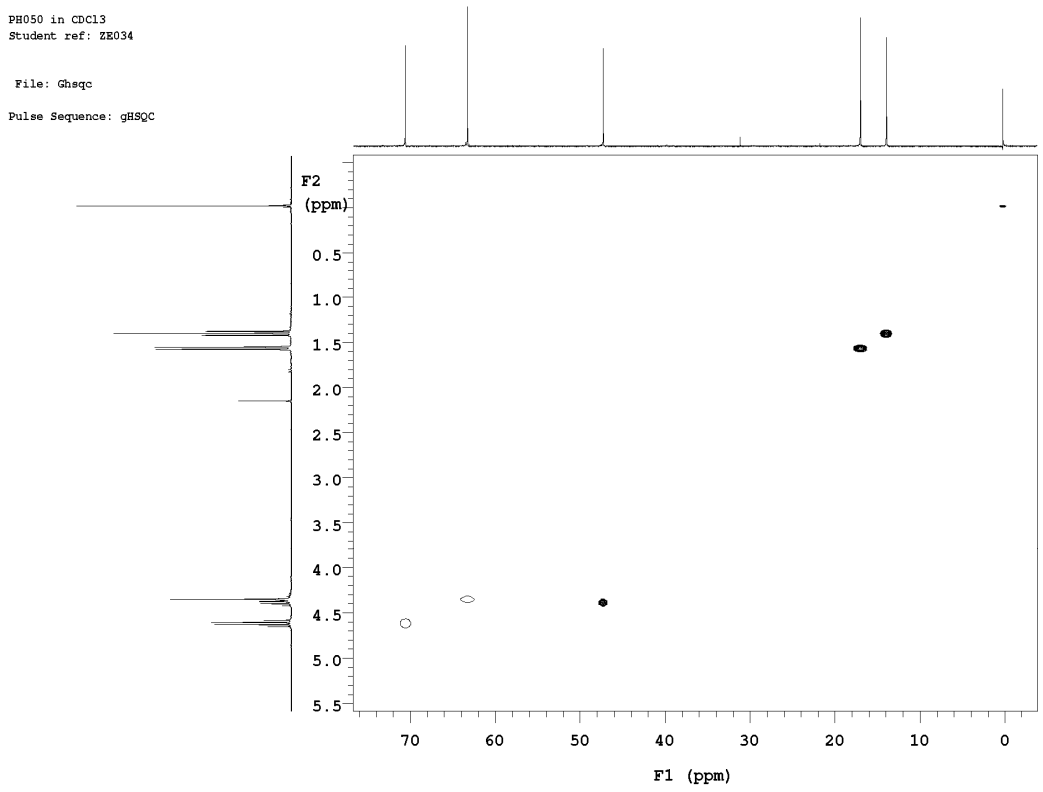

Figure 3-3: Heteronuclear Single Quantum Correlation (HSQC) of X_{D1}

3.3.3 Tetra functional Xanthate

3.3.3.1 Synthesis of 2,2-bis((2-(ethoxycarbonothioylthio)propanoyloxy)methyl) propane-1,3-diyl bis(2-(ethoxycarbonothioylthio)propanoate[4] (X_{T1})

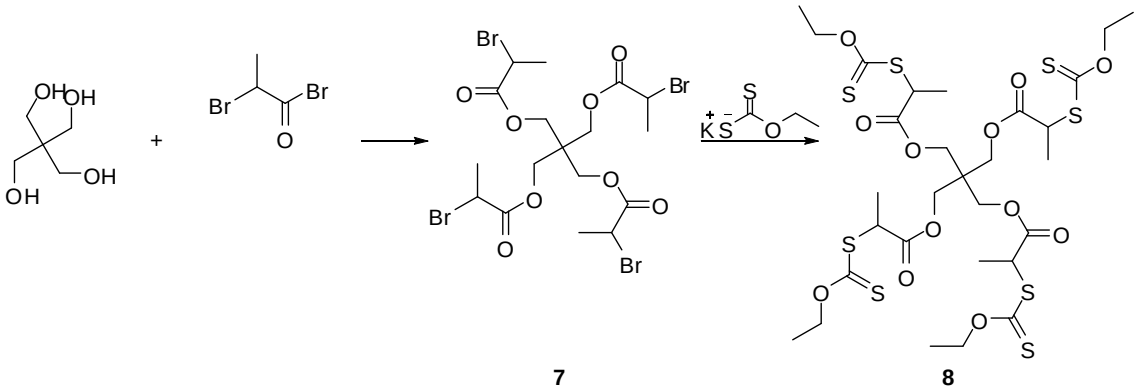

7 **8**

Scheme 3-2: The synthesis of the tetra functional RAFT agent X_{T1}

Method:

Pentaerythritol (5.01 g, 3.68×10^{-2} mol), triethylamine (2.03 g, 2.01×10^{-2} mol), 4-dimethyl amino pyridine (spatula tip) and 300 mL dichloromethane (DCM) were placed in a 500 mL three neck round bottom flask and fitted with a condenser. The mixture was allowed to dissolve with stirring, before a solution of *2*-bromopropionyl bromide (39.58 g, 1.83×10^{-1} mol) in 75 mL DCM was added dropwise to the dissolved mixture which was kept at 0 °C via an ice bath. The reaction was allowed to slowly reach room temperature and to run for 18 hours. This procedure was repeated several times see table 3.1 for experimental values.

The reaction mixture was washed with 8×60 mL 1M HCl solution and then 8×60 mL concentrated $NaHCO_3$ solution. The product **7** was allowed to dry over anhydrous $MgSO_4$ for two hours and then removed via filtration. Product **7** was concentrated on the rotavap under reduced pressure at 38 °C. Crystals appeared in product **7**. The crystals were recrystallized by dissolving in DCM and became turbid by slow dropwise additions of pentane. The cloudy solution was then placed in the fridge and product **7** was allowed to recrystallize overnight. The crystals of product **7** were filtered and allowed to dry at room temperature. The gravimetric yield was 32 %.

Product **7** was then added to the potassium *O*-ethyldithiocarbonate (7.91 g, 1.17×10^{-2} mol) in 25 mL THF. The round bottom flask was stoppered and allowed to stir at room temperature for three days.

The organic layer was diluted with 50 mL distilled water and extracted with 3×50 mL diethyl ether. The extracted layer was dried over anhydrous $MgSO_4$ overnight. The solution was filtered and then concentrated under reduced pressure at 38 °C.

Table 3-1 A summary of the experimental molar ratios used to synthesise X_{T1}

Reagent	A mol	B Mol	C Mol
Pentaerythritol	3.68×10^{-2}	3.71×10^{-2}	7.37×10^{-2}
Tri ethylamine	2.01×10^{-2}	1.83×10^{-1}	3.59×10^{-1}
4-dimehtyl amino pyridine	Spatula tip	2.46×10^{-3}	3.33×10^{-2}
2-bromopropionyl bromide	1.83×10^{-1}	1.83×10^{-1}	3.82×10^{-1}

The concentrated viscous yellow oil was analyzed by TLC and was purified by washing with pentane over fifteen centimetres of silica. The eluent system used was gradually polarized, by slowly increasing the fraction of ethyl acetate. The yellow fraction product **8** was concentrated under reduced pressure at 38˚C. Product **8**, a yellow oil was obtained with 36% gravimetric yield and 92% was determined by ^{1}H NMR spectroscopy.

^{1}H-NMR and ^{13}C-NMR spectroscopy analyses were performed on product 8. ^{1}H-NMR δ (ppm): 4.64 (q, J=7.1, CH_3-C<u>H</u>$_2$, 8H), 4.44 (q, C<u>H</u>-S, 4), 4.17 (m, C-C<u>H</u>$_2$-O, 8H), 1.57 (d, CH-C<u>H</u>$_3$ 12H), 1.43 (t, CH_2-C<u>H</u>$_3$, 12H) ^{13}C-NMR δ (ppm): 211.95 (O-C=S), 170.74 (C=O), 70.6(C), 62.82(<u>C</u>H-CH_3), 47.01(O-<u>C</u>H_2-C), 42.38(CH_2-O) , 16.58 (<u>C</u>H_3-CH), 13.70 (<u>C</u>H_3-CH_2)

MS (figure 3-4): The isotopic pattern for C29H44O12S8, K^+ 860.84 g/mol was observed

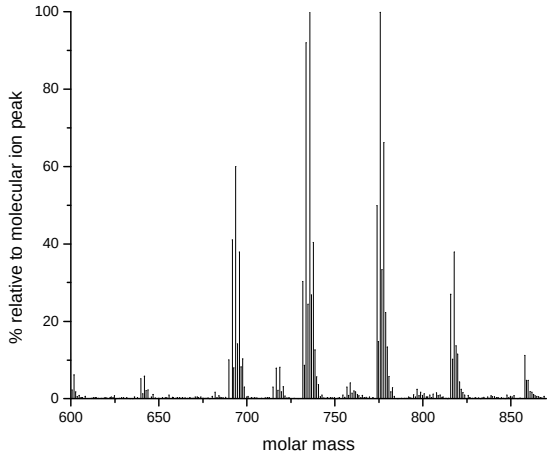

Figure 3-4: Mass spectrum of the tetra functional xanthate X_{T1}

3.3.3.2 Synthesis of 1,2,4,5-Tetrakis[(o-ethyl xanthyl) methyl]benzene[5] X_{T2}

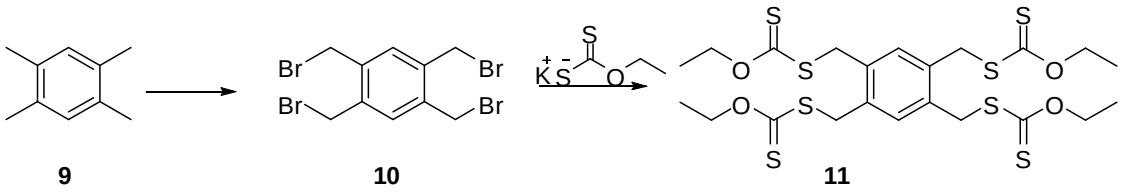

9 **10** **11**

Scheme 3-3: Reaction scheme for the synthesis of 1,2,4,5-tetrakis[(O-ethyl xanthyl) methyl]benzene X_{T2}

Method:

1,2,4,5-Tetrakis[(*O*-ethyl xanthyl) methyl]benzene (**11**) was synthesized as described in the procedure of Kwon et al.[6]

After synthesis a reaction vessel quantity of distilled water was added to the reaction mixture of benzene and product **10** (scheme 3-3). Product **10** was then extracted with benzene (3×50 mL). The solution was dried over anhydrous $MgSO_4$ for 16 hours. $MgSO_4$ was removed via filtration and product **10** was concentrated under reduced pressure at 38 °C. Product **10** was purified by filtering it over 10 cm of silica with PET/pentane as the eluent. The colourless eluent containing product **10** was concentrated under reduced pressure at 38 °C. Product **10** spontaneously formed

ivory crystals upon concentration; these crystals were allowed to dry under reduced pressure for 18 hours.

Product **10** (4.19 g, 9.31×10^{-03} mol) and potassium *O*-ethyl dithiocarbonate (6.56 g, 4.09×10^{-02} mol) were dissolved in 40 mL of THF. The solution was allowed to stir at room temperature for 3 days. After 3 days the mixture was washed with brine (3×50 mL). Product **11** was extracted from the water by adding 3×50 mL diethyl ether and allowed to dry over anhydrous $MgSO_4$ overnight. The $MgSO_4$ was removed via filtration. Product **11** crystallized out during concentration under reduced pressure at 38 °C. The product was recrystallized from pentane: DCM with a ratio of 3:1 (v/v). From table 3.2, D resulted in a white solid, 91% purity according to ^{1}H NMR spectroscopy and a gravimetric yield of 68 % was achieved.

Table 3-2: Experimental molar ratios used in individual synthesis of X_{T2}

Chemical	A n(mol)	B n(mol)	C n (mol)	D n(mol)
N-bromo succinimide	4.17×10^{-2}	4.21×10^{-2}	4.21×10^{-2}	4.17×10^{-2}
1,2,4,5-tetramethylbenzene	1.62×10^{-1}	1.64×10^{-1}	1.62×10^{-1}	1.62×10^{-1}
AIBN	1.53×10^{-2}	1.53×10^{-2}	1.52×10^{-2}	1.52×10^{-2}
Product 10	8.90×10^{-3}	1.10×10^{-2}	8.46×10^{-3}	9.31×10^{-3}
Potassium *O*-ethyl dithiocarbonate	3.94×10^{-2}	4.84×10^{-2}	3.72×10^{-2}	4.09×10^{-2}

^{1}H NMR (400 MHz, $CDCl_3$) δ (ppm): 1.44 (t, *J*=7.12 Hz, $C\underline{H}_3$-CH_2-O, 12 H); 4.41 (s, Ar-$C\underline{H}_2$-S, 8 H) ; 4.68 (q, *J*=7.02 Hz, O-CH_2-CH_3, 8 H); 7.40 (s, $C\underline{H}_{Ar}$,2 H)

T_m: 86.2 - 87.1°C

From infrared spectroscopy the following bands were observed C=S (s) 1060 cm^{-1}, C(S)O (vs.) 1225 cm^{-1} very clearly, the absorbance bands were summarized in table 3.3 and seen in figure 3-5.

Table 3-3: IR band assignments of 1,2,4,5-Tetrakis[(o-ethyl xanthyl) methyl]benzene

Band Assignment	Wavenumber (cm^{-1})
Aromatic C=C-H in plane	1275 (w), 1195 (w)
C(S)O	1225 (s)
C=S	1060 (s)
Ethyl Ester	2975 (m), 2950 (w), 2900 (w), 1475(w), 1460 (w), 1380 (m)

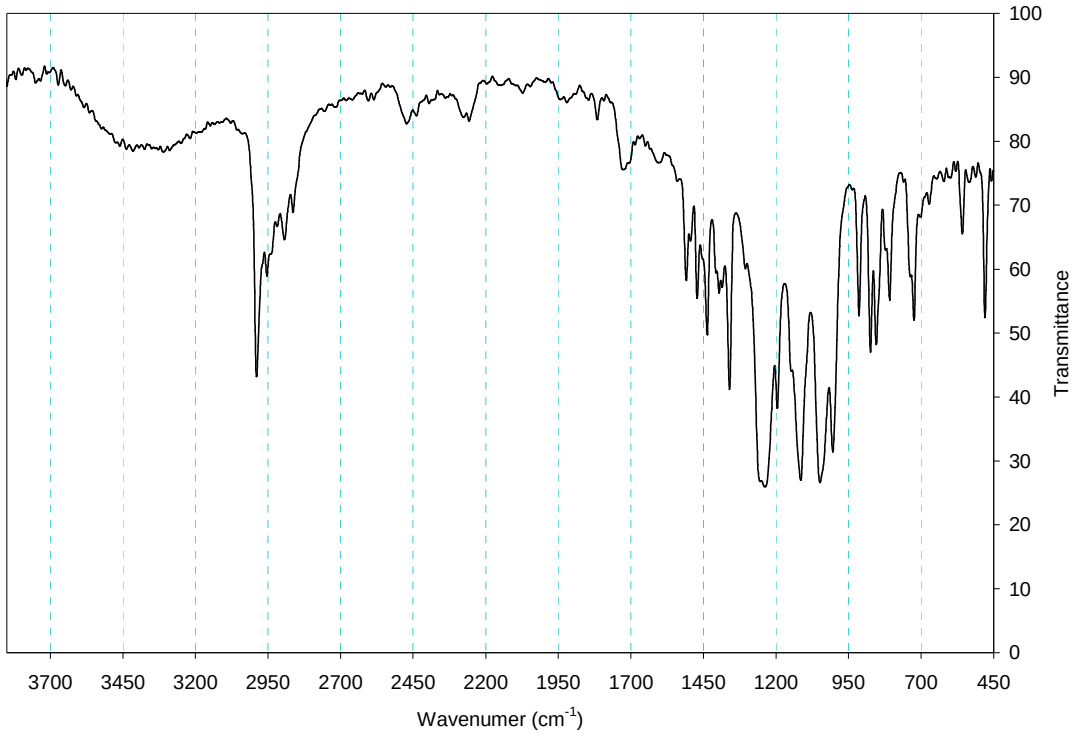

Figure 3-5: IR spectrum of 1,2,4,5-Tetrakis[(o-ethyl xanthyl) methyl]benzene

3.3.4 Multi functional RAFT

3.3.4.1 Synthesis of cyclodextrin based multifunctional xanthate X_{M1}

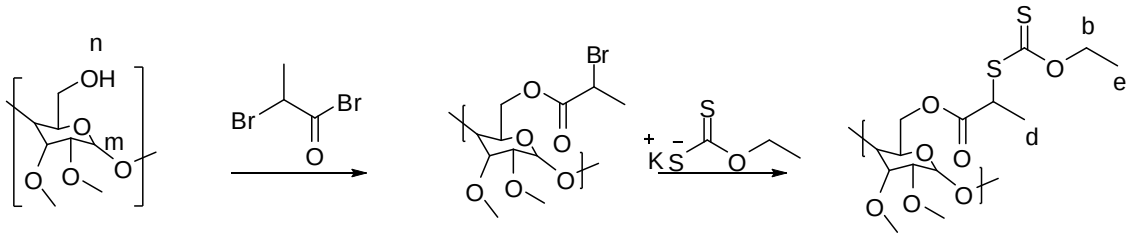

Scheme 3-4: Synthesis of multi functional Xanthate X_{M1}

Method:

Stage 1: Cyclodextrin (4.82 g, 3.68×10^{-3} mol), triethylamine (18.88 g, 1.87×10^{-1} mol), DMAP (0.49 g, 4.01×10^{-3} mol) and 200 mL DCM were added to a three neck 500 mL round bottom flask, the solids were allowed to dissolve via stirring and then a condenser was attached. A mixture of bromopropionyl bromide (60 mL, 5.73×10^{-1} mol) in 50 mL DCM was added dropwise at 0 °C (ice bath) to the closed system. The mixture was allowed to reach room temperature and stirred overnight.

The reaction mixture was washed with 1M HCl (5×50 mL) solution and then with concentrated $NaHCO_3$ solution (5×50 mL). The organic layer was dried over $MgSO_4$ for an hour. The $MgSO_4$ was removed by filtration and the solution was concentrated under reduced pressure at 38 °C. The concentrate was purified by column chromatography with an eluent mix of 1:5 ethyl acetate to pentane. The yellow fraction was collected and concentrated under reduced pressure at 38 °C. Product **13** (scheme 3.4), a glassy yellow solid, was obtained with a gravimetric yield of 85%.

^{13}C-NMR δ (ppm): $CDCl_3$ 173.38 C(O)O) and 169.69 C(CH_3)Br

ESI-MS: MS+ 1703 g/mol which equates to four additions 135 g/mol with atomic pattern of C3H4BrO of bromopropionyl bromide addition to the original cyclodextrin.

Stage2: Product **13** (6.22 g, 3.64×10^{-3} mol) and potassium *O*-ethyl dithiocarbonate (4.44 g, 2.77×10^{-2} mol) were dissolved in 25 mL of THF and allowed to stir overnight at room temperature. The reaction mixture was washed with 50 mL of brine and

product **14** was extracted with 3×100 mL diethyl ether. The organic layer was dried over anhydrous $MgSO_4$ overnight. The $MgSO_4$ was removed via filtration and product **14** was concentrated under reduced pressure at 38 °C. Upon concentration, product **14** crystallized out resulting in 82% gravimetric yield.

^{13}C-NMR δ (ppm): $CDCl_3$ 211.84 (C=S); 171.17 C(O)O

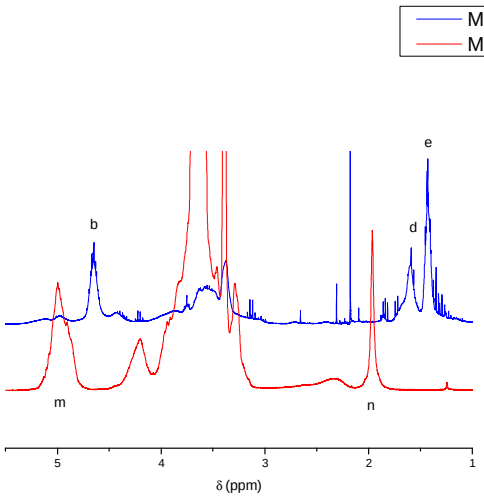

Figure 3-6 ^{1}H NMR X_{M1} vs. pure cyclodextrin

From figure 3-6 a 100% xanthate functionalization was expected as all the **m** (CH) peaks and **n** (OH) peaks (see schematic 3.4) from the starting product (β-cyclodextrin) were consumed.

ESI-MS: M+ = 1970 g/mol which equates to three xanthate arm additions with the atomic pattern of C6H9O2S2 = 177 g/mol additional to the original β-cyclodextrin 1310 g/mol.

The ^{1}H NMR results couldn't be supported by MS results as the molar mass of a 100 % functionalized X_{M1} (C98H154O49S14 = 2565.15 g/mol). This could simply mean that this method was not ideal for the determination of the molar mass of such a large molecule, prone to fragmentation and outside the range of the machine (i.e. > 2000 g/mol).

3.4 Polymerization

Equation 3.1 was used to calculate the initial molar ratios of RAFT agent to monomer required for individual target molar masses. The molar ratio of AIBN : RAFT was kept at 1:5. The RAFT equation was used to target specific molar masses, but in designing experiments high molar masses were targeted and reactions stopped in the range of 30 to 60 % conversions. This method was used to prevent side reactions of the NVP due to long inhibition periods at 60 °C, caused by a high RAFT agent concentration.

$$M_{n_{Th}} = \frac{c[M_0]}{[RAFT]} * M_{w_{MONOMER}} + M_{w_{RAFT}} \qquad (3.1)$$

Method

The RAFT agent X_{T2} (0.37 g, 2.25×10^{-3} mol) and AIBN (0.08 g, 4.79×10^{-4} mol) were weighed into a dry pear-shaped reaction vessel. *N*-vinylpyrrolidinone was added by measuring a precise volume (15 mL) as quickly as possible to prevent oxygen contamination. The vessel was then sealed and frozen in liquid nitrogen. The frozen vessel was degassed under reduced pressure for one minute, thawed and frozen again. This step was repeated in four freeze pump thaw cycles. After the final cycle the reaction vessel was filled with ultra high purity argon and placed in a 60 °C pre-heated oil bath. The reaction was allowed to run for 2 h 40 min.

The polymerization mixture was precipitated into diethyl ether. The precipitated polymer was recovered immediately by filtration and dried under reduced pressure overnight before analysis. Care has to be taken at this point to keep the polymer dry, cool and preferably under argon environment to prevent the loss of chain end functionality. All the polymerizations were executed using the same method. The experimental data are summarized in table 3.4.

Table 3-4 Summary of bulk polymerization results with N-vinylpyrrolidinone

Exp Ref	RAFT agent Ref	NVP (mol)	RAFT (mol)	AIBN (mol)	RAFT: AIBN	Target M_n (g/mol)	% Conv	$M_{n\ exp}$ (g/mol)	M_{n} exp GPC HFIP PMMA (g/mol) (PDI)	M_{n} exp GPC DMF PMMA (g/mol) (PDI)	M_{n} exp GPC DMAc PMMA (g/mol) (PDI)	%Unsat
L1	X_{L1}	9.91×10^{-2}	1.16×10^{-3}	1.38×10^{-4}	8	9636	81	7805	8300(1.3)		4406(1.4)	46%
L2	X_{L1}	9.93×10^{-2}	5.94×10^{-4}	6.94×10^{-5}	9	18752	83	15564	16200(1.3)		8008(1.4)	5%
L3	X_{L2}	9.36×10^{-2}	2.16×10^{-3}	4.42×10^{-4}	5	1622	30	928			954 (1.0)	23%
L4	X_{L2}	4.68×10^{-2}	7.96×10^{-4}	2.39×10^{-4}	3	1481	20	1090			1021 (1.0)	5%
D1	X_{D1}	9.91×10^{-2}	7.14×10^{-4}	7.13×10^{-5}	10	15821	42	6915	5198(1.4)	4179(1.4)	2631 (1.3)	8%
D2	X_{D1}	9.93×10^{-2}	3.21×10^{-4}	3.11×10^{-5}	10	34761	71	21972	20732(1.5)			0%
D3	X_{D1}	9.92×10^{-2}	7.75×10^{-4}	7.59×10^{-5}	10	14638	37	5557	4312(1.4)			27%
D4	X_{D1}	$9.91\times10\text{-}^{2}$	3.70×10^{-4}	3.71×10^{-5}	10	30110	45	19061	11051(1.5)			30%
T1	X_{T2}	1.87×10^{-1}	4.99×10^{-4}	1.01×10^{-4}	5	14374	33	10669		6413(1.6)		0%
T2	X_{T2}	1.87×10^{-1}	6.66×10^{-4}	1.51×10^{-4}	4	10777	33	9545		3148(1.6)		50%
T3	X_{T2}	1.41×10^{-1}	1.02×10^{-3}	2.06×10^{-4}	5	5717	33	10456		3116(1.9)		100%
T4	X_{T2}	1.41×10^{-1}	2.25×10^{-3}	4.79×10^{-4}	5	6053	79	10139		5563(1.1)		60%
T5	X_{T2}	1.41×10^{-1}	1.78×10^{-3}	3.76×10^{-4}	5	7581	79	12687		4994(1.2)	11786(1.5)	73%
T6	X_{T2}	9.36×10^{-2}	2.11×10^{-3}	4.29×10^{-4}	5	2058	29	4433		5062(1.1)	3661 (1.3)	12%
T7	X_{T2}	9.36×10^{-2}	1.53×10^{-3}	3.12×10^{-4}	5	3106	37	10187		7216(1.1)	5506 (1.4)	15%
T9	X_{T2}	9.36×10^{-2}	1.14×10^{-3}	1.89×10^{-4}	6	2038	16	3268			3270 (1.3)	15%
T10	X_{T2}	1.87×10^{-1}	9.13×10^{-4}	1.88×10^{-4}	5	15371	65	13808			9956(3.5)	4%
T11	X_{T2}	1.87×10^{-1}	1.31×10^{-3}	3.27×10^{-4}	4	10238	61	7002			10899	100%
T12	X_{T2}	2.34×10^{-1}	1.45×10^{-3}	2.70×10^{-4}	5	1496	5	2805			3100(1.5)	12%
T13	X_{T2}	1.87×10^{-1}	2.12×10^{-3}	4.24×10^{-4}	5	5694	52	7131			6775 (1.4)	22%
T14	X_{T2}	1.87×10^{-1}	2.31×10^{-3}	4.27×10^{-4}	5	2324	23	3539			3034 (1.3)	11%
M1	X_{M1}	9.36×10^{-2}	1.21×10^{-3}	4.20×10^{-4}	3	3006	6	5011		6534(1.2)		13%

The average molar mass ($M_{n\ exp}$) determined via ^{1}H NMR spectroscopy was calculated in the following way. The peak integration of (a) in figure 3-7, which is equal to either two or four or eight protons depending on the topology of the RAFT agent used observed at δ=4.6 ppm (CH_3-C$\underline{H}_2$; q; 2H ;4H ;8H) was set to a reference value (topology dependent). In setting the reference value a ratio is obtained for the integration of the polymer peaks between δ=4.0-3.5 ppm (b). This ratio equates directly to the average number of monomer units per polymer chain. This ratio was multiplied by the molar mass of *N*-vinylpyrrolidinone (111.14 g/mol) and in doing so the molar mass of the polymer $M_{n\ exp}$ ^{1}H NMR was determined[7].

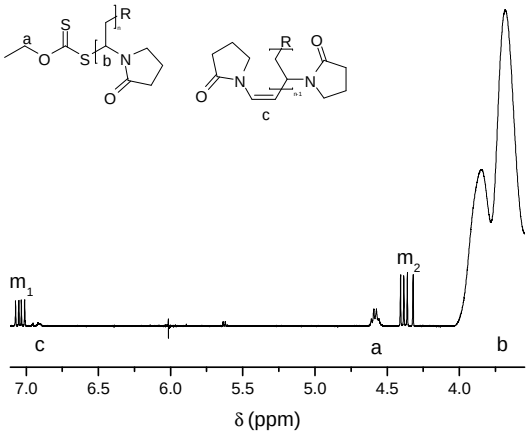

Figure 3-7: Peak assignment used in the determination of ^{1}H NMR molar mass.

In spite of the lowered polymerization temperature and shortened polymerization time unsaturated chain ends still form through the thermolysis of the xanthate chain end during polymerization. The approximate percentage unsaturation of the polymer relevant to the functional chain ends was determined by using equation 3.2. The percentage unsaturation of each polymerization was summarized in table 3.4.

$$\%Unsaturation = \frac{A_{7.0-6.8}}{A_{4.6}} \times 100 \qquad (3.2)$$

$$\text{Reference}\ \delta_{4.0\text{-}3.5} = 100 \qquad (3.3)$$

3.5 Cross linker synthesis

3.5.1 Synthesis of 2,2(bisacryloyl oxymethyl)propane-1,3diyl diacrylate (TEA)

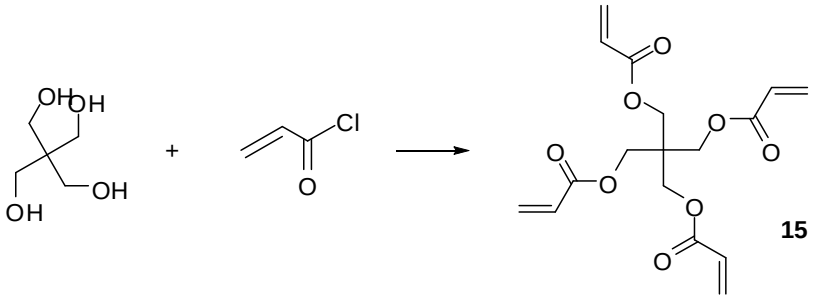

Scheme 3-5 A Schematic for the synthesis of TEA

Method:

Pentaerythritol (4.97 g, 3.7×10^{-2}mol), triethylamine (25.44 mL, 1.83×10^{-1} mol), DMAP (0.45 g, 3.71×10^{-3} mol) and a spatula tip of hydroquinone were added to 75 mL of chloroform in a 100 mL three neck reaction vessel fitted with a condenser. The mixture was stirred for 30 min at room temperature. To this mixture a solution of acryloyl chloride in 25 mL of chloroform was added dropwise through a dropping funnel. The reaction vessel was kept at 0 °C with an ice bath during the addition of acryloyl chloride. The system was allowed to thaw and was stirred overnight.

The reaction mixture was washed with 8×60 mL of 1M HCl and then with 8×60 mL of a saturated aqueous $NaHCO_3$ solution. An excess of NaCl was added to the final washing steps. Product **15** was allowed to dry over $MgSO_4$ for a couple of hours at which time the drying agent was removed via filtration. Product **15** was concentrated under reduced pressure at 38 °C.

Table 3-5: Molar ratios used during two separate synthesis of Product 15

Reagents	A n (mol)	B n (mol)
Acryloyl chloride	2.22×10^{-1}	1.83×10^{-1}
Pentaerythritol	5.19×10^{-2}	3.70×10^{-2}
Triethylamine	2.58×10^{-1}	1.83×10^{-1}
DMAP	5.17×10^{-3}	3.71×10^{-3}

Product **15** was completely insoluble in water and only partially soluble in DMSO.[8]

^{1}H NMR, 400 MHz, δ (ppm), (DMSO-*d*) 6.39-6.27 (m, C$\underline{H}_{2a}$=CH, 8H); 6.21-6.09 (m, CH_2=C$\underline{H}$, 4H); 6.00-5.91 (m, C$\underline{H}_{2b}$=CH, 8H); 4.28-4.25 (s, C$\underline{H}_2$-O, 8H)
Product **15**, a bright orange solid with a gravimetric yield of 30 % and a purity determined via ^{1}H NMR spectroscopy of 80 % was obtained.

3.5.2 Synthesis of di-acrylate poly(ethylene glycol) (DIAC PEG)

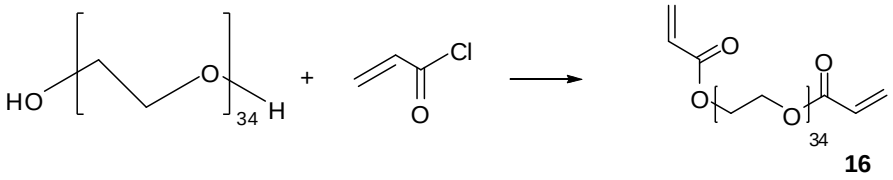

16

Scheme 3-6: Synthesis of DIAC PEG

Method:
The same method as explained in 3.1.5.1 was used and the molar masses are shown in table 3.6. Product **16** was synthesized successfully, with 53 % gravimetric yield. The white waxy product is completely water soluble.

^{1}H-NMR 400 MHz, $CDCl_3$ δ (ppm), 6.45-6.35 (m, C$\underline{H}_{2a}$=CH, 4H); 6.19-6.07 (m, CH_2=C$\underline{H}$, 2H); 5.86-5.79 (m, C$\underline{H}_{2b}$=CH, 4H); 3.65-3.60 (s, C$\underline{H}_2$-C$\underline{H}_2$-O, 408H)

$$PEG\ \text{DiAc}\ g/mol = \frac{A_{\delta_{3.65-3.60}}}{4_{\text{protons refeence}} * 3_{\text{protons per repeat unit}}} * 44\ \text{g/mol (repeat unit)} \qquad (3.4)$$

$$PEG\ \text{DiAc}\ g/mol = 1496\ \text{g/mol}$$

The molar mass provided by the supplier indicated 1500-1600 g/mol thus it was concluded that a nearly 100 % acrylate functionalization was obtained.

Table 3-6: Molar ratios used in DIAC PEG

Reagents	n (mol)
Acryloyl chloride	2.09×10^{-2}
Poly(ethylene glycol)	1.01×10^{-2}
Triethylamine	7.17×10^{-2}
DMAP	1.39×10^{-3}

3.5.3 Synthesis of N-methylolmaleimide

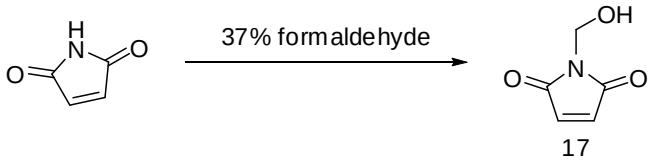

17

Scheme 3-7 The synthesis of maleimide crosslinker

Method

Maleimide (24.5 g, 2.5×10^{-1} mol) was added to a three neck flask, with a condenser. Formalin was added through a dropping funnel and the mixture was allowed to mix at 30 °C for 30 minutes. A 5% solution of NaOH was allowed to add over 10 minutes (0.75 mL). The solution was removed from heat and allowed to cool down for 3 hours before filtering the off white crystal product **17** (scheme 3-7). The crystals of product **17** were recrystallized in ethyl acetate in the freezer for 16 hours.

References:

1. Ting, S. R. S.; Gregory, A. M.; Stenzel, M. H., Polygalactose Containing Nanocages: The RAFT Process for the Synthesis of Hollow Sugar Balls. *Biomacromolecules* **2009,** 10, 342-352.
2. Bouhadir, G.; Legrand, N.; Quiclet-Sire, B.; Zard, S. Z., A New Practical Synthesis of Tertiary S-Alkyl Dithiocarbonates and Related Derivatives. *Tetrahedron Lett.* **1999,** 40, 277-280.
3. Pound, G.; McLeary, J. B.; McKenzie, J. M.; Lange, R. F. M.; Klumperman, B., In-Situ NMR Spectroscopy for Probing the Efficiency of RAFT/MADIX Agents. *Macromolecules* **2006,** 39, 7796 - 7797.
4. Bernard, J.; Favier, A.; Zhang, L.; Nilasaroya, A.; Davis, T. P.; Barner-Kowollik, C.; Stenzel, M. H., Poly(vinyl ester) Star Polymers via Xanthate-Mediated Living Radical Polymerization: From Poly(vinyl alcohol) to Glycopolymer Stars. *Macromolecules* **2005**, 5475-5484.
5. Nguyen, T. L. U.; Eagles, K.; Davis, T. P.; Barner-Kowollik, C.; Stenzel, M. H., Investigation of the Influence of the Architectures of Poly(vinyl pyrrolidone) Polymers Made via the Reversible Addition–Fragmentation Chain Transfer/Macromolecular Design via the Interchange of Xanthates Mechanism on the Stabilization of Suspension Polymerizations. *J. Polym. Sci., Part A: Polym. Chem* **2006,** 44, 4372–4383.
6. Kwon Tae Seok; Takagi Koji; Kunisada Hideo; Yuki Yasuo, Synthesis of star polystyrene by radical polymerization with 1,2,4,5-tetrakis(p-tert-butylphenylselenomethyl)benzene as a novel photoiniferter. *Eur. Polym. J.* **2003**, 1437–1441.
7. Pfukwa, R. Synthesis and Characterization of Telechelic Hydroxyl Functional Poly(N-vinylpyrrolidone). MSc, University of Stellenbosch, Stellenbosch, 2008.
8. Wang N.; Dong A.; Radosz M.; Shen Y., Thermoresponsive degradable poly(ethylene glycol) analogues. *J. Biomed. Mater. Res. Part A* **2007**, 148-157.

4. Hydrogels: Synthesis & Analysis

In this chapter chemical crosslinked PVP hydrogels were synthesized via the Michael addition reaction and Schiff base formation between PVP SH and PVPALD of di functional, 4 arm star and multifunctional stars. The effect of pH and molar ratio of reactants on hydrogel formation was investigated.

Synthesized hydrogels were analyzed with equilibrium swelling experiments, % equilibrium swelling experiments, ^{1}H NMR, IR and SEM.

4.1 Reagents

Tetrahydrofuran (98 %, Saarchem), dichloromethane (98 %, Saarchem), NaH_2PO_4 (reagent grade, Merck), Na_2HPO_4 (reagent grade, Merck), cyclohexylamine (≥99.5 %, Fluka), $NaCNBH_3$ (≥95.0 %, Fluka), *D-L*-Dithiothreitol (DTT) (sigma grade, Sigma Aldrich), 5,5'-Dithiobis(2-nitrobenzoic acid) (≥97.5 %, Fluka).

4.2 Analysis

High Performance Liquid Chromatography (HPLC)

The HPLC setup comprised of the following units: Waters 2690 Separations Module (Alliance); Agilent 1100 series variable wavelength UV detector; PL-ELS 1000 detector. The data was recorded and processed using PSS WinGPC unity (Build 2019) software. A C18 silica column was used (Luna RP C18 3 μm 150×4.60 mm, Phenomenex) at 30 °C. The mobile phase composition was water (de-ionized, with 0.1% formic acid): acetonitrile at a flow rate of 0.5 mL/min. Samples were prepared in the same solvent composition as the mobile phase (80:20) at a concentration of 0.5 mg/mL. The gradient of each sample injection started with the ratio of (80:20)

this was gradually changed to (65:35) over 30 minutes. The injection volume was 10 μL.

HPLC MS: The optimized gradient HPLC conditions were used. The instrument used was a Waters API Q-TOF Ultima and scanning 400-1990. Sample introduction 300 μL/min Waters UPLC, sample injection 5 μL. ESI+ capillary voltage 3.5 kV, cone voltage 35, RF1 40, Source 100 °C, desolvation Temp 350°C, desolvation gas 350 L/h and cone gas 40 L/h was used.

Scanning electron microscopy SEM

A LEO 1430VP Scanning Electron Microscope was used. Prior to imaging, samples were sputter coated with gold. Images were acquired at various magnifications. An accelerating voltage of 7 kV and spot size of 150 was used.

4.3 Methods: Functionalization & Crosslinking

4.3.1 Thiol functionalization

4.3.1.1 Aminolysis

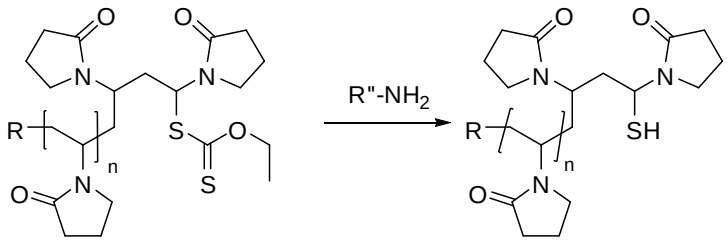

Scheme 4-1: Schematic representation of the aminolysis reaction

The aminolysis (scheme 4-1) experiments A1-A4 (table 4.1) were performed using the following method.

The xanthate chain end functional PVP L1_A1 (0.7 g, 9.07×10^{-5}mol) was dissolved in 30 mL of dry THF. A twenty times molar excess of cyclohexylamine (0.04 g, 3.78×10^{-4} mol) was added to the solution at 30 °C. The mixture was allowed to stir overnight. The polymer was precipitated directly from this step into diethyl ether, dried under

reduced pressure and stored in a dry cool environment. It became apparent that this long period of reaction leads both to side reactions and the formation of di-sulphide bridges.

The aminolysis experiments A5-A8 (table 4.1) were performed using the following method.

A solution of the polymer T6_A5 (2.10 g, 4.73×10^{-4} mol) in THF was purged with high purity argon for 30 minutes. The isolated reaction mixture (under argon atmosphere) was allowed to stir for two hours at 30 °C. At this point degassed cyclohexylamine (3.28 g, 3.30×10^{-2} mol) was in 10 mL THF was added to the solution. The reaction was allowed to run for two hours before it was precipitated into diethyl ether.

In an attempt to increase the conversion of xanthate chain ends into thiols, a final experiment using the aminolysis method was performed as follows. The entire reaction setup was kept under argon atmosphere, by bubbling it through the solution at a constant rate. Both the solution of the polymer T9_A9 (1.55 g, 4.74×10^{-4} mol) in THF and the cyclohexylamine (2.94 g, 2.96×10^{-2} mol) in 15 mL of THF each were degassed separately for 20 min before mixing. The mixture was allowed to stir for 2 hours at 30 °C. An excess of DTT was added to a 2 mL aliquot of reaction mixture via a syringe. The degassed DTT plus the reaction mixture was returned to the mother reaction mixture and allowed to stir for another hour. A solution of DIAC PEG (2.29 g, 1.53×10^{-3} mol) in 1mL THF was degassed and added to the mother reaction mixture.

Table 4-1: Data summary of aminolysis experiments

Exp Reference	PVP mass (g)	PVP n (mol)	Cyclohexylamine mass (g)	Cyclohexylamine n (mol)
L1_A1	0.71	9.07×10^{-5}	0.04	3.78×10^{-4}
T1_A2	1.99	1.86×10^{-4}	0.01	1.04×10^{-4}
T2_A3	1.98	2.07×10^{-4}	0.04	3.78×10^{-4}
T3_A4	2.10	2.01×10^{-4}	0.08	7.78×10^{-4}
T6_A5	2.10	4.73×10^{-4}	3.28	3.30×10^{-2}
T7_A6	2.20	2.16×10^{-4}	2.41	2.43×10^{-2}
L1_A7	1.14	1.46×10^{-4}	0.35	3.49×10^{-3}
L3_A8	0.16	1.70×10^{-4}	0.35	3.49×10^{-3}
T9_A9	1.55	4.74×10^{-4}	2.94	2.96×10^{-2}

Ellman's Test was performed to determine the concentration of thiol functionalized chain ends as prescribed in the original 1958 paper[1]. Ellman's reagent acts as a UV indicator that can be directly correlated to the concentration of free thiols in a solution by measuring the absorbance at 412 nm (equation 4.1; 4.2).

$$c_{thiol} = \frac{A_{412nm}}{13600} \qquad (4.1)$$

$$\%\,\text{Thiol functionalization} = \frac{c_{thiol}}{c_{initial}} * 100 \qquad (4.2)$$

In this calculation, to determine the initial concentration of PVP in mol/L ($c_{initial}$), the molar mass of the PVP must be know. The experimental molar mass of each PVP sample was determined ^{1}H NMR spectroscopy (see Figure 3.6).

4.3.1.2 Reduction method to obtain thiol chain ends

The polymer T11 (2.15 g, 3.07×10^{-4} mol) was dissolved in 200 mL distilled water. To this solution $NaBH_4$ (7.57 g, 2.00×10^{-1} mol) was added to obtain a 1 M solution. The mixture was left to stir for 2 hours at room temperature.

The excess $NaBH_4$ was neutralized with 1 M HCl solution. The mixture was supplemented with 0.1 M Na_2HPO_4 and the pH adjusted to pH 8.2 before the addition

of excess Ellman's reagent. This was done to prevent anomalous results which would result due to the reduction of the Ellman's reagent itself.

The mixture was dialyzed against water for a week to remove any excess Ellman's reagent. The dialyzed mixture was freeze dried immediately, resulting in a light yellow powder. The powder was then analyzed according to Ellman's test. Further analysis was complicated by the formation of a gel in solvent upon exposure to air. This gelation was assigned to the formation of disulphide bridges due to oxidation from oxygen in solvents and air.

4.3.1.3 Michael addition:

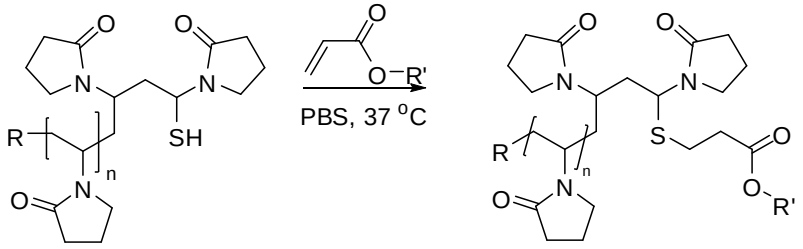

Scheme 4-2 Schematic representation of the Michael addition reaction

The PVP SH T6_A5_M4 (0.21 g, 4.78×10^{-5} mol) was dissolved in 0.8 mL of 0.1 M PBS buffer pH 7.4. In a different vessel the DIAC PEG (0.06 g, 4.24×10^{-5} mol) was dissolved in PBS buffer pH 7.4. The two components were mixed to obtain a solution of 58 wt%. The gel point was determined by the tilting method. The tilting method means that if the liquid no longer flows but adheres to the bottom of the vial even when the vial is inverted, then a gel has formed. In this case it was observed after 2 hours. All the other Michael additions were performed in this manner see table 4.3 for the experimental values.

4.3.2 Aldehyde functionalization

4.3.2.1 Hydrolysis:

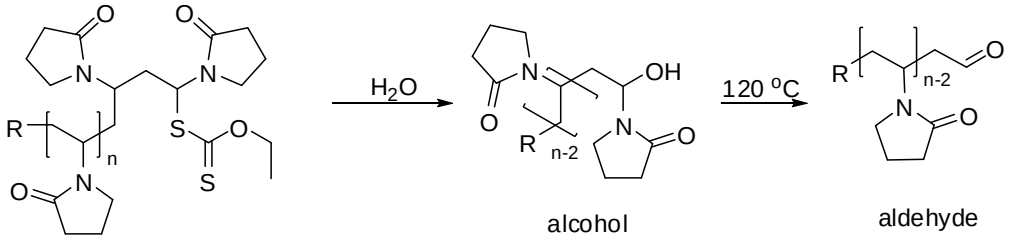

Scheme 4-3 Schematic representation of the hydrolysis reaction with PVP xanthate

Distilled water (30 mL) was added to T4_H6 (6.59 g, 6.50×10^{-4} mol). The solution was stirred at 37 °C for 22 hours. This solution was then dialysed using snake skin dialysis tubing (Pierce, molecular weight cut off 3500 g/mol) for 2 days in distilled water, refreshing the water roughly every 8 hours. The polymer was recovered via freeze-drying and heated at 120 °C under reduced pressure for 22 h. Upon drying in the oven, the polymer consisting of aldehyde functional PVP (PVP ALD), was cooled under reduced pressure and directly placed in a cool and dry environment. All other hydrolysis experiments were executed using this method (table 4.5).

4.3.2.2 Schiff base formation

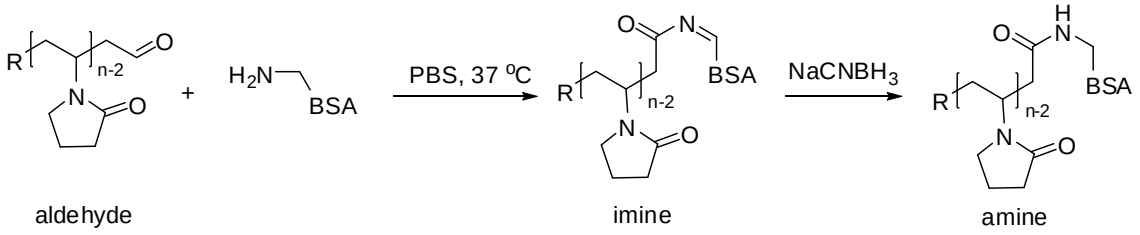

Scheme 4-4 Schematic representation of Schiff base formation between PVP ALD and a lysine residue on BSA, and subsequent reduction to a secondary amine.

PVP ALD T5_H7_S10 (0.094 g, 9.27×10^{-6} mol) was dissolved in 0.1 M PBS buffer at 37 °C. Bovine serum albumin (BSA) (0.30 g, 4.68×10^{-6} mol) was sprinkled onto 0.1 M PBS buffer and allowed to dissolve slowly taking care to avoid bubbles before being added to the solution of PVP ALD in PBS. After an hour $NaCNBH_3$ (0.25 M) was

added to reduce the Schiff base. This method was used for all other Schiff base reactions, unless specified otherwise (table 4.6).

4.4 Results and discussion

4.4.1 Chain end analysis of PVP

4.4.1.1 Gradient HPLC (G HPLC)

Gradient high performance liquid chromatography (GHPLC) coupled to an ELSD detector may not be used on its own to determine the end group composition of chain end functionalized PVP, but it has been shown to be useful in a comparative manner in combination with ^{1}H NMR analysis. The reported critical conditions for the separation of linear PVP topologies with xanthate end groups from their products of aminolysis and hydrolysis was used for our multi functional topologies[2].

The separation of linear topologies from multifunctional topologies by liquid chromatographic means in SEC mode is complicated by the fact that this technique separates on the basis of hydrodynamic volume. Multifunctional molecules may occupy the same hydrodynamic volume as linear molecules but have vastly different molecular topologies and molar masses. However we were still hopeful that because in GHPLC, close to critical conditions, separation would occurs based on chemical composition and that it would be possible to separate the xanthate moiety from chain end modified versions.

The gradient profile started with a water:acetonitrile volume ratio of 80:20 and the acetonitrile content was gradually increased over 30 minutes to 65:35.

In figure 4-1 the GHPLC elution profile of the xanthate, aminolysis and hydrolysis products are compared, it appears as if there were two main elution profiles at the same elution time irrelevant of post polymerization treatment. This observation does not bring us any closer to chain end identification as was seen with linear PVP molecules were the different chain ends eluted at different times. This either indicates that this technique is not suitable to separate star molecules according to

the nature of their functional endgroups, or that different conditions are required for the separation as compared to the linear polymers.

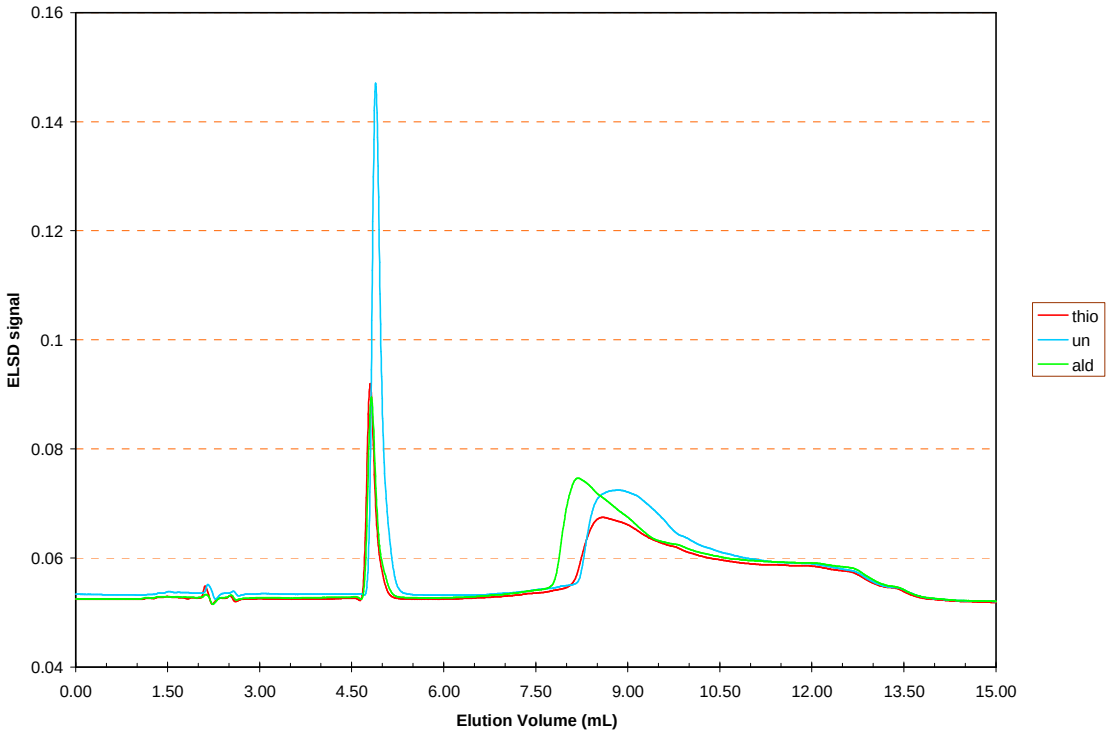

Figure 4-1: GHPLC elution profile of PVP (T5) in all three functionalities.

In figure 4-2 the signal of the elution profiles indicates that only the PVP SH does not have absorption at the second elution profile at 25 minutes, which would indicate that this is the UV absorption of the xanthate chain end indicating the presence of non functionalized chain ends in the hydrolysis sample.

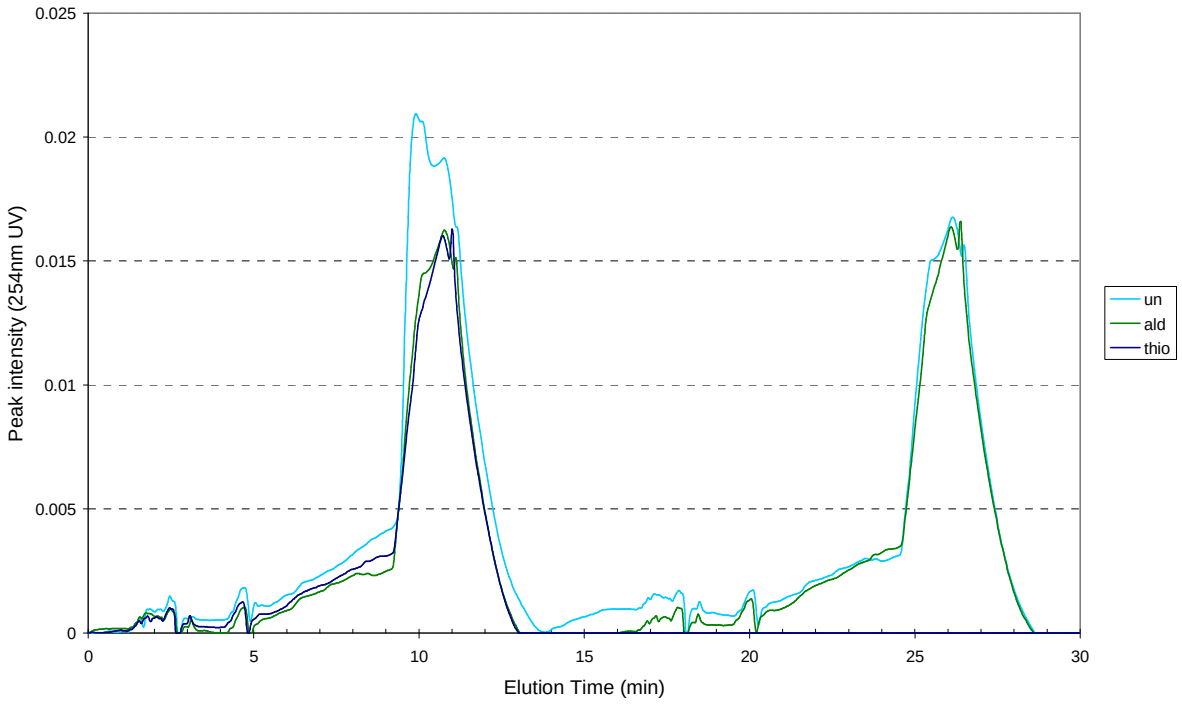

Figure 4-2: UV elution profile of PVP (T5) all three functionalities.

4.4.1.2 HPLC MS

Gradient high pressure liquid chromatography coupled to mass spectroscopic analysis was used for chain end identification of 4 arm star molecules as G HPLC on its own was inconclusive and matrix assisted laser desorption ionization time of flight mass spectroscopy (MALDI-ToF) was unsuccessful.

The previously determined G HPLC method was transferred to the MS setup. The total molar mass of the polymer is on the border of the measurable range of this system, but some valuable information was still obtained from the isotope distribution patterns observed with this method. The theoretically possible chain end moieties and the atomic loss during modification are summarized in scheme 4.5 and table 4.2.

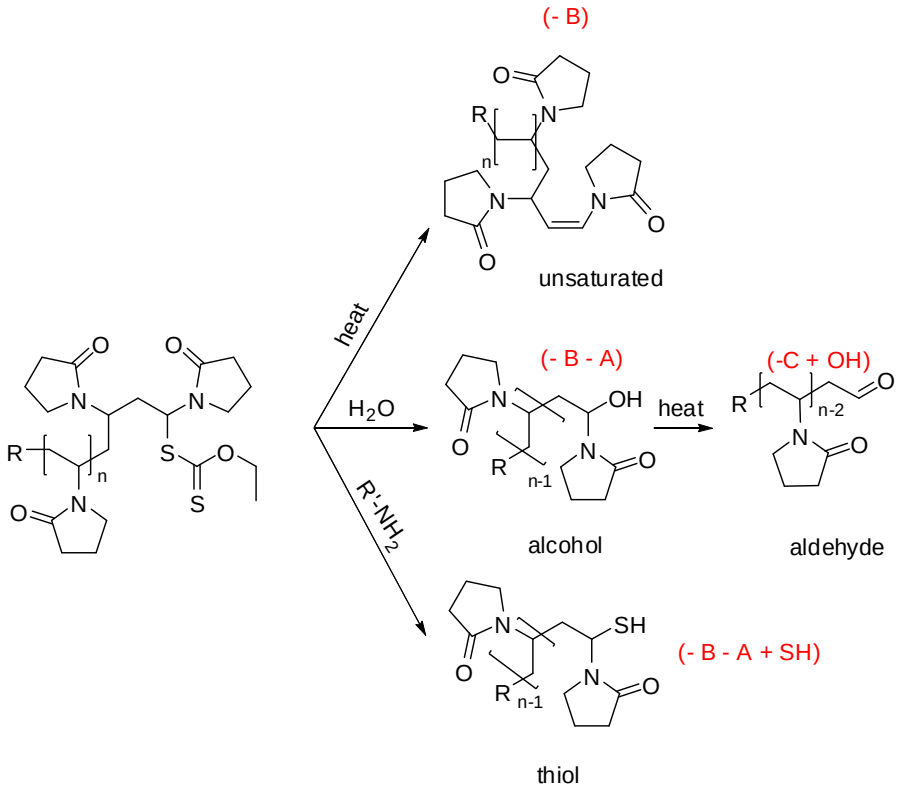

Scheme 4-5: Chain end modification scenario schematic[3]

Table 4-2 Theoretical atomic and molar mass changes with chain end modification

A	Repeating unit	C6H9NO	111 g/mol
B	Xanthate end	C3H5OS2	120 g/mol
C	OH chain end	C6H10NO2	128 g/mol

The chain end moiety modification and consequent loss in molar mass was observed successfully with this analysis technique and the molar mass changes matched the theoretical values (table 4.2) very well, data are summarized in table 4.3.

Table 4-3: Experimental HPLC MS data of PVP 34_3

Chain end functionality	PVP (xanthate)	PVP ALD	PVP SH	Average molar mass change from 1281 g/mol	Molar mass change in atoms from 1281 g/mol
Xanthate	1281.40	/	/	/	/
Unsaturated	1156.97	1156.93	1156	124.77	- C3H5OS2
Alcohol	1045.66	1045.66	1045.66	235.74	-C6H9NO -C3H5OS2
Aldehyde	/	934.58	934.59	111.07	- C6H10NO2 +OH
Thiol	/	/	1059.07	222.33	- C6H9NO -C3H5OS2 +SH

In table 4.3 it is shown that experimental values match very well with the theoretically predicted values in table 4.2 for the three PVP chain end scenarios (non functionalized, thiol functionalized and aldehyde functionalized).

Each sample although being exposed to different experimental variables contained unsaturated chain ends. This was expected as the loss of the xanthate chain end functionality through thermolysis to form unsaturated chain ends is inevitable, but the degree can be controlled by careful sample preparation and storage.

The alcohol chain end functionalized PVP was also observed in all three sample preparation methods. The presence of this can easily be explained as the loss of xanthate chain ends through hydrolysis. The presence of the aldehyde moiety is consequently also explained (see scheme 4-3).

The thiol chains ends however are only present in the sample that underwent aminolysis.

4.4.2 Thiol PVP results

Aminolysis and Michael addition experimental data and results are summarized in table 4.4. The $\times$ indicate that a gel was not formed and the $\surd$ that a hydrogel was successfully formed. The ratio mentioned in table 4.4 was based on equation 4.3.

$$\text{Ratio} = \frac{\text{Mol PVPSH}_{M_n\,^1HNMR}}{\text{Mol CROSSLINKER}} \times \frac{\text{Number Arms PVP}}{\text{Number Acrylate groups}} \qquad (4.3)$$

Table 4-4: Experimental data summary of Michael addition reactions

	Exp Ref	% Thiol	PVP SH Mass (g)	PVP SH n (mol)	PEG DiAc mass (g)	PEG DiAc n (mol)	TEA mass (g)	TEA n (mol)	Molar ratio Thiol: Acrylate	DTT mass (g)	DTT n (mol)		Gel
A	T1_A2_M1	21	1.73	1.62×10^{-4}	0.14	9.59×10^{-5}			3.38				×
B	T2_A3_M2	28	1.42	1.49×10^{-4}	0.20	1.34×10^{-4}			2.23				×
C	T3_A4_M3	31	1.62	1.55×10^{-4}	0.47	3.12×10^{-4}			0.99				×
D	T6_A5_M4	44	0.21	4.78×10^{-5}	0.06	4.24×10^{-5}			1.78	0.0045	2.92×10^{-5}	16h00min	√
E	T7_A6_M5	64	0.23	2.21×10^{-5}	0.03	2.15×10^{-5}			1.95	0.0035	2.27×10^{-5}	16h00min	√
F	T6_A5_M6	44	0.06	1.32×10^{-5}	0.01	7.60×10^{-6}			1.15			1h44min	√
G	T6_A5_M7	44	0.05	1.03×10^{-5}	0.01	7.60×10^{-6}			0.80			16h55min	√
H	T6_A5_M8	44	1.59	3.59×10^{-4}	0.06	3.91×10^{-5}	0.1108	3.15×10^{-4}	1.63			16min	√
I	T9_A9_M9		1.55	4.74×10^{-4}	2.29	1.53×10^{-3}			0.62	excess		5min	√

Observations from Table 4.4:

A-C. The solution became milky after mixing, but no gels were formed, thus indicating that a 21-31 % (1.2 arms) thiol functionalization was insufficient for hydrogel formation via the Michael addition reaction.

D&E. The phosphate buffer solution used was pH 7.4 and temperature of 37 °C. A small amount of DTT was added to break disulphide bonds prior to the addition of the DIAC PEG. As DTT has been used as a crosslinker agent with multi arm PEG acrylate[4] it could be possible that instead of acting as just a reducing agent that it also acted as a secondary thiol nucleophile Michael donor molecule. This competitive situation could have resulted in a slowing of the overall hydrogel formation.

F&G. The phosphate buffer solution used was pH 7.6 and no DTT was added to the PVP SH to break disulphide bridges. The only variable in this experiment was the molar ratio of reactants being just higher and lower than unity. In F the mixture was extremely viscous and gel like after 1 h 10 min, but only completely gelled after 1 h 45 min a gel has formed as detemined by the sample inversion method. G was also very viscous after the same amount of time but only partially gelled according to the sample inversion method.

H. The phosphate buffer solution pH used was pH 7.5. The polymer was not reduced with DTT. Two different topology crosslinkers were added, TEA (4) and DIAC PEG (2), but the total molar ratio of acrylate:thiol was the same as in previous experiments. Solid segments appeared after 16 minutes, but macroscopic gel formation was only confirmed after 16 hours at 37 °C according to the sample inversion method.

I. A completely oxygen free synthetic method was employed. The reaction turned dark yellow and a precipitation of gel like segments formed directly after the addition of DIAC PEG. It was impossible to prepare a ^{1}H NMR sample as the sample did not

dissolve, but only swelled in the deuterated solvent. Once dried to a constant mass, a dark brown transparent solid was obtained.

4.4.2.1 Conclusion PVP PEG hydrogels

A thiol conversion according to Ellman's Test of larger than 40% (1.6 arms) was required to obtain a PVP PEG hydrogel.

The molar ratio of acrylate: thiol (T6_A5) directly affected the rate of hydrogel formation as was seen in comparing M6-8 (table 4.4)

4.4.3 Hydrolysis and Schiff base formation

In table 4.5 the hydrolysis experimental procedures and results are summarized. The fractions of functional chain ends were determined via equation 4.1.

Table 4-5: A summary of the reaction and the resulting aldehyde conversion as determined via 1H NMR.

Exp Ref	Mass PVP (g)	Mol	Fraction of functional chain ends
D1_H1	2.01	2.90×10^{-4}	0.68
D2_H2	2.01	9.16×10^{-5}	0.88
D3_H3	2.03	3.64×10^{-4}	0.58
D4_H4	2.04	1.07×10^{-4}	0.44
T1_H5	0.10	9.71×10^{-6}	0.38
T4_H6	6.59	6.50×10^{-4}	0.56
T5_H7	5.83	4.59×10^{-4}	0.50
T8_H8	7.75	7.55×10^{-4}	0.38
T10_H9	2.98	1.43×10^{-4}	1.00
T11_H10	1.00	3.57×10^{-4}	1.00
T12_H11	1.00	5.24×10^{-4}	0.85
T13_H12	3.74	5.66×10^{-4}	0.81
T14_H13	2.00	2.13×10^{-4}	0.82
M1_H14	1.07	3.57×10^{-4}	0.32

$$\text{Fraction of Functional ends} = \frac{\text{Aldehyde} + \text{Alcohol}}{\text{Unsaturated} + \text{Aldehyde} + \text{Alcohol}} \quad (4.4)$$

$$\text{Fraction of Functional ends} = \frac{A_{\delta_{9.5}} + A_{\delta_{6.0}}}{A_{\delta_{7.0-6.8}} + A_{\delta_{9.5}} + A_{\delta_{6.0}}}$$

The reference integration of the repeat unit ($\delta_{4.0-3.5}$) was set as equal to 100

The results of the Schiff base reaction are summarized in table 4.6. The pH, molar ratios and different crosslinking topologies were varied to assess their influence on this reaction. The molar ratio of amine:aldehyde as referred to in table 4.6 was determined via equation 4.5.

$$\text{Ratio} = \frac{\text{Mol PVPALD}_{M_n\ ^1HNMR}}{\text{Mol CROSSLINKER}} \times \frac{\text{Number Arms PVP}}{\text{Number Amine groups}} \quad (4.5)$$

Table 4-6: Data summary of Schiff base crosslinking reactions

	Experiment Reference	Amine	pH	Ratio	Gel
a	(D1_H1+D2_H2+D3_H3+D4_H4) _S1	Lysozyme, BSA	6.2	2.9	√
b	T5_H7_S2	BSA	6.0	0.7	√
c	T4_H6_S3	BSA	6.0	0.1	√
d	D2_H2_S4	Lysozyme	5.4	0.7	√
e	T1_H5_S5; T5_H7_S6; T5_H7_S7; T5_H7_S8	Bis-(2amino ethyl)amine	6.1	0.06;0.02; 0.02; 4.5	x
f	T5_H7_S9	Egg white	6.0	Excess	√
g	T5_H7_S10; M1_H14_S11; M1_H14_S12; T8_H8_S13	BSA	7.4	0.1;0.6; 0.8; 1.1	√ x x x
h	T5_H7_S14-S17	BSA	4.4;5.4; 7.4; 8.1	0.3	x √ x x
i	T5_H7_S18	Poly(lysine)	7.4	67	x

Observations from Table 4.6:

a. Consisted of difunctional polymer that was crosslinked with bovine serum albumin and lysozyme. After 48 hours the mixture was very viscous but not a gel (less than 1%wt of PVP and BSA in solution). The mixture was then dialyzed for 2days and

freeze dried. The dried white fluffy powder was swollen in pH 6.12 phosphate buffer solution at 37 °C. This resulted in a clear solid gel.

b & c. In both these cases no reducing agent was used. After 18 hours sample appears solid. The solid gel material was dried to a stable mass in the oven at 40 °C before swelling studies were performed.

d. Consisted of difunctional polymer (D2_H2_S4) with Lysozyme in pH 5.4 phosphate buffer solution. After 24 hours, the mixture appeared viscous but not a gel. The mixture was freeze dried. The dried white powder (0.20 g) was swollen in 0.4 mL of pH 6.12 phosphate buffer solution. The mixture appeared solid after 4 days at 40 °C. The solid disk was removed from the polytop container and dried to constant mass in an oven at 40 °C under reduced pressure for 16 hours before swelling studies were performed.

e. No gels formed, using the difunctional crosslinker and 4 arm star PVP at pH 6.0 This did not change when the molar ratios of reagents or the temperature was varied. Solid segments did form in viscous liquid, but the mixtures remained turbid and on tipping over a layer remained behind.

f. The PVPALD was added directly to the egg white and the egg kept at 37 °C. A gel formed within an hour. Xanthate functionalized PVP was added to freeze dried egg white and no hydrogel was formed, confirming that this was indeed Schiff base formation and not an artefact.

g. Hydrogel was successfully formed using T5_H7_S10 after 3 days at 37 °C. None of the other experiments at the same pH with different PVPALD samples were successful. This indicated clearly the effect of the fraction of functional chain ends on the Schiff base reaction.

h. In this experiment only the pH was varied.

- pH 4.4 there was no gel, BSA appeared un-dissolved and dry

- pH 5.4 a turbid gel was formed after 16 hours
- pH 7.4 the mixture was very viscous but not a gel at 32hours
- pH 8.0 the mixture seemed to contain solid segments (chunky) and appears wet

i. An experiment was designed to investigate the possible influence of a large excess of primary amines relative to aldehydes on the formation of primary cycles or non idealities. The mixture did not gel after 2 days. The viscous solution was allowed to dry on a clean dry flat surface (in air at room temperature) before swelling studies and fluorescence microscopy were performed on it.

T5_H7_S2

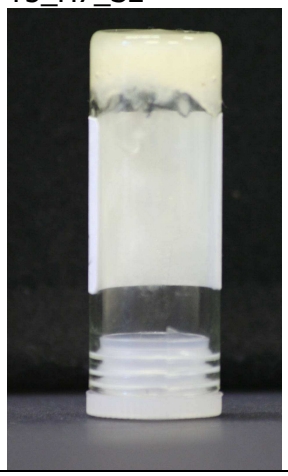

(D1_H1+D2_H2+D3_H3+D4_H4)_S1

T5_H7_S15

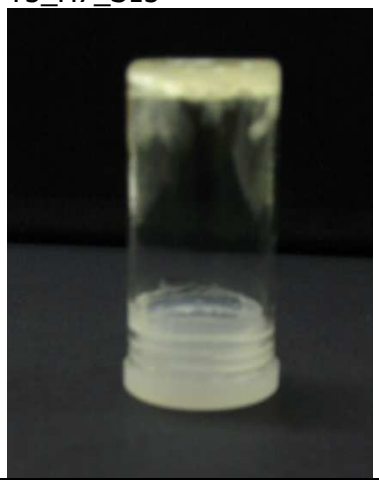

T5_H7_S11

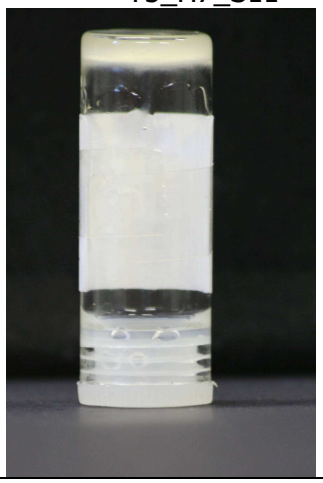

T5_H7_S10

Image 4-1: Pictures of hydrogels referred to in Table 4.5

4.4.3.1 Conclusion Schiff base hydrogels:

PVPALD systems that performed the best in hydrogel formation needed a fraction of functional chain ends of at least 0.88 (88% of 2 = 1.8 arms) for the difunctional PVP and 0.50 (50% of 4 = 2.0 arms) for the 4-arm star PVP. To obtain hydrogels, an average PVP functionality of two was required for crosslinkers of 7 (lysozyme) or more functionalities (60 lysine residues on BSA). Crosslinker molecules with a larger amount of functionalities outperformed crosslinkers of small functionality (2), irrelevant of which PVPALD was used.

The optimal pH for Schiff base covalent bond formation was shown to be pH 5.4-6.4. The molar ratio played an important role in gelling efficacy. An optimum amine:aldehyde molar ratio of between 0.7-1.0 was observed.

4.5 Swelling Studies

4.5.1 Equilibrium swelling experiments:

Equilibrium swelling experiments were used to determine the structural characteristics (see equations 4.6 - 4.11) of the hydrogels obtained via Michael addition (PVP-PEG) or via Schiff base formation (PVP-Amine). The volumes directly after crosslinking V_{CR}, dried to a constant mass V_D and swollen for 24 hours in PBS V_S (table 4.7) were determined sequentially by measuring the displaced volume of these hydrogels in a non solvent (ethanol).

$$u_{2,cr} = \frac{V_d}{V_{cr}} \tag{4.6}$$

$$u_{2,s} = \frac{V_d}{V_s} \tag{4.7}$$

$$\frac{1}{M_c} = \frac{2}{M_n} - \frac{\left(\frac{\bar{u}}{V_1}\right)\left\{\ln(1-u_{2,s}+u_{2,s}+\chi u_{2,s}^2\right\}}{u_{2,r}\left\{\left(\frac{u_{2,s}}{u_{2,cr}}\right)^{\frac{1}{3}} - \frac{1}{2}\left(\frac{u_{2,s}}{u_{2,cr}}\right)\right\}} \tag{4.8}$$

$$\text{n} = \text{bonds between crosslinks} = \frac{\overline{3M_c}}{M_r} \tag{4.9}$$

$$\alpha_s = u_{2,s}^{-\frac{1}{3}} \tag{4.10}$$

$$\xi = \alpha_s\left(C_n n l^2\right)^{\frac{1}{2}} = \text{Average Mesh size} \tag{4.11}$$

Table 4-7: Summary of constants5, 6 for PVP as used in equation 4.6-4.11

Universal constants for PVP			
ū	specific volume of monomer	0.962	mL/g
V_1	molar volume of water	18.100	mL/mol
χ	polymer-solvent interaction parameter	0.490	
C_n	characteristic ratio of polymer	2.000	
l	bond length of gel's polymeric backbone	1.530	A
M_r	molecular weight of repeat unit	111.14	g/mol
d_p	density of the polymer	1.160	g/mL
v_1	specific volume of water	1.006	mL/g
Experimentally determined			
V_d	Volume of the dry hydrogel		
V_{cr}	Volume of the hydrogel directly after crosslinking		
V_s	Volume of the hydrogel after equilibrium swelling (24hrs)		
ξ	Average mesh size (Angstrom)		
M_c	Molar mass between crosslinks		

4.5.2 Equilibrium Swelling

After the equilibrium swelling experiments, the hydrogels were dried to constant mass under reduced pressure at 60 °C overnight. The dry gel was then weighed (W_o) and placed in large excess of buffer at pH 7.4, 37 °C. The hydrogels were weighed at set time intervals (W_t). The wet hydrogels were gently patted dry with filter paper to remove excess moisture before being weighed. From these values and by using equation 4.12 the swelling for each hydrogel could be tracked over time. The data was summarized in figures 4-3 & 4-4.

$$\%Swelling = \frac{W_t - W_o}{W_o} \times 100 \qquad (4.12)$$

4.5.3 Swelling Results

4.5.3.1 PVP Aldehyde

The results of structural characteristics as determined by equation 4.3 of the most successful non reduced Schiff base hydrogels are summarized in Table 4.8. As T5_H7_S2 has a larger molar mass than T4_H6_S3 larger molar mass between crosslinks were expected, this was confirmed by swelling calculations. From the swelling calculations a pore size was estimated in angstrom and this value was seen to be tunable by varying the initial molar mass of the 4 arm star used.

Table 4-8: Structural characteristic summary of 4 arm star PVP-BSA hydrogels

	T5_H7_S2	T4_H6_S3
Arms	4	4
M_n (g/mol)	12687	10139
X-link M_W BSA (g/mol)	64000	64000
M_c (g/mol)	6214	5042
Aldehyde: Amine K=60	0.7	0.1
ξ (Å)	136	119
n	168	136

The swelling of imine and amine crosslinked hydrogels was measured over time in a large excess of PBS. The data is summarized in figure 4.3. Reducing the Schiff base hydrogels was seen to directly affect their degradation profile.

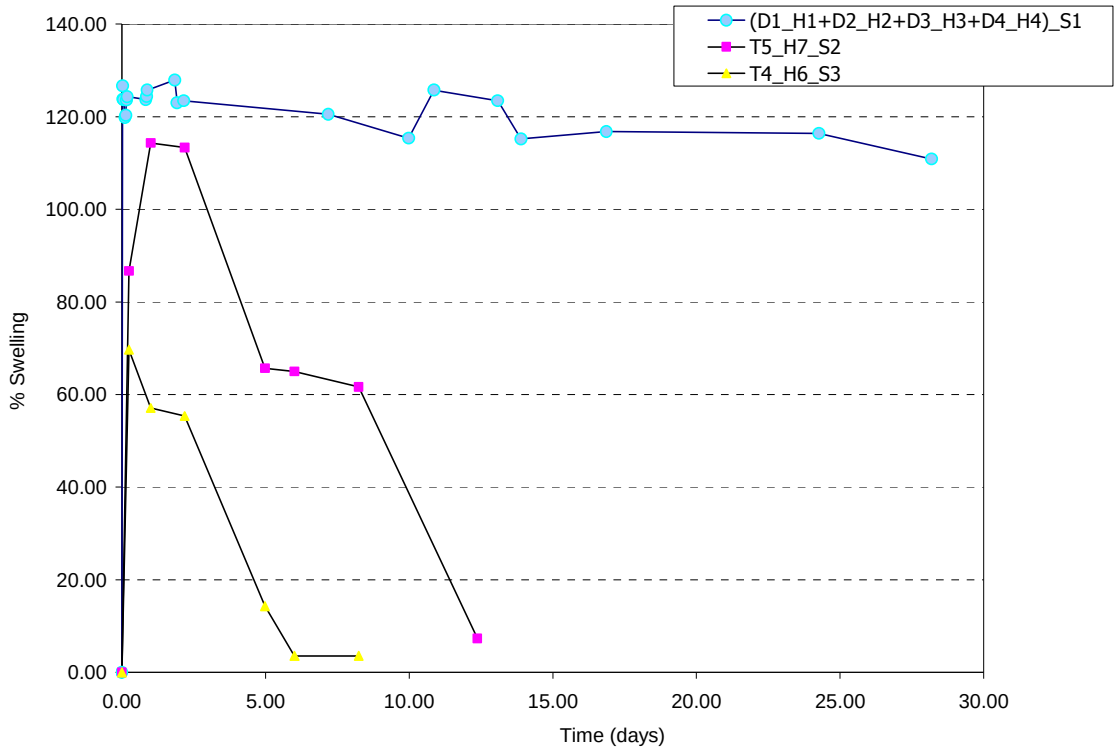

Figure 4-3: % Swelling of PVP BSA reduced vs non reduced hydrogels over time at pH 7.4 37 °C

4.5.3.2 PVP Thiol

The structural characteristics of PVP PEG hydrogels as determined by equation 4.6-4.11 is summarized in table 4.9.

Table 4-9: Structural characteristic summary of 4 arm star PVP-PEG hydrogels

Sample	T6_A5_M7	T6_A5_M6	T6_A5_M4	T7_A6_M5	T6_A5_M8
M_n (g/mol)	4433	4433	4433	10187	4433
X-link M_W di (g/mol)	1500	1500	1500	1500	1500
4 arm star (g/mol)					352
M_c (g/mol)	1891	2121	1335	3648	1390
ξ(Å)	41	38	22	58	41
n	51	57	36	98	38

The swelling over time of PVP PEG hydrogels with varying reagent molar ratios and crosslinking morphologies is summarized in figure 4-4.

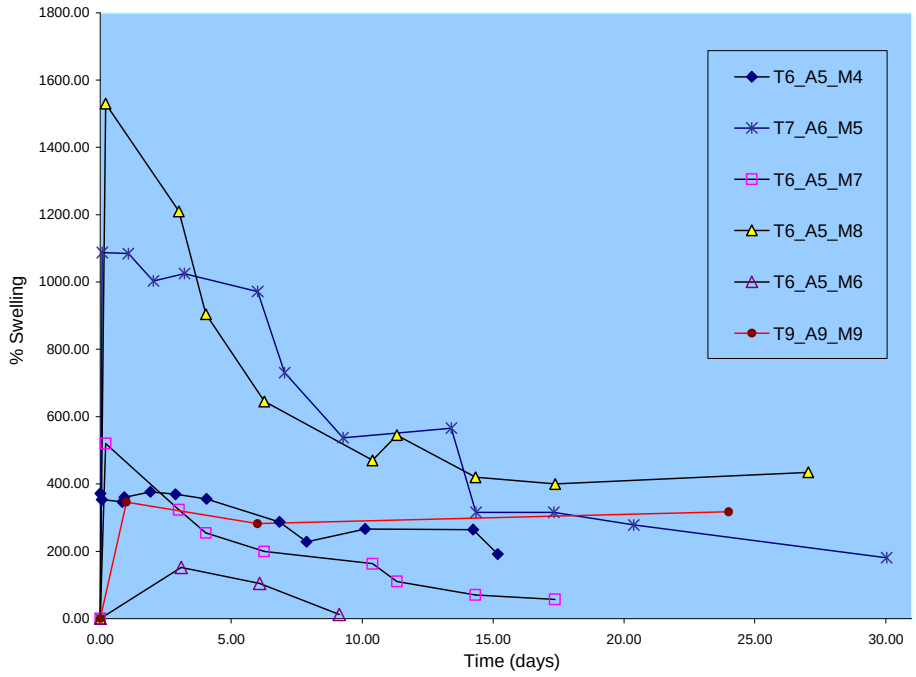

Figure 4-4: The % swelling of PVP PEG hydrogels over time at pH 7.4 PBS 37 °C

4.5.3.3 Conclusions from swelling studies

PVP-BSA non-reduced hydrogels degraded much faster than the reduced hydrogel as is seen in figure 4-3. Also PVP-BSA unreduced hydrogels with a lower stoichiometric ratio of aldehyde : amine, were observed to degrade faster as is seen in figure 4-3.
In PVP PEG hydrogels the stoichiometric ratio of reagents and chain length of the PVP arms influenced the material properties of the hydrogel as seen in figure 4-4.
These experiments indicate that the mechanical characteristics of the synthesized hydrogels were modified through varying the molar ratios of polymers to crosslinkers.

4.6 SEM

A sample of each hydrogel was freeze-dried, resulting in a soft fluffy powder. The SEM samples were prepared by coating a small piece of double sided tape on the SEM mount with the hydrogel powder. The mounted sample was then coated with gold before being placed in the SEM cavity.

In Image 4-2 it is clear that both imine crosslinked PVP BSA hydrogels and amine crosslinked PVP BSA hydrogels exhibited porous structures.

The addition of TEA, a crosslinker with a tetra functional topology affected the molecular weight between thioether-crosslinks and also the crosslinking density as was calculated through equilibrium swelling studies (table 4.9). The effects of these changes on the morphology are visualized in image 4-3 sample T6_A5_M8.

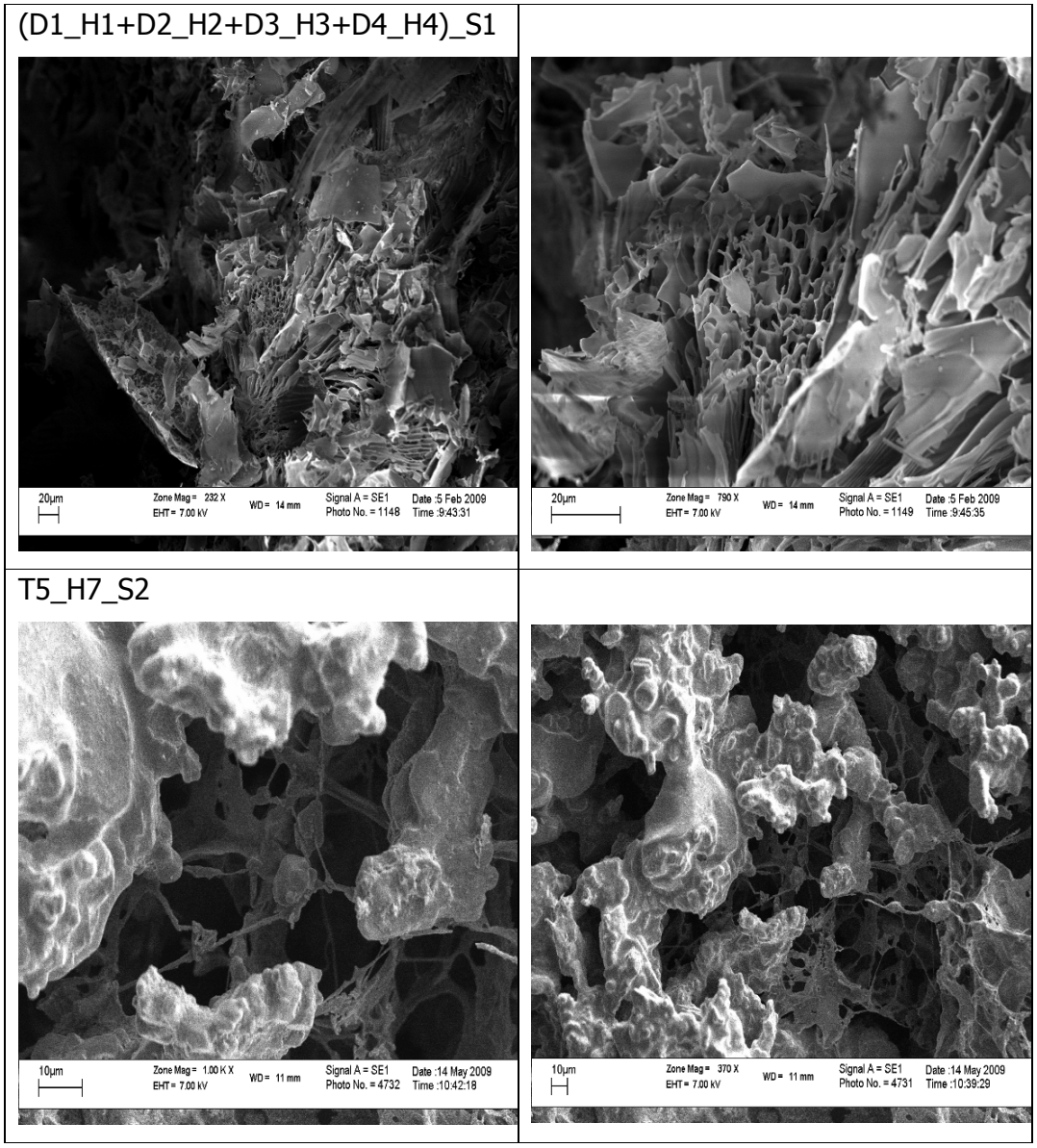

Image 4-2: SEM images of reduced and non reduced PVP-BSA hydrogels.

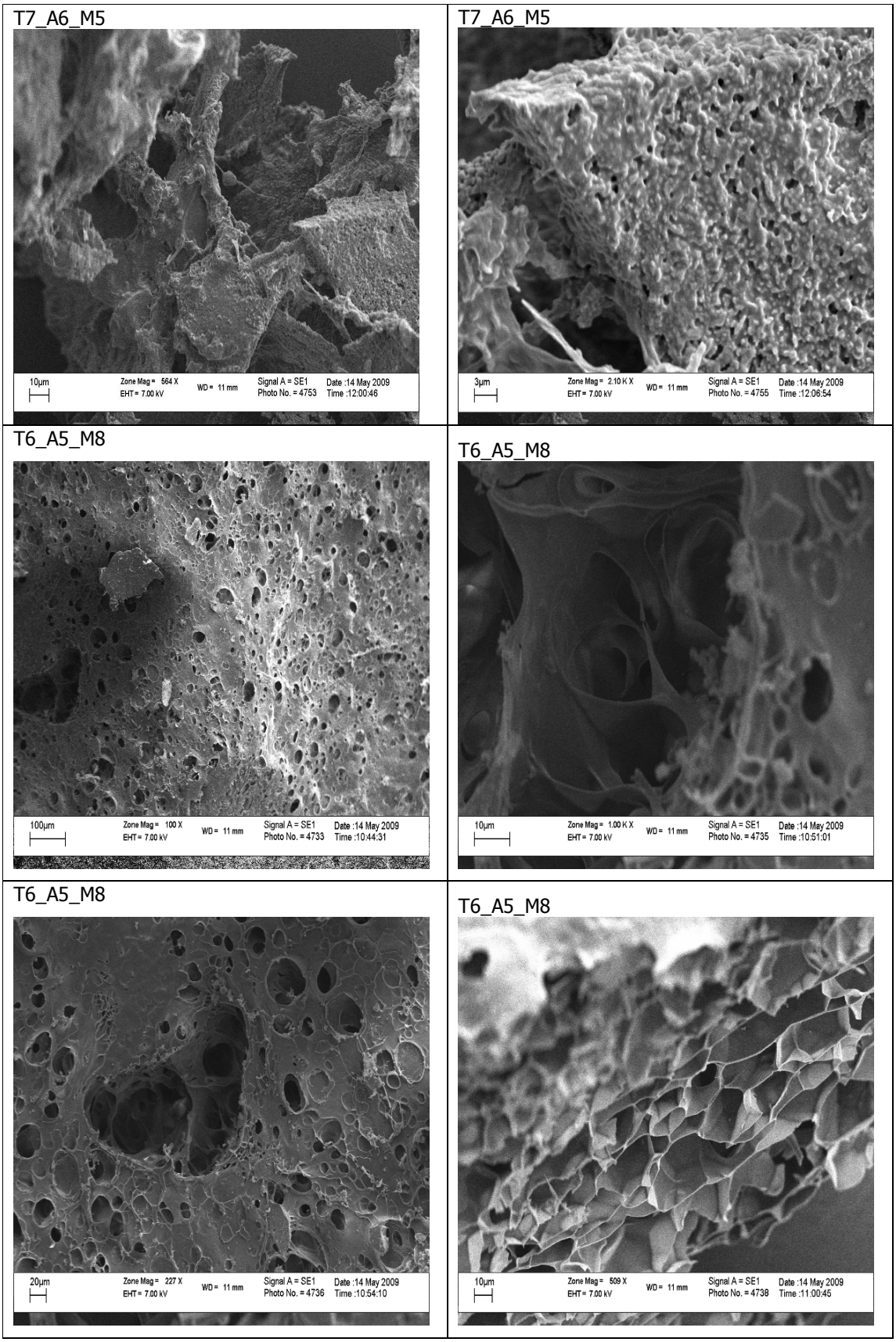

Image 4-3 : SEM images of PVP-PEG hydrogels with varying molar mass between crosslinkings M_c.

4.7 Non idealities

In an ideal hydrogel, the initial mass swelling ratio and ideal mass swelling ratio should be the same. Therefore all the chains connected in a three dimensional network are affected in a cooperative manner and have similar elasticity. By analysis of PVP PEG systems a deviation from expected gelling behaviour was observed (Initial swelling vs. Ideal swelling ratios). This deviation from expected values can be seen in Figure 4.5 based on equations 4.14 & 4.15.

$$Q_m = \frac{W_{\text{initial}}}{W_o} = \text{Mass Swelling Ratio} \qquad (4.14)$$

$$\mathrm{Q}_{\text{m ideal}} = \frac{U}{(Q_m - 1)} \times \mathrm{v}_1 + U \qquad (4.15)$$

The experiments of T6_A5_M4; T6_A5_M6; T6_A5_M7 showed lower than expected $Q_{m\ experimentl}$ vs $Q_{m\ initial}$ ratios. This can be ascribed to the formation of cycles or rather non ideal intramolecular covalent bonds (scheme 4-6). Non ideal networks have less elastically active chains, lower crosslinking density which results in macroscopic hydrogel behavioural changes[4, 7].

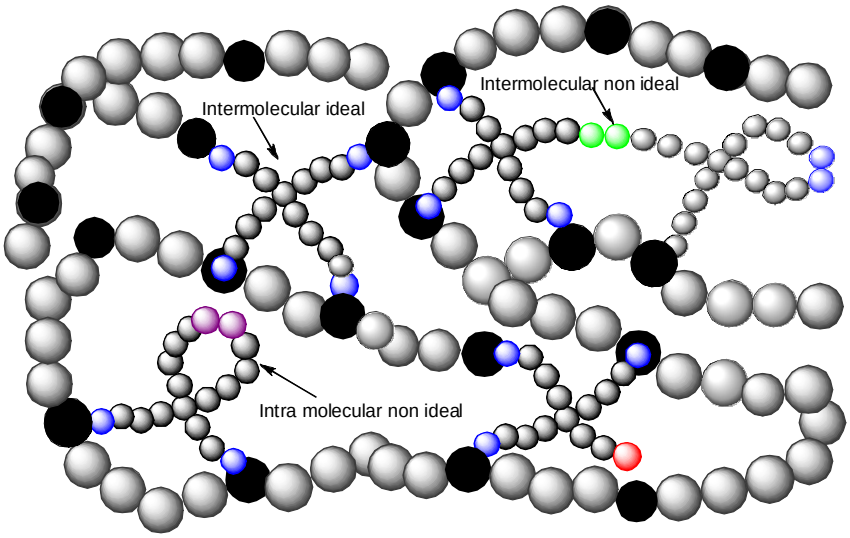

Scheme 4-6 Schematic representation of ideal and non ideal crosslinks

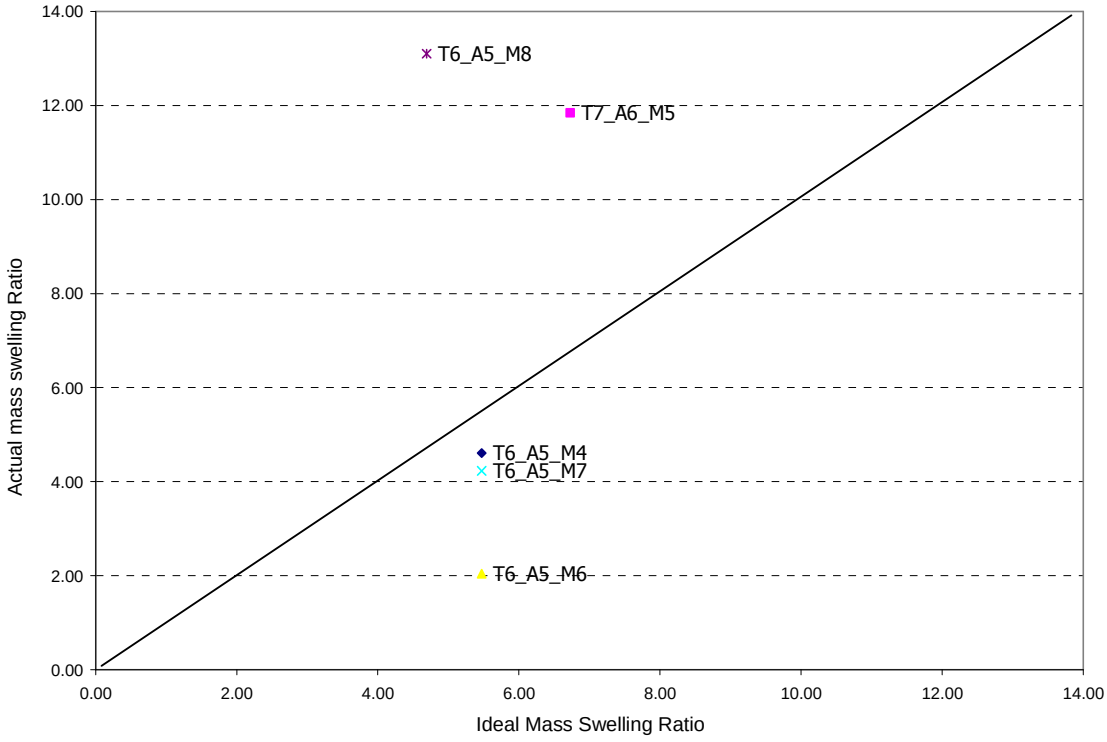

Figure 4-5: Ideal mass swelling ratios vs. experimentally determined initial mass swelling ratios

The $Q_{m\ experimentl}$ vs $Q_{m\ initial}$ ratios of experiments T7_A6_M5 and T6_A5_M8 were observed to be higher than expected (figure 4.5). This would suggest a higher than expected crosslinking density, non ideal intermolecular bonds, which could only arise from the presence of disulphide bridge formation in this case.

An experiment was designed to visually illustrate the presence of non idealities poly(lysine), 0.01% FITC labelled, was reacted with T5_H7. From closer inspection through Fluorescence Microscopy the presence of non idealities are visible as seen in Images 4.4 & 4.5. The globules of intermolecular reactions observed in SEM (100μm) were also observed in Fluorescence microscopy.

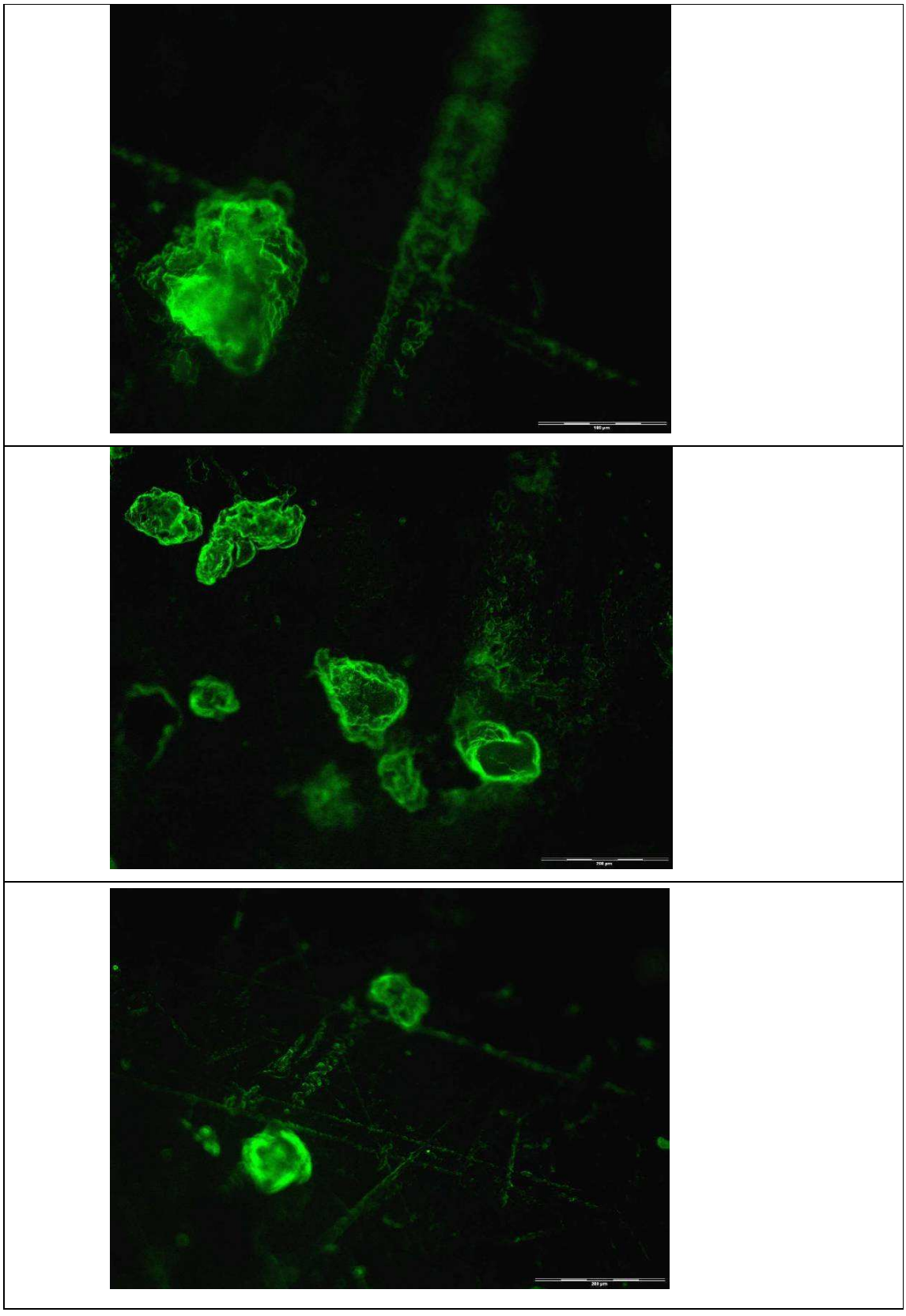

Image 4-4: Fluorescence Microscopy Images of PVP-Lysine

Image 4-5 SEM images of PVP-Lysine

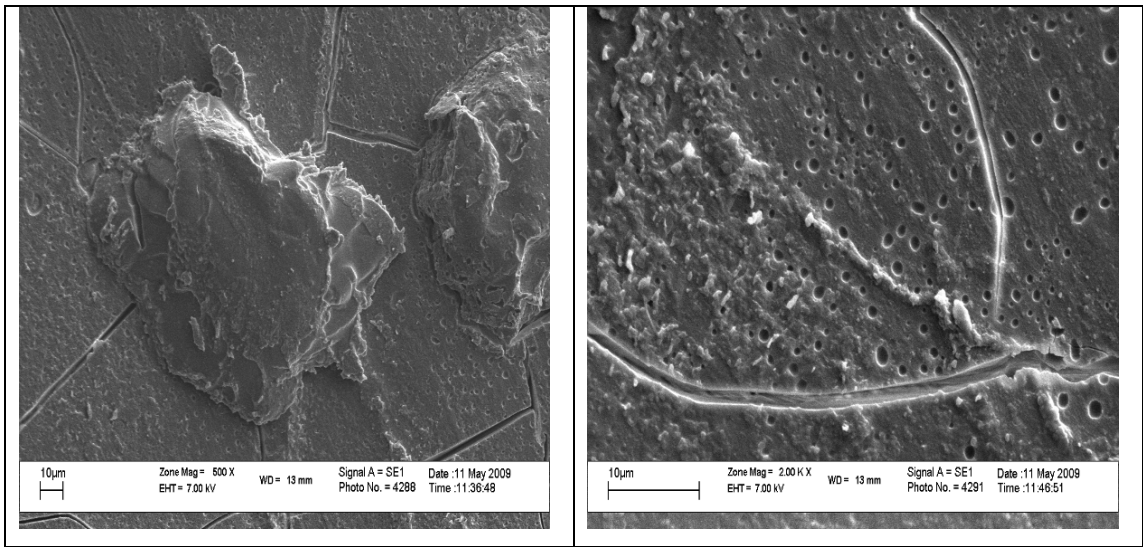

4.8 Conclusions

PVPALD systems that performed the best in hydrogel formation needed a fraction of functional chain ends value of at least 0.88 (1.8 arms) for di functional PVP and 0.50 (2 arms) for 4 arm star systems. Therefore for successful hydrogel formation the average arm distribution should be at least two for crosslinkers with a functionality of seven (lysozyme) or more. This was observed to be true as crosslinker molecules with 7 or more functionalities formed hydrogels and crosslinkers with less functionality (two) did not form hydrogels irrelevant of which PVPALD was used.

The optimal pH for covalent bond formation between PVPALD and primary amines were observed to be between pH 5.4-6.4. The molar ratio played an important role in gelling efficacy, the optimum molar ratio was established to be 0.7-1.0.

Non-reduced imine crosslinked hydrogels degraded much faster than the reduced amine crosslinked hydrogels. Also PVP-BSA imine crosslinked hydrogels with a lower molar ratio of aldehyde : amine, were observed to degrade faster. This indicates that the characteristics of the hydrogel e.g swelling properties and pore size, of the PVP

BSA hydrogels were modified through stoichiometric ratios to obtain variable properties.

PVP SH systems with higher crosslinking efficacy had a thiol conversion according to Ellman's Test of larger than 40%. The molar ratio of reagents and chain length of arms influenced the material properties of the hydrogels. This indicates that the properties of the hydrogel e.g swelling properties and mesh size, of the PVP DIAC hydrogels were modifiable through stoichiometric ratios.

References

1. Ellman, G. L., A colorimetric method for determining low concentrations of mercaptans. *Arch. Biochem. Biophys.* **1958,** 74, 443-450.
2. Pound, G. Reversible Addition Fragmentation Chain Transfer (RAFT) Mediated Polymerization of *N*-Vinylpyrrolidone. Phd, University of Stellenbosch, Stellenbosch, 2007.
3. Pound, G.; McKenzie, J. M.; Lange, R. F. M.; Klumperman, B., Polymer–protein conjugates from x-aldehyde endfunctional poly(N-vinylpyrrolidone) synthesised via xanthate-mediated living radical polymerisation. *Chem. Commun* **2008**, 3193-3195.
4. Metters, A.; Hubbell, J., Network Formation and Degradation Behavior of Hydrogels Formed by Michael-Type Addition Reactions. *Biomacromolecules* **2005,** 6, 290-301.
5. Kaplan, H.; Güner, A., Characterization and Determination of Swelling and Diffusion Characteristics of Poly(N-vinyl-2-pyrrolidone) Hydrogels in Water. *J. Appl. Polym. Sci.* **2000,** 78, 994-1000.
6. Flebbe, T.; Hentschke, R.; Hadicke, E.; Schade, C., Modeling of polyvinylpyrrolidone and polyvinylimidazole in aqueous solution. *Macromol. Theory Simul.* **1998,** 7, 567-577.

5. Kinetics and the bigger picture

For the synthesis of three dimensional networks, the reactants must have an average functionality of more than two[1]. In the present case, networks were formed with end functionalized PVP stars by the formation of covalent bonds with either PVPALD and the primary amine of lysine residues on BSA_{30} or between PVP SH and a DIAC PEG

The rate of the crosslinking reaction of the thiol functional stars was much lower than expected, in the range of hours as opposed to minutes. This determining step could be affected by four factors under our control:

1. effective production of four armed stars. Stars comprising less than four arms may have been formed due to the core first RAFT mediated polymerization method not being efficient
2. human error during synthesis, resulting in loss of xanthate chain end functionality (thermolysis or hydrolysis) and thus a reduced total number of arms available for crosslinking (*n,* less than four)
3. the efficacy of the functionalization reaction consisting in the conversion of the xanthate chain ends to the moiety of choice (thiol or aldehyde)
4. the efficacy of the Michael addition reaction itself with thiol end functional PVP molecules as the nucleophile at physiological pH

In this section we investigated points 1 and 4 of these rate determining factors in depth by performing *in situ* ^{1}H-NMR spectroscopy experiments with experimentally equivalent temperatures and stoichiometric ratios to mimic actual systems.

In this chapter the efficacy of the core first RAFT as selective controlling agent is evaluated as well as the post polymerization Michael addition reaction of PVP SH. Through in depth analysis, it becomes possible to optimize these hydrogels from polymer synthesis through to post polymerization reactions.

5.1 Kinetic study with X_{T2}

In modelling the core first RAFT mediated polymerization it was aimed to investigate initial chain growth from the central core of the RAFT agent. A distribution in topologies would have a definite effect on further applications (scheme 5.1). The modelling of core first RAFT mediated polymerizations is a complex task as in addition to the normal reactions applicable to linear RAFT mediated polymerizations the arms also have to be incorporated in the kinetic model.

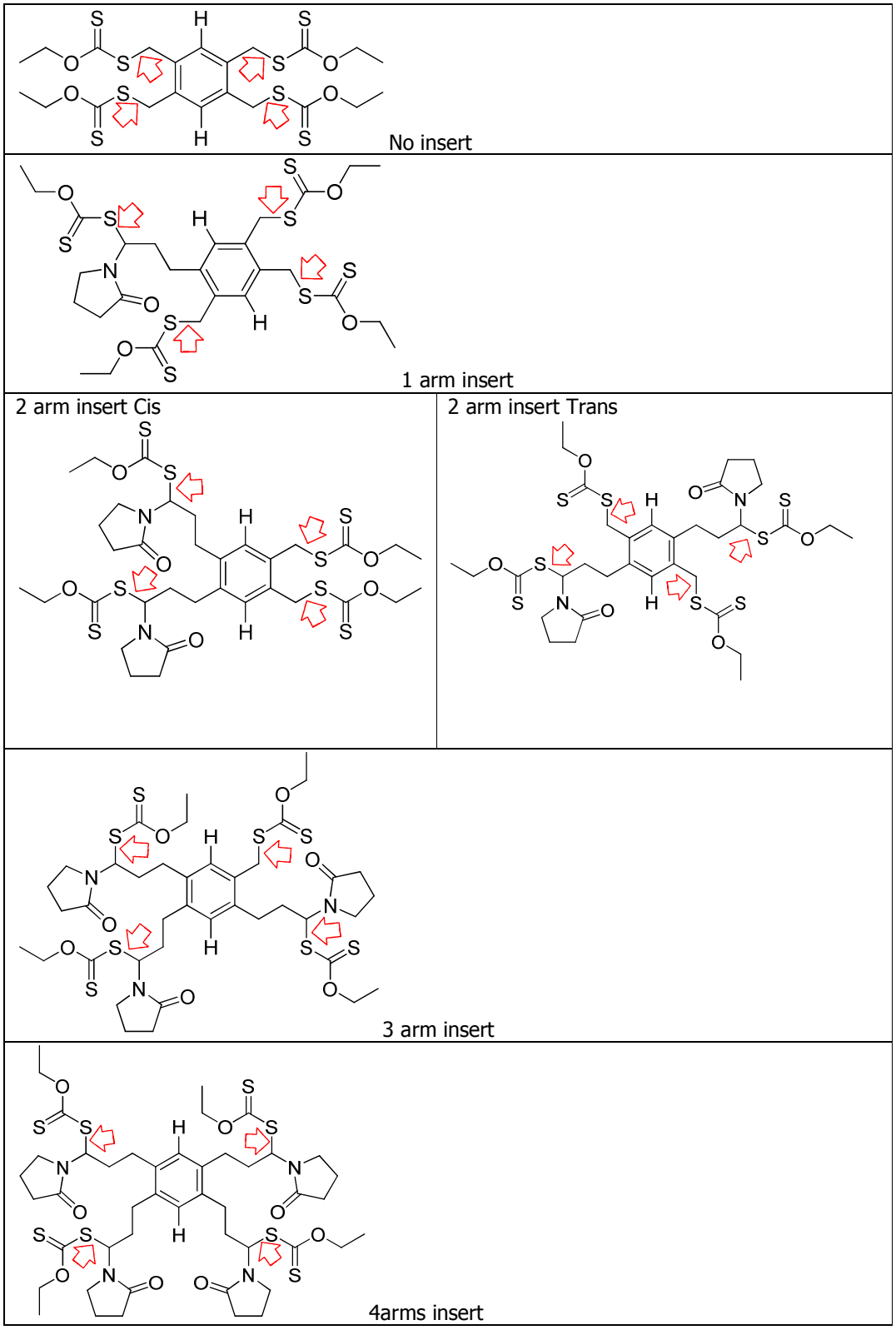

Scheme 5-1: Monomer insertion scenarios

To understand the kinetics of this core first RAFT polymerization it is necessary to understand all of the reactions taking place[2]. Additional to the conventional linear RAFT polymerization radical coupling reactions are also possible:

- between arms in the same star
- between arms in different stars (i.e. between stars)
- between an arm and a linear polymer chain

Of significance in our system are the following coupling reactions:

- between arms of different stars resulting in star-star couplings
- between arms in the same star resulting in cyclic chain
- between a star and a linear chain resulting in a dead arm

All of the above reactions result in the loss of the Z group, limiting the degree of post polymerization functionalizability of the synthesized PVP star.

Another possible issue could be the degradation of the RAFT agent itself, resulting in a macro RAFT agent species which consumes monomer, but does not necessarily produce star topology polymers. This would result in a broadening of the molar mass distribution and the loss of star functionality, which has a snow ball effect on the final material properties of the hydrogel.

Method

In the *in situ* experiment the ratio of AIBN: RAFT: NVP used were 0.8 : 1 : 20 and 0.5 : 1 : 40 respectively. The method of synthesis and the purity of the RAFT agent X_{T2} were discussed in Chapter 3.

The experiment was performed using the following method: AIBN (0.0068 g, 4.1×10^{-5} mol) and the X_{T2} (0.0506 g, 8.2×10^{-5} mol) were weighed and added to NVP (0.3658 g, 3.3×10^{-3} mol),in C_6D_6 (0.4231 g, 5.0×10^{-3} mol) and *N,N*-dimethyl formamide DMF (25 µL = 1.9×10^{-6} g, 2.9×10^{-08} mol) (reference material). The mixture was transferred to a J-young type NMR tube, degassed via four consecutive freeze pump

thaw cycles and filled with ultra high purity argon. The tube was kept cooled to prevent premature initiation during transport to the NMR laboratory.

In situ ^{1}H NMR spectroscopy experiments were carried out on a 600 MHz Varian Unity *Inova* spectrometer. A 5 mm inverse detection PFG probe was used for the experiments and the probe temperature was calibrated using an ethylene glycol sample in the manner suggested by the manufacturer using the method of Van Geet[3, 4]. ^{1}H NMR spectra were acquired with a 3 μs pulse width and a 4 s acquisition time. For the ^{1}H NMR kinetic experiments, samples were 25 °C reference spectrum was collected. The sample was removed from the magnet and the cavity of the magnet was heated to the required temperature of 60 °C. The sample was reinserted and the delay time until start of experiment was recorded. A delay time was experimentally required (approximately 5 minutes) to optimize the system by further shimming at elevated temperature.

Results and discussion:

The integration values were referenced to the known DMF concentration value of 0.32 mol/L. In this manner the concentrations of all the compounds were determined.

The two protons in the benzene ring of the RAFT agent's core provide a look into monomer insertion as each insertion scenario results in a distinct aromatic peak in the range of 7.0-7.2 ppm. The initial singlet at 7.18 ppm (scheme 5-1 no inserts) splits into several singlet peaks between 7.18 - 7.02 ppm upon insertion of one or more monomer units.

Four distinct insertion scenarios were observed after a couple of monomer insertion , the concentration of the initial $C\underline{H}_{Ar}$ X_{T2} were seen to decrease over time. By adding the concentration values of the four insertion scenarios together, the initial $C\underline{H}_{A}$ X_{T2} concentration was obtained *e.g.* **25 + 26 + 27 + 28 = 29** (figure 5-1) This indicated that a very small amount of 0.01 mol/L X_{T2} could have been consumed in the formation of a macro RAFT agent or that it is simply an experimental error.

Table 5-1: 1H NMR integral peak assignment

Shift (ppm)	No of shift
[1.016 - 1.020]	3
[5.20 - 5.25]	14
[5.25 - 5.31]	15
[5.32 - 5.38]	16
[5.52 - 5.58]	17
[5.61 - 5.71]	18
[5.83 - 5.90]	19
[5.90 - 5.95]	20
[6.082- 6.13]	21
[6.72 - 6.79]	22
[6.80 - 6.84]	23
[6.89 - 6.94]	24
[6.96 - 6.99]	25
[7.031 - 7.061]	26
[7.061 - 7.10]	27
[7.12 - 7.16]	28
[7.16 - 7.20]	29

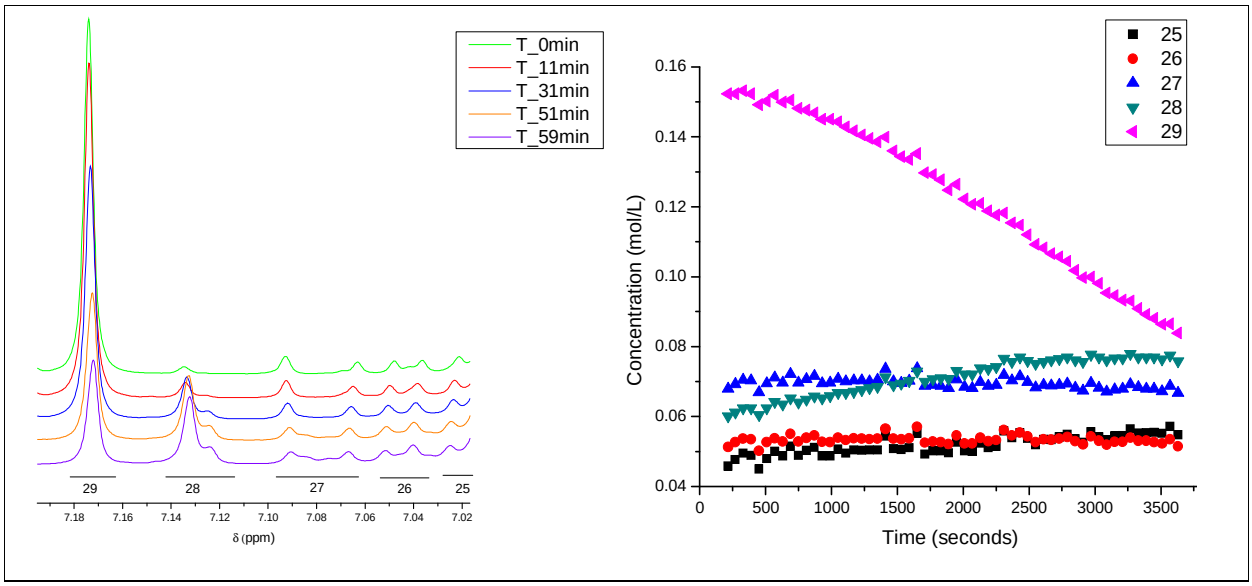

Figure 5-1 The aromatic protons (s, C<u>H</u>, 2H) of the four insertions scenario after the first couple of monomer insertions and corresponding concentration profile.

Peaks corresponding to the first couple of monomer adducts were visible at the following integrations **16** quartet; **18** quartet; **19** multiplet, **20** triplet; **21** doublet (figure 5-2 a). These assignments match those indicated by predictive ^{1}H NMR software and those previously reported[4]

A straight line is expected from the consumed (X_{T2}) concentration profile *vs.* the formed insertion product concentrations. This was not clearly visible from analyzing the CH_{Ar} singlet concentrations of concentrations of consumption *vs.* creation alone. The system had to be analyzed in its entirety including the concentration of the C<u>H</u>S (CHS = (**18+19+20+21**)/4) and the C<u>H</u>$_{Ar}$ (CH_{Ar} = (**28+27+26+25**)/4) see figure 5-2 b. From this we believe that in RAFT mediated polymerization with a core first RAFT agent technique the RAFT agent is consumed simultaneously with the formation of four monomer insertion scenarios.

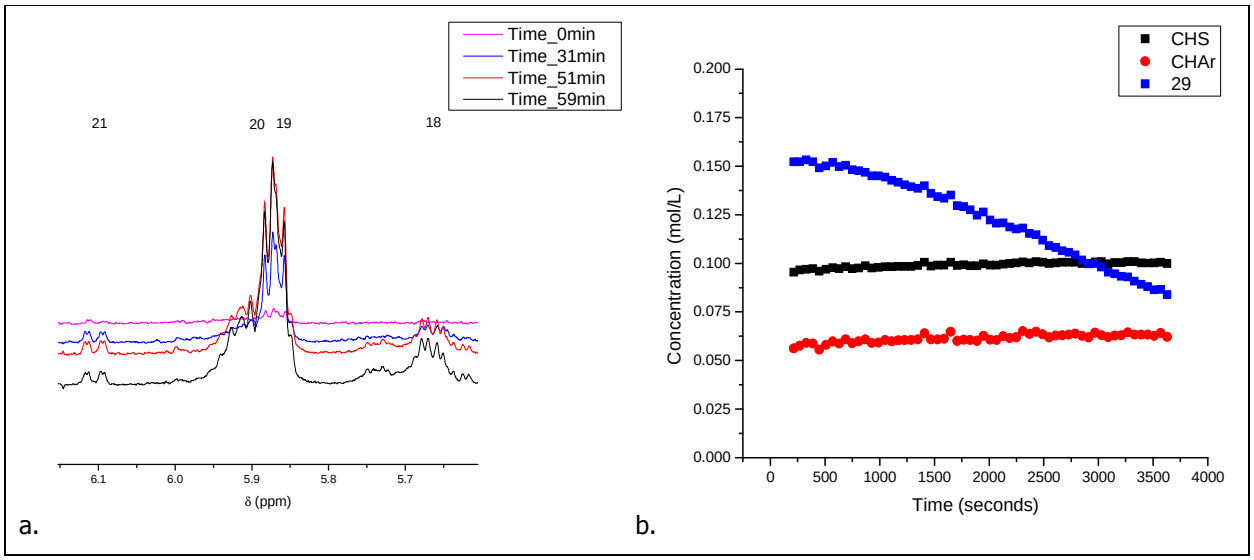

Figure 5-2 The peak assignment and concentration profile of consumed XT2 CHAr protons vs. first couple of monomer adduct CHS & CHAr

Unexpected side reactions involving NVP in RAFT polymerization systems have been reported in a publication by our group[4] and even though strict control was executed over the reaction conditions and reactant purity, hydration products in ratio of protons 2H:6H (figure 5-3) were observed in the present experiment, as previously reported in the polymerization of NVP with mono-functional xanthate RAFT agents[4].

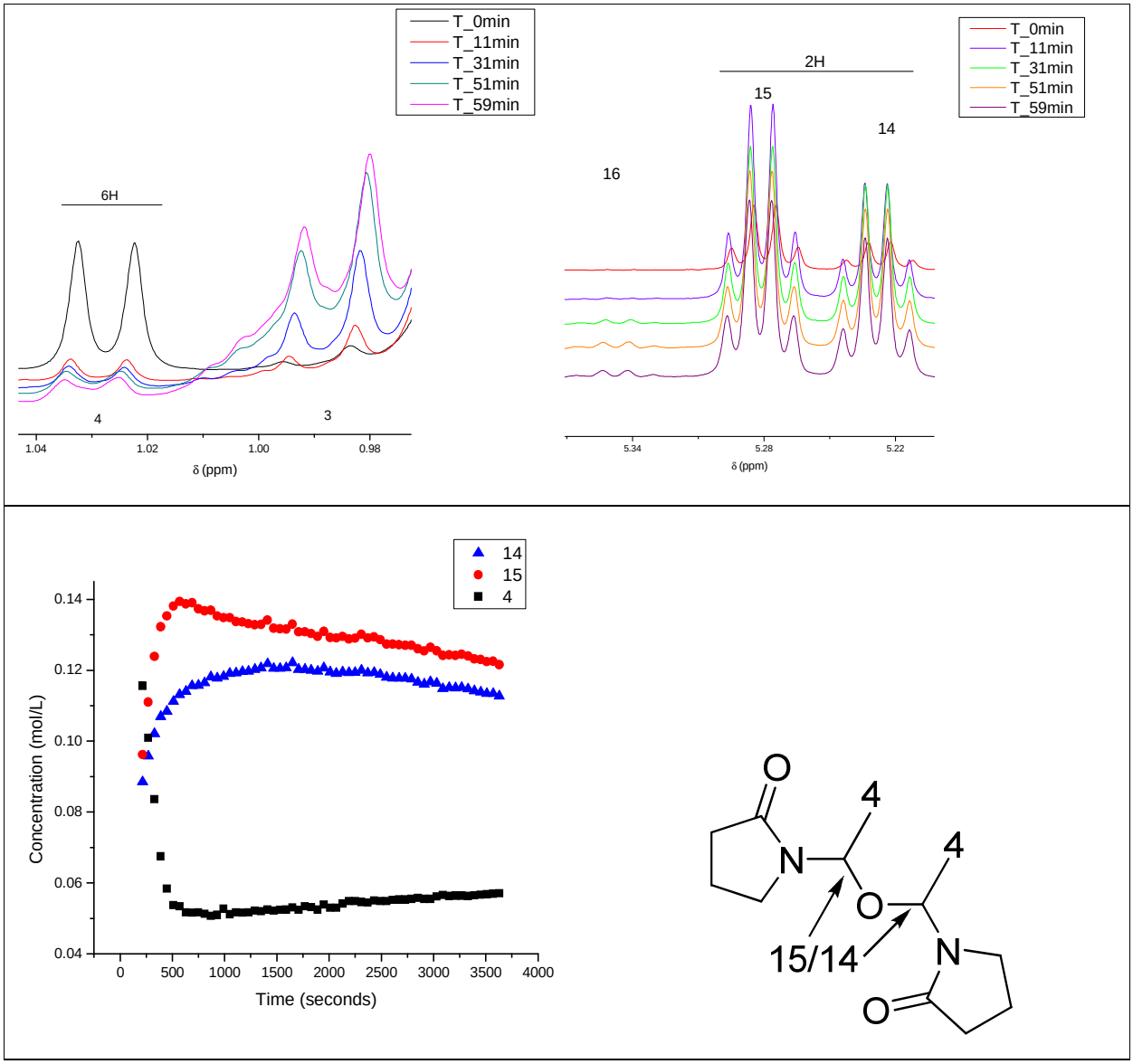

Figure 5-3 The peak assignment and concentration profile of hydration side products

5.2 Geometry optimization and energy calculations with Spartan

Chaffey-Millar et al. constructed a model in PREDICI® to model the molecular weight distribution of the arms during star polymerisation[2]. The model is based on the assumption that polymeric stars with *n* arms can be considered to consist of *n* equivalent sites at which polymer chains can grow. This assumption that all the initial n sites were equivalent was not observed in our experimental ^{1}H NMR spectroscopy

studies. Multiple insertion arm scenarios were observed indicating the presence of 4; 3; 2; 1 first monomer insertion topologies (scheme 5-1). To shed light on these observations the following calculations geometry optimization and energy calculations (of the first monomer insertion structures) were performed with the aid of Spartan 04, on a normal Pentium 4 desktop with computational time ranging from several hours to several days.

Longer bonds will be energetically more favourable to act as insertion points as it requires less energy to break them. The bond length probability was estimated from the table 5-2 by looking at the C-S bond length without rounding off (1st) and then round off to the second decimal (2nd). The results were summarized as 2 x 1 arm; 4 x 2arms; 1 x 3arm; 3 x 4arm.

Table 5-2 Data summary as calculated by the Spartan program

	E(RHF) (kcal/mol)	ΔE	Multiple reactivity *	C-S bond length (Å)				1st	2nd
RAFT	$-2.69\times10^{+6}$	$0.00\times10^{+0}$	1	1.81726	1.81838	1.81686	1.81689	4	
1 arm	$-2.91\times10^{+6}$	$-2.24\times10^{+5}$	1.08	1.81731	1.82623	1.81697	1.81740	1	4
2 $_{arms(cis)}$	$-3.13\times10^{+6}$	$-4.48\times10^{+5}$	1.17	1.83049	1.83081	1.81753	1.81705	2	
2 $_{arms(trans)}$	$-3.13\times10^{+6}$	$-4.48\times10^{+5}$	1.17	1.81777	1.82712	1.81767	1.83148	1	2
3 arms	$-3.36\times10^{+6}$	$-6.72\times10^{+5}$	1.25	1.82670	1.83178	1.83149	1.81789	2	3
4 arms	$-3.58\times10^{+6}$	$-8.97\times10^{+5}$	1.33	1.82640	1.82675	1.83462	1.83146	2	4

* $\Delta E_{arm} / \Delta E_{no\ insert}$

The multiple of reactivity ratio of $\Delta E_{arms}/\Delta E_{no\ insert}$ was calculated for each scenario (1arm; 2arm $_{cis/trans}$; 3arm; 4arm). The multiple of reactivity and the sum of the bond length probability per scenario was multiplied e.g. 1 arm = 1.08×2. These values were visualized as percentages in a pie chart see figure 5-4. To summarize, a distribution in topology of molecules is expected from this RAFT agent and can be arranged in decreasing order of probability 2,4,1,3 arms and was represented schematically in figure 5-4.

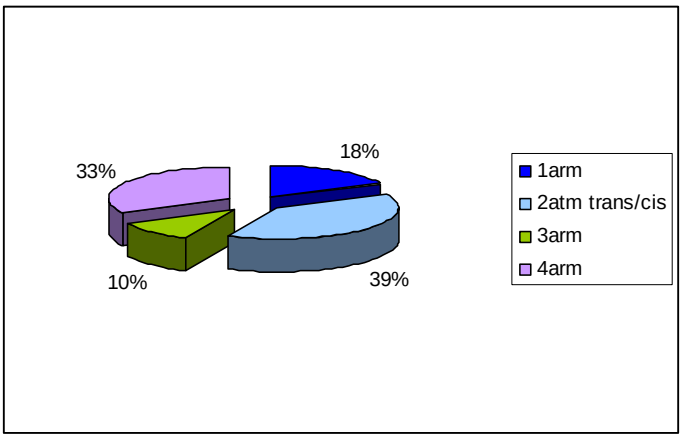

Figure 5-4: Arm distribution percentage

These calculations combined with *in situ* ^{1}H NMR observations indicate possible termination reactions from star kinetics that would result in a loss of chain end functionality through use of core first RAFT polymerization technique. This would have to be compensated for in further reaction steps. To make three dimensional networks the reactants must have an average functionality of more than two[1], we therefore advise that a cross linker with a functionality $n>4$ would be able to compensate for the loss of functionality inherent in the RAFT star polymer. This was already seen to be successful in the higher success rate of crosslinking to $n > 30$ *LYS* functional BSA molecules. The optimization of the polymerization conditions to minimize side reactions *e.g.* low temperature initiating system was also investigated (see chapter 6).

5.3 Michael Addition Reaction kinetics with thiol end functionalized PVP:

The Michael addition, named after Arthur Michael, is a straightforward reaction between nucleophiles and activated olefins or alkynes in which the nucleophile adds across a carbon-carbon multiple bond. Advantages of this crosslinking method are: a general lack of sensitivity to oxygen and the absence of low molar mass byproducts. This method has been used to successfully synthesize crosslinked polymers such as hydrogels, thermoset resins, and coatings, where rapid cure and high conversion are necessary for performance[5].

Reactions involving non-enolate nucleophiles as donors *e.g.* amines, thiols and phosphines are commonly referred to as 'Michael-type additions'. The Michael acceptor possesses an electron withdrawing and resonance stabilizing activating group, which stabilize the anionic intermediate *e.g.* maleimides, alkyl methacrylates, acrylate esters and vinyl sulfones.

It was shown by Lutolf et al[1] that the de-protonated thiols (thiolates) rather than the thiols are the reactive species in this reaction. The reaction rate is thus affected by indirect factors that change the thiolate concentration *e.g.* pH or electrostatic environment of the thiol.

Another factor that affects the reaction rate is the stoichiometric ratio of thiol to acceptor molecule. To this respect the tendency for disulfide bridge formation via oxidation of thiols in a concentrated system would decrease the effective concentration of free thiols[6].

The Michael addition reaction for our system of star functional PVP molecules was investigated by synthesizing template linear xanthate end functional PVP molecules. The linear PVP molecules were aminolyzed, to achieve mono functional PVP molecules with one thiol end group per molecule. The thiol end functional PVP was crosslinked under physiological conditions with model template Michael acceptor molecules in a molar ratio Michael acceptor to thiol larger than unity, in deuterated phosphate buffer of physiological pH 7.4. The progress of the reaction was followed via *in situ* ^{1}H NMR spectroscopy.

5.3.1 Method

PVP SH samples L1_A1 and L1_A8 were used in the *in situ* Michael addition reactions (see table 5.2). N-methylolmaleimide was synthesized as described in Chapter 3. Ethyl acrylate, vinyl acetate and *N*-phenylmaleimide were purchased from Sigma Aldrich and used as received.

In situ ^{1}H NMR spectroscopy: The PVP-SH and Michael acceptor molecules were weighed (molar ratio 1:1.1) and to this 0.8 mL of deuterated buffer pH 7.4 was added and the solids dissolved before transferring to an NMR tube. The tube was sealed and placed in an ice bath during transport to the ^{1}H NMR laboratory. The spectra were recorded according to the same method as described in the previous section. In this case the temperature in the cavity of the spectrometer was set to 37 °C.

The NMR tube containing the reaction mixture was removed from the NMR spectrometer after 4 hours and placed in oil bath at 37 °C. The reaction was allowed to run for 3 days from start of reaction. At this point the final 25 °C ^{1}H NMR spectrum was taken and the solution was precipitated into diethyl ether. The precipitated polymer was analyzed via infrared spectroscopy.

Model Michael acceptor compounds investigated in this manner were: ethyl acrylate, vinyl acetate, *N*-phenylmaleimide and *N*-methylolmaleimide.

Table 5-3 Experimental data summary of In situ Michael addition reactions

Exp Ref	PVP SH Mass (g)	PVP SH n (mol)	Michael Acceptor	Mass (g)	Acceptor (mol)
L3_A8_IM_1	0.0640	6.90×10^{-5}	Ethyl Acrylate	0.0084	8.39×10^{-5}
L1_A1_IM_2	0.0866	1.11×10^{-5}	Ethyl Acrylate	0.0094	9.39×10^{-5}
L1_A1_IM_3	0.0846	1.08×10^{-5}	Ethyl Acrylate	0.0040	4.00×10^{-5}
L1_A1_IM_4	0.0695	8.90×10^{-6}	Vinyl Acetate	0.0016	1.86×10^{-5}
L1_A1_IM_5	0.0718	9.20×10^{-6}	N-phenylmaleimide	0.0017	9.82×10^{-6}
L1_A1_IM_6	0.0800	1.02×10^{-5}	N-methylolmaleimide	0.0074	5.82×10^{-5}

5.3.2 Results:

5.3.2.1 Ethyl acrylate:

Acrylates are well documented[6-8] Michael acceptor molecules for thiolate Michael donor molecules. Three experiments were performed on ethyl acrylate as a model acrylate acceptor molecule the concentration and reactant ratios were kept constant. The differences between these experiment were the following:

1. in L3_A8_IM_1 the polymer had a lower molar mass than in the other experiments and it was prepared with X_{L2} RAFT agent
2. in L1_A1_IM_2 the polymer had a molar mass approximately seven times higher than L3_A8_IM_1 and it was prepared with X_{L1}
3. in L1_A1_IM_3 the experimental conditions were the same as for IM_2, except for the addition of an excess of (0.0196 g, $1.27x10^{-4}$ mol) DTT as a reducing agent

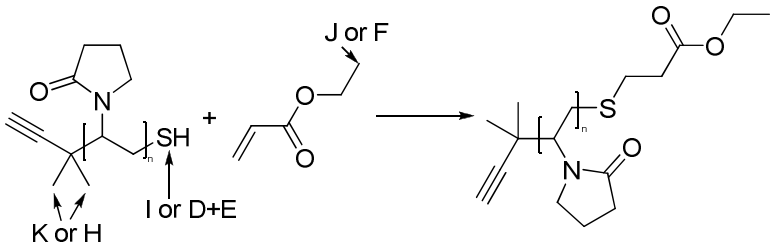

Scheme 5-2 Reaction scheme and expected Michael addition product for experiment from L3_A8_IM_1 and peak assignment

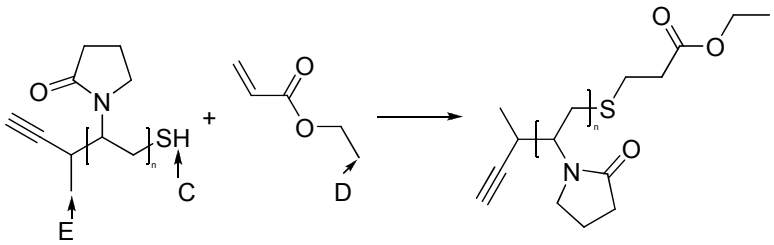

Scheme 5-3 Reaction scheme and expected Michael addition product from L1_A1_IM(2-3) and peak assignment

The ^{1}HNMR chemical shift ranges for relevant protons in the structures presented in scheme 5-5 and 5-6 peaks were assigned and are reported in table 5.3.

Table 5-4: Integration and Peak assignment Ethyl Acrylate to PVP SH

L3_A8_IM_1			L1_A7_IM_2			L1_A7_IM_3		
Shift (ppm)	*	No	Shift (ppm)	*	No	Shift (ppm)	#	No
[0.80 - 0.90]	H	4	[0.95 - 1.059]	D	0			
[0.90 - 1.16]	I	5	[1.059 - 1.16]	E	1	[1.12 - 1.28]	C	0
[1.16 - 1.33]	J	6	[1.18 - 1.24]	F	2	[1.28 - 1.35]	D	1
[1.34 - 1.59]	K	7	[1.38 - 1.58]	H	4	[1.35 - 1.47]	E	2

* as indicated in Scheme 5-5; #as indicated in Scheme 5-6

After 4 hours of reaction 20% of the functional groups were consumed in both reactions, indicating that a maximum of 80% of the starting reagents were still available.

In figure 5.5, L3_A8_IM_1 is compared to L1_A7_IM_2. By comparing the rate of reactant consumption, it was observed that in the system with longer chains the consumption of the three reagent peaks occurred at the same rate (figure 5.5 F & H *vs.* K & J).

In comparing L3_A8_IM_1 to L1_A7_IM_2 the rate of –SH (figure 5-5 I *vs.* E+D) consumption was faster. This would suggest that di-sulphide bridge formation is favoured in the shorter chain system.

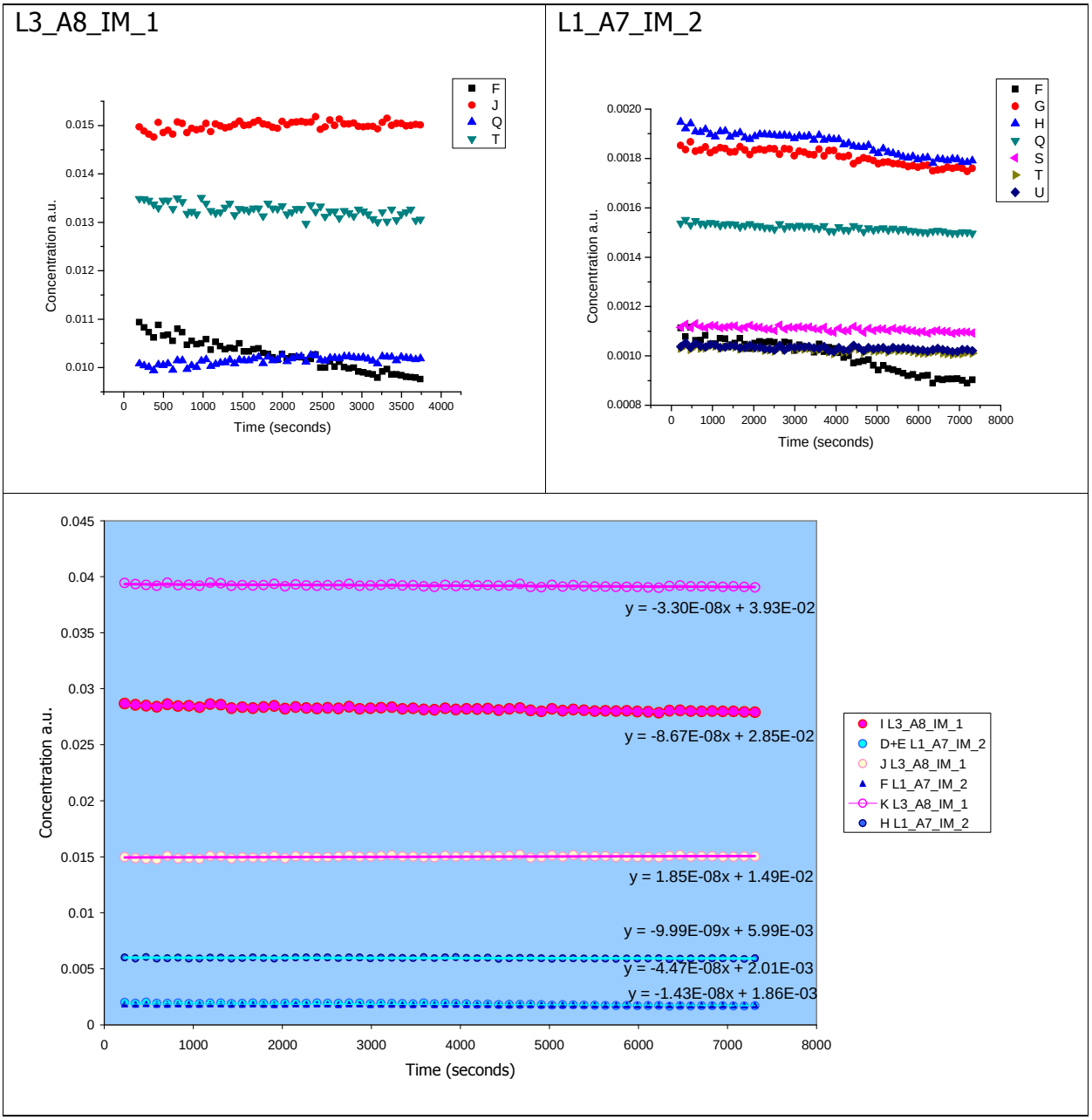

Figure 5-5 The reaction rate comparison between long and short PVP chains during the Michael addition reaction (L3_A8_IM_1 vs. L1_A7_IM_2)

The addition of the reducing agent DTT did not have a pronounced effect on the rate of the reaction as seen in figure 5-6.

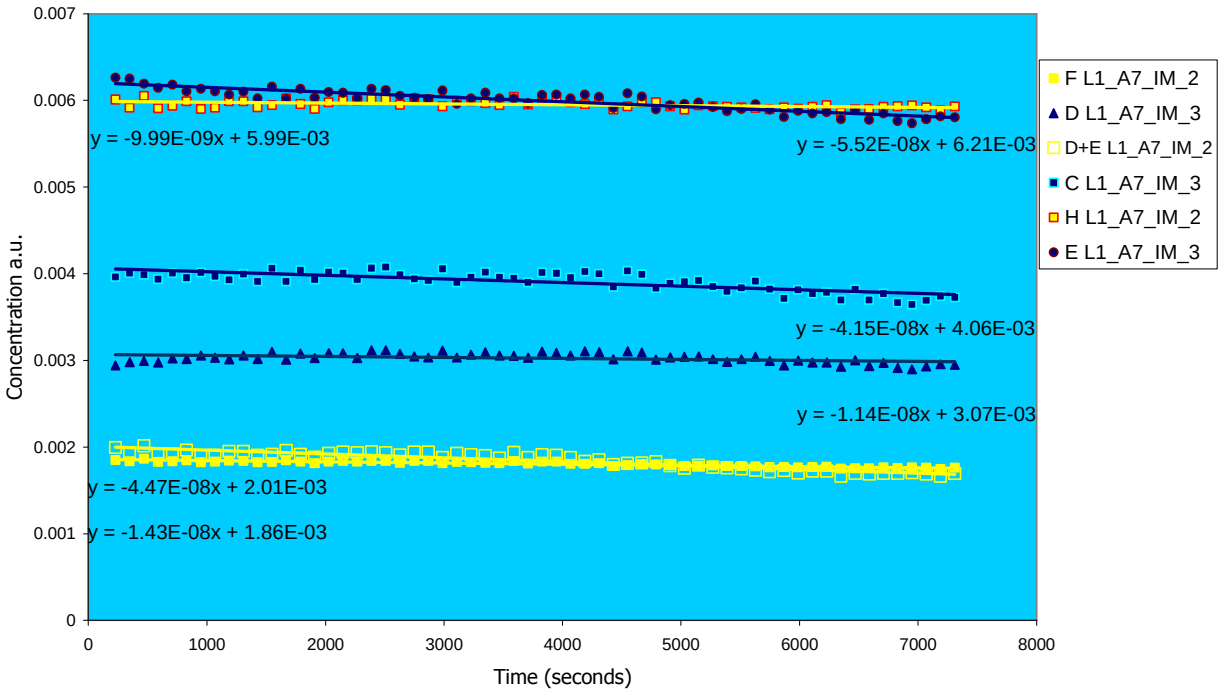

Figure 5-6 The reaction rate of reactants being consumpted with and without the addition of DTT (L1_A7_IM_2 vs. L1_A7_IM_3) was compared.

From the IR analysis of precipitated polymer it was observed that CH_2-S-CH_2 bands were present in both experiments, but some unsaturated ethyl ester bonds were still present after 4 days in L3_A8_IM_1 . The results are summarized in the table 5.4.

Table 5-5: IR band comparison between Michael addition of long (L1_A7_IM_2) vs. short (L1_A8_IM_1) chain PVP SH molecules to ethyl acrylate.

Band Assignment[9]	Reference wavenumber value[9] (cm^{-1})	L1_A8_IM_1 (cm^{-1})	L1_A7_IM_2 (cm^{-1})
Ethyl Ester	2980 (m)	x	2968
	2950(w)	2950	2944
	2900(w)	2926	2916
	1475(m-w)	1472	1492
	1455(m)	1456	1458
	1375 (m)	1370	1368
CH_2-S (aliphatic)	2950-2920(m)	2950	2944
	2880-2845(m)	2880	2870
	1435-1400(m)	1420	1420
1,2,3 tri-substituted pyrolisone C=O	1670-1655	1670	1674
β-α unsaturated ethyl ester	1740-1705	1724	X
Primary aliphatic nitrile	560-525	526	530
C-SH	2600-2550	x	X

5.3.2.2 Vinyl Acetate

When vinyl acetate was used as a Michael acceptor no appreciable reaction was observed (experiment L1_A1_IM_4). The concentration decrease of reactants was below the detection limit of this method (5%) (see scheme 5-4 a). The small decrease in concentration of reactants can be seen in scheme 5.4.

Table 5-6: 1H NMR shift to peak assignments table.

Shift (ppm)	Letter*
[1.11 - 1.27]	E
[1.27 - 1.47]	F
[1.48 - 1.69]	G
[2.23 - 2.66]	H

* as indicated in scheme 5-4 b

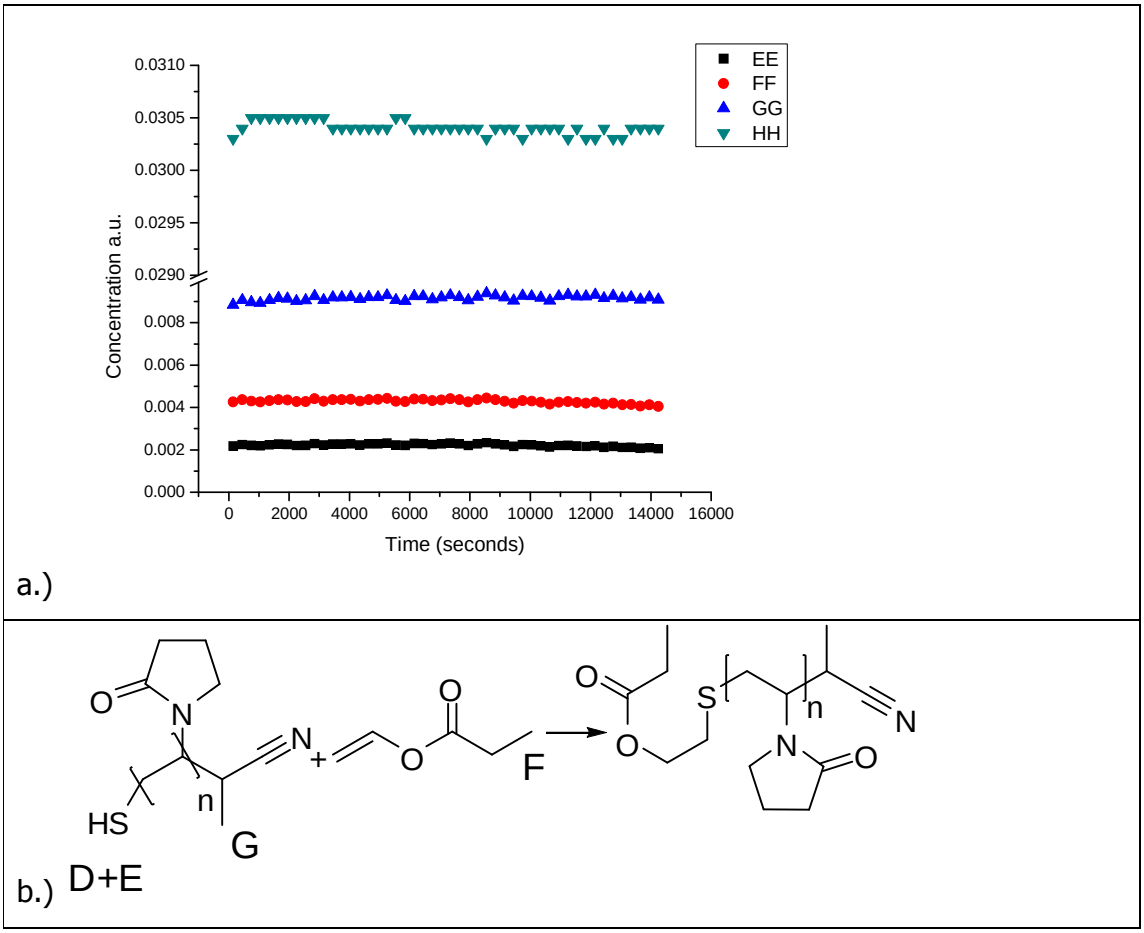

Scheme 5-4: The Michael Addition of PVP SH to vinyl acetate as acceptor molecule

The IR analysis of the precipitated polymer after four days of reacting at 37 °C indicated the presence of CH_2-S-CH_2, but also still showed significant presence of non-reacted vinyl acetate (1670 cm^{-1}).

Table 5-7: IR band comparison between Michael addition PVP SH to vinyl acetate

Band Assignment[9]	Reference wavenumber value (cm^{-1})	$Wavenumber_{Exp}$ (cm^{-1})
CH_2-S (aliphatic)	2950-2920 (m)	2944
	2880-2845 (m)	2872
	1435-1400 (m)	1420
	1270-1220 (s)	1270
	660-630	648
1,2,3 tri-substituted pyrrolidone C=O	1670-1655	1670
β-α unsaturated ketone	1700-1660 (vs)	1670
Primary aliphatic nitrile	560-525 (s)	530
C-SH	2600-2550 (w)	X

5.3.2.3 Maleimide

In the experiment with N-phenylmaleimide deuterated acetone-d_6 was used as the reaction medium (L1_A7_IM_5). A water soluble alternative was also investigated, *N*-methylolmaleimide (L1_A7_IM_6) according to a similar method to previous experiments in deuterated buffer.

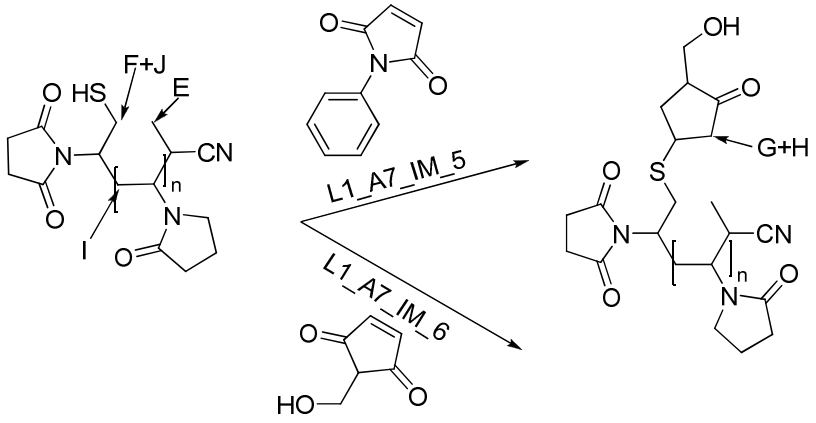

Scheme 5-5: PVP SH reaction products with maleimide acceptor molecules.

Table 5-8: ^{1}H NMR peak assignments table

L1_A7_IM_5			L1_A7_IM_6		
Shift (ppm)	Letter[ϰ]	No	Shift (ppm)	Letter	No
[1.0024 - 1.12]	F	2	[1.00 - 1.15]	D	0
[1.21 - 1.26]	G	3	[1.19 - 1.35]	E	1
[1.38 - 1.54]	I	5	[4.51 - 4.70]	F	2
[1.86 - 2.44]	K	7	[4.73 - 4.85]	G	3
[2.68 - 2.97]	L	8	[4.89 - 5.09]	H	4

[ϰ]As indicated in Scheme 5-9

The reaction in acetone was not satisfactory as the rate was much slower than expected from literature between a thiol and maleimide. In the deuterated buffer system much faster reaction rates were observed as seen in Scheme 5.10.

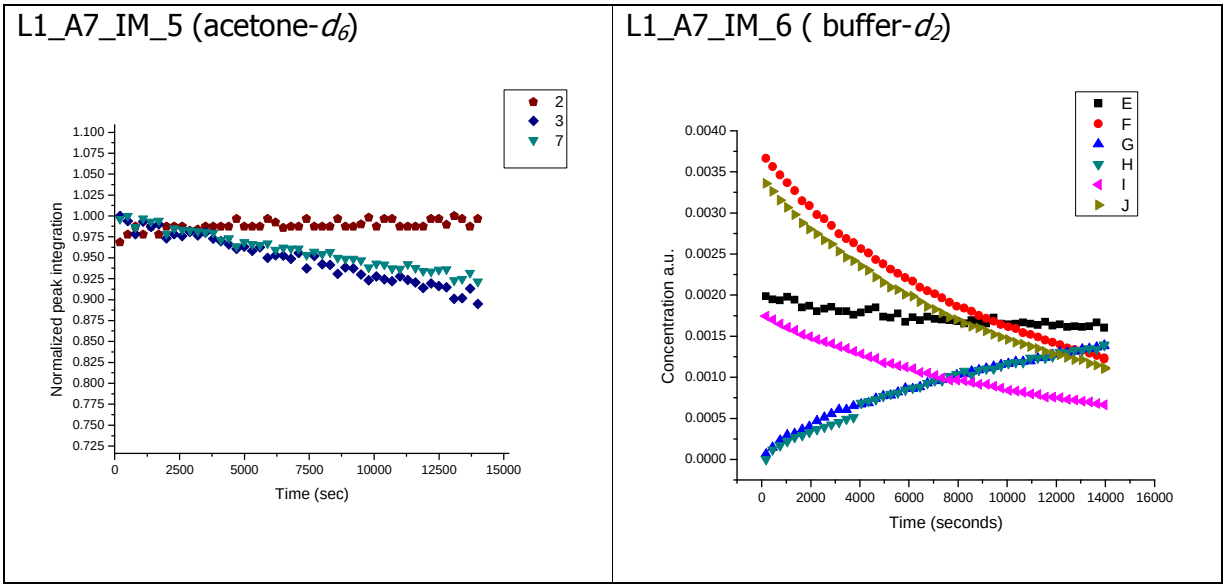

Scheme 5-6 Maleimide reaction in deuterated buffer compared to the same reaction in acetone-d_6

IR analysis of the precipitated polymer indicated that CH_2-S-CH product was synthesized in both systems as seen in Table 5.9

Table 5-9: IR band comparison between Michael addition of PVP SH two different Maleimides in deuterated buffer (L1_A7_IM_5) and in acetone-d_6 (L1_A7_IM_6)

Band Assignment[9]	Reference value (cm^{-1})	L1_A7_IM_5 (cm^{-1})	L1_A7_IM_6 (cm^{-1})
CH_2-S (aliphatic)	2950-2920 (m)	2948	2948
	2880-2845 (m)	2880	2886
	1435-1400 (m)	1440	1422
	660-630 (w)	660	642
1,2,3 tri-substituted pyrolisone C=O (similar in structure to pyrrolidone)	1670-1655 (s)	1672	1672
-OH (broad)	3600-3000	x	3588-3098

5.4 Conclusions

From this study it was concluded that PVP SH Michael addition acceptors can be arranged with increasing reactivity vinyl acetate<<ethyl acrylate<maleimides. The reaction kinetics was not measurably increased by the addition of a reducing agent, but the choice of solvent was essential.

Factors that would increase the thiolate concentration may positively influence the reaction rate, *e.g.* an increase in pH. It was also shown that peptides containing cysteine residues adjacent to a positively charged arginine group resulting in a lowered pK_a of the cysteine increased the rate of the Michael reaction by a factor of two[1]. The increase of pH would not be feasible for *in vivo* crosslinking strategies but the modification of thiol end groups to result in a lowered pK_a for the thiol in PVP SH may be an interesting strategy to investigate.

References:

1. Lutolf, M. P.; Hubbell, J. A., Synthesis and Physicochemical Characterization of End-Linked Poly(ethylene glycol)-*co*-peptide Hydrogels Formed by Michael-Type Addition. *Biomacromolecules* **2003,** 4, 713-722.

2. Chaffey-Millar, H.; Busch, M.; Davis, T. P.; Stenzel, M. H.; Barner-Kowollik, C., Advanced Copmutational Strategies for Modelling the Evolution of Full Molecular Weight Distributions Formed During Multiarmed (Star) Polymerisations. *Macromol. Theory Simul.* **2005,** 14, 143-157.

3. Van Geet, A. L., *Anal. Chem.* **1968,** 40, 2227-2229.

4. Pound, G.; Eksteen, Z.; Pfukwa, R.; McKenzie, J. M.; Lange, R. F. M.; Klumperman, B., Unexpected reactions associated with the xanthate-mediated polymerization of N-vinylpyrrolidone. *J. Polym. Sci., Part A: Polym. Chem.* **2008,** 46, 6575-6593.

5. Mather, B. D.; Viswanathan, K.; Miller, K. M.; Long, T. E., Michael addition reactions in macromolecular design for emerging technologies. *Prog. Polym. Sci.* **2006**, 487-531.

6. Hiemstra, C.; Van der Aa, L. J.; Zhong, Z.; Dijkstra, P. J.; Feijen, J., Rapidly in Situ-Forming Degradable Hydrogels from Dextran Thiols through Michael Addition. *Biomacromolecules* **2007,** 8, 1548-1556.

7. Wang N.; Dong A.; Radosz M.; Shen Y., Thermoresponsive degradable poly(ethylene glycol) analogues. *J. Biomed. Mater. Res. Part A* **2007**, 148-157.

8. Mi-Sook, K.; Yoon-Jeong, C.; Insup, N.; Giyoong, T., Synthesis and characterization of *in situ* chitosan-based hydrogel via grafting of carboxyethyl acrylate. *J. Biomed. Mater. Res. Part A* **2007,** 83A, 674-682.

9. Socrates, G., *Infrared characteristic group frequencies*. 2nd ed.; John Wiley & Sons Ltd.: Chichester, 1980.

Appendix

Table 5-10: The complete peak assignment of XT2 (figure 5-1 to 5-3)

Shift (ppm)	No of shift
[0.597-0.639]	0
[0.803-0.877]	1
[0.898 - 1.016]	2
[1.0162 .. 1.0196]	3
[1.0196 .. 1.0411]	4
[1.1681 .. 1.2189]	5
[2.3350 .. 2.3761]	6
[2.4152 .. 2.4601]	7
[2.7220 .. 2.7631]	8
[3.8205 .. 3.9202]	9
[4.1137 .. 4.1606]	10
[4.1723 .. 4.2329]	11
[4.2340 .. 4.3658]	12
[4.5714 .. 4.6437]	13
[5.1969 .. 5.2535]	14
[5.2535 .. 5.3083]	15
[5.3181 .. 5.3747]	16
[5.5233 .. 5.5780]	17
[5.6054 .. 5.7051]	18
[5.8321 .. 5.8966]	19
[5.8989 .. 5.9544]	20
[6.0816 .. 6.1325]	21
[6.7170 .. 6.7913]	22
[6.7952 .. 6.8421]	23
[6.8656 .. 6.9379]	24
[6.9574 .. 6.9848]	25
[7.0317 .. 7.0610]	26
[7.0610 .. 7.1021]	27
[7.1158 .. 7.1549]	28
[7.1549 .. 7.1959]	29

6. Cell Viability in the presence of PVP hydrogels

Poly (*N*-vinylpyrrolidinone) PVP hydrogels synthesized via free radical polymerization with suitable crosslinkers have previously been tested as cell culture or biocompatible materials for clinical use, with promising but contradictory results[1-3]. The contradiction comprised the non adherence of platelets onto blood contact devices[3] and the inflammation of rabbit eyes after injection of PVP hydrogels[2] as possible vitreous liquid substitutes. Curiously, with cytotoxicity tests in static cultures, the proliferation of 3T3 Swiss mouse fibroblasts was observed[4]. The novel RAFT mediated, PVP hydrogels synthesized during this work also needed to be tested for cytotoxicity, in order to establish the applicability of such materials as "tissue-mimetic" substances.

6.1 Materials & Methods:

6.1.1 Reagents:

3-(4,5-dimethylthiazol-2-yl)-2,5-diphenyltetrazoliumbromide 98 % TCC (M2128-5g 28597EJ) and Dulbecco's Modified Eagle's Medium LOT 019K2402 07/2010, D5671 was obtained from Sigma Aldrich; Fetal Calf Serum free of mycoplasma CN3332 was from Highveld Biological (Pty) Ltd., and Trypan blue stock (0.4 %(w/v) in PBS was supplied by Cell Culture Laboratory, University of Stellenbosch.

Rat heart myoblast (H9c2) cells were donated by Mark Thomas of the Cell Death Group of the Physiology Department University of Stellenbosch. Cells were grown as a monolayer in Dulbecco's Modified Eagle's Medium (DMEM) supplemented with 1 % Penicillin/streptomycin (PS), Fetal calf serum 10 % and L-glutamine 1% at 37 °C in 5% CO_2 incubator.

All treatments were autoclaved at 120 °C to ensure treatments were sterile before being brought into contact with the cells.

6.1.2 Methods:

6.1.2.1 Trypan Blue dye exclusion stain

Trypan blue is a diazo dye that cannot be absorbed through the selectively permeable membranes in viable cells. Conversely, dead cells will absorb the dye and will thus become stained light blue.

Two time experiments were performed on H9c2 myoblast cells, 24 h and 48h after treatment. The treatment profile used for controls was 0.01 g/mL for BSA and T5_H7 PVPALD in 2 mL of Medium. The hydrogel concentration profile of treatments was 0.01; 0.005; 0.0025 g/mL for (D1_H1+D2_H2+D3_H3+D4_H4)S1 for the BSA-PVP hydrogel and T6_A5_M8 for the PVP-DIAC PEG hydrogel in 2 mL of Medium.

Five 6-well plates were seeded with 5×10^4 cells/well in 2 mL of medium and allowed to attach to plates over night before treatment. The following morning the cells were removed from the incubator and washed with sterile PBS, after which 0.5 mL of trypsin was added to each well. The cells were then incubated at 37 °C for 5 min until they became clearly visible and detached from the dish. After addition of 1 mL of 37 °C medium to deactivate the trypsin, the cell suspension was transferred to a Falcon™ tube and centrifuged for 3 min at 360 G- force (*g*). The supernatant was decanted and the cell pellet re-suspended in 0.5 mL of warm medium. 0.05 mL of the cell suspension was transferred to a black 1.5 mL Eppendorf tube. To the eppendorf tube 0.05 mL of Trypan blue stock solution was added and mixed with the cell suspension. This mixture was allowed to cure at RT for 5 min before placing 0.05 mL onto a haemocytometer. The dead blue cells and viable unstained cells were then counted.

6.1.2.2 MTT cell activity assay

To verify the results obtained from the Trypan blue staining the 3-(4,5-dimethylthiazol-2-yl)-2,5-diphenyltetrazoliumbromide (MTT) cell activity assay was performed. The MTT cell activity assay indicates the percentage of metabolically viable cells post treatment. The absorption at 540 nm directly correlates with the ability of vital reduction enzymes in the mitochondria of healthy cells to reduce MTT.

Two time experiments were performed on H9c2 myoblast cells, 24 h and 48 h after treatment. Treatment profile used was 0.01 g/mL for controls, BSA and PVPALD. The hydrogel concentrations were 0.01; 0.005; 0.0025 g/mL for BSA-PVP hydrogels and PVP-DIAC PEG hydrogels. After 24 h and 48h the supernatants of the cells were discarded and 1.5 mL of warm PBS added. To this 0.5 mL of MTT solution (0.01g MTT/mL PBS), prepared just prior to the removal of supernatant, was added to each well containing the cell monolayer and treatment. The wells were carefully transferred to an incubator and incubated for 2 h at 37 °C in a humidified 5 % CO_2 atmosphere.

After incubation, cells were carefully covered with tin foil to avoid light exposure. In the wells where cells appeared to be detached from the plate, the supernatant was removed to 2 mL black centrifuge tubes and spun down for 2 min at 160 *g*. The supernatant was gently decanted and 0.5 mL of the solution mixture was added. The solution and cells were gently re-suspended and returned to their respective wells. A total of 2 mL solution was added to each well, being careful not to expose the plates to prolonged periods of light.

The tin foil-covered wells were placed on a shaker device and shaken vigorously for 5 min, after which the contents of each well were transferred to labelled 2 mL black centrifuge tubes and spun down for 2 min at 314 *g*.

The absorbance of each tube's supernatant was measured with a spectrophotometer at 540 nm using relevant blanks. Each treatment was measured in triplicate for 24 h and 48 h experiments and absorbance values calculated as a percentage versus untreated blank controls. Each experiment was performed in triplicate and by use of the student *t*-test, at a 95% confidence level with 2 degrees of freedom[5].

After MTT assay, the cells and hydrogel treatments were washed with an excess warm PBS solution before adding 2 mL of nutrient medium and incubating them overnight at 37 °C in a humidified 5 % CO_2 atmosphere.

6.2 Results

6.2.1 Trypan Blue dye exclusion

The results obtained from the Trypan Blue staining are summarized in figure 6.1. A very small percentage of cell mortality (no more than 14 % in 48 h) was observed.

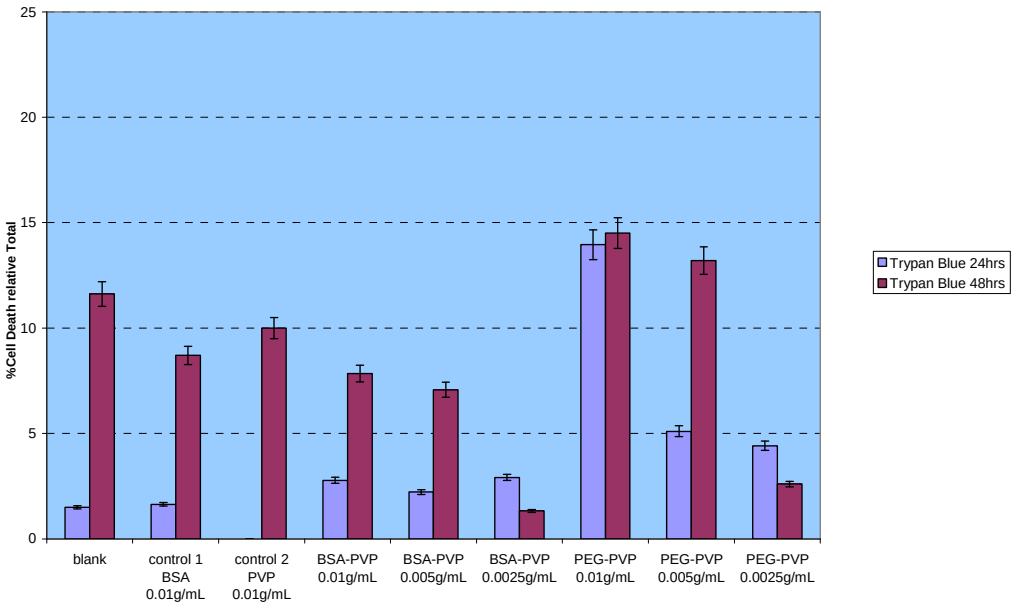

Figure 6-1: % Cell Death with Trypan Blue staining 24 h and 48 h after treatment.

6.2.2 MTT cell activity assay

The results are summarized in figure 6-2 and it is observed that at the highest concentration of BSA-PVP treatments after 48 h, cells were still more than 60% viable. Treatments of 0.005 g/mL and 0.0025 g/mL have similar results and on a positive note, viability seems to have increased after 48 h compared to 24 h being larger than 80% for both treatments. As observed in PVP-DIAC PEG free radical crosslinked hydrogels with fibroblast cells[1], the myoblast cells in the current study seemed to have experienced a stimulatory effect.

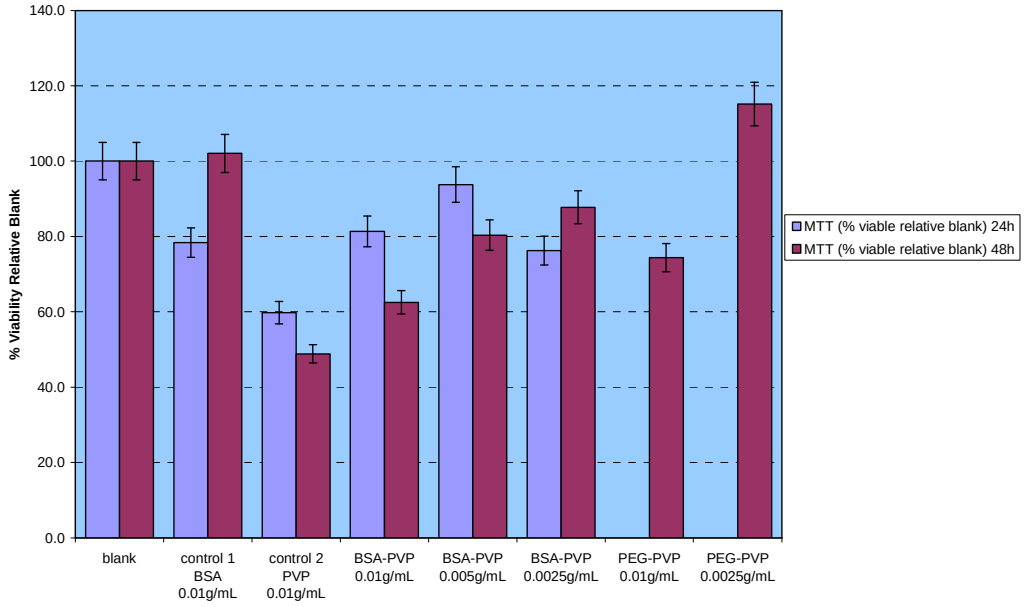

Figure 6-2: %Cell Viability using MTT assay 24 h and 48h after treatments.

In figure 6-3, the two different hydrogels at separate time treatments are compared. The largest mortality (>50%) was observed on treatment with PVPALD (control 2) The PVP-DIAC PEG hydrogels out-perform the BSA-PVP hydrogels as a biocompatible material, but only marginally. The difference between the two methods for determining cell viability was never larger than 20 %. To verify the validity of this data it was required to perform a t-test

between the treatment sets of the two different methods, equation 6.1 and 6.2 were used to calculate this.

$$t = \frac{\overline{D}}{s_d}\sqrt{N} \qquad (6.1)$$

$$s_d = \sqrt{\frac{\sum\left(D_i - \overline{D}\right)^2}{N-1}} \qquad (6.2)$$

$$N_{\text{per treatment}} = 3$$

After 24 h the t values at 2 degrees of freedom are: 0.01 g/mL BSA 1.42 ; 0.01 g/mL BSA-PVP 2.15; 0.005 g.mL BSA-PVP 0.34; 0.0025 g/mL 2.79. The t value at 95% confidence level for 2 degrees of freedom is 4.30. Therefore, $t_{calc}<t_{table}$ and there is no significant difference between the two methods.

After 48 h the t values were : 0.01 g/mL BSA 0.73; 0.01 g/mL PVPALD 23.51 ; 0.01 g/mL BSA-PVP 8.84; 0.005 g.mL BSA-PVP 2.26; 0.0025 g/mL 2.64; 0.01 g/mL PVP-DIAC PEG 0.92; 0.0025 g/mL PVP-DIAC PEG 0.89. The t value at 95% confidence level for 2 degrees of freedom is 4.30. Therefore, $t_{calc}<t_{table}$ and there is no significant difference between the two methods except in the case of 0.01 g/mL PVPALD and 0.01 g/mL BSA-PVP.

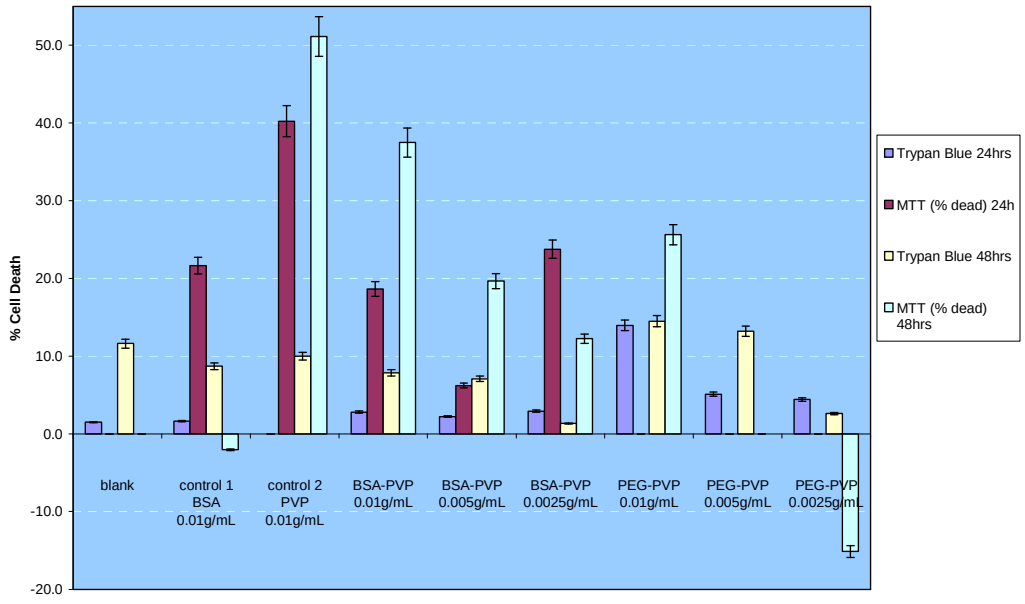

Figure 6-3: Summary of data comparison % Cell death Trypan Blue vs. MTT

6.2.3 Optical and Fluorescence Microscopy

In image 6-1 the red circles indicate cells that seem to have adhered to the clear hydrogel.

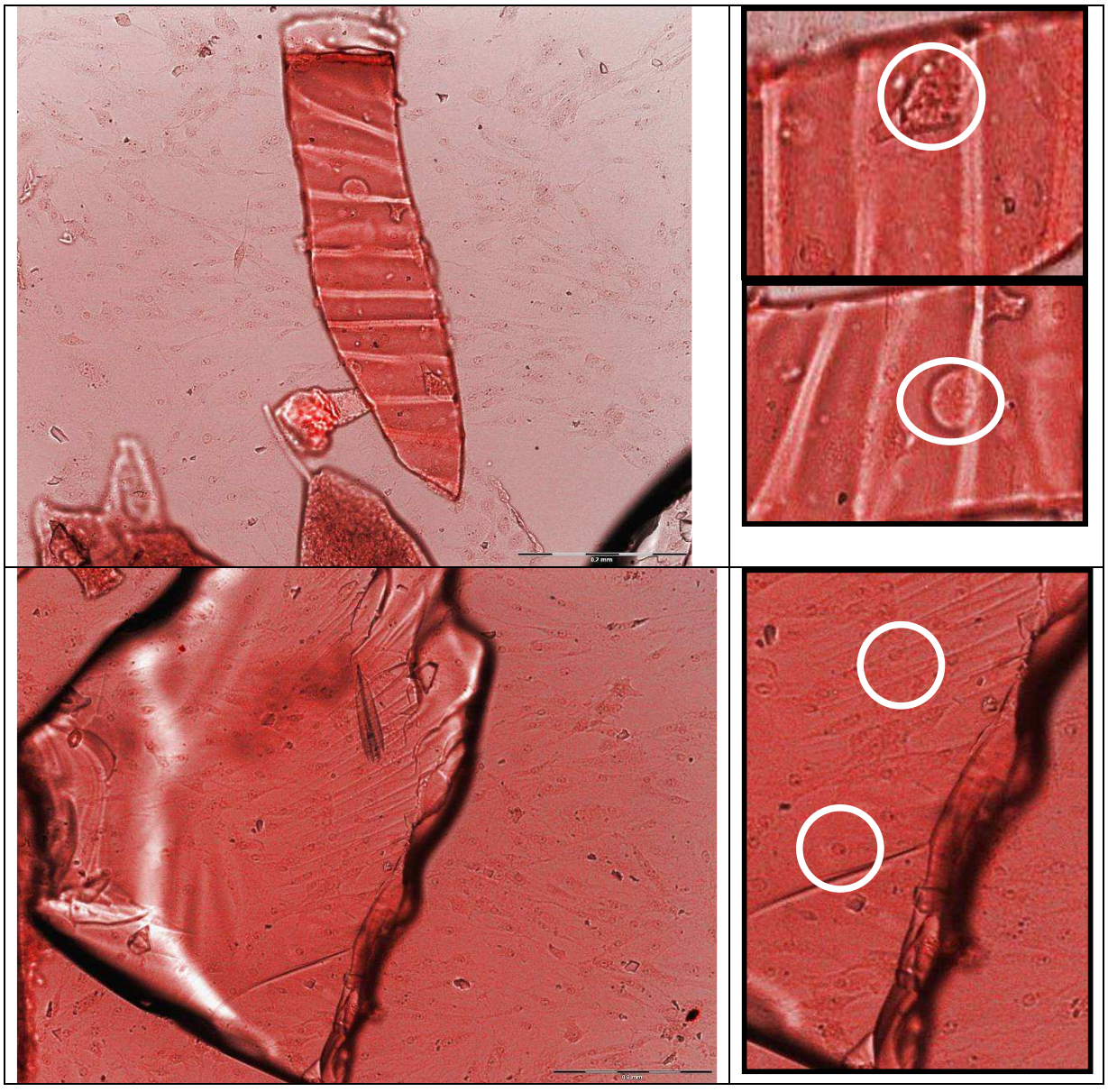

Image 6-1: Images of PVP-BSA hydrogel Fluorescence Microscopy in the presence of H9c2 myoblast cells.

The PVP-DIAC PEG hydrogel contained a very low concentration of Rhodamine B as fluorescent staining agent. In image 6.2 the cells seem to be adhered to the transparent hydrogel.

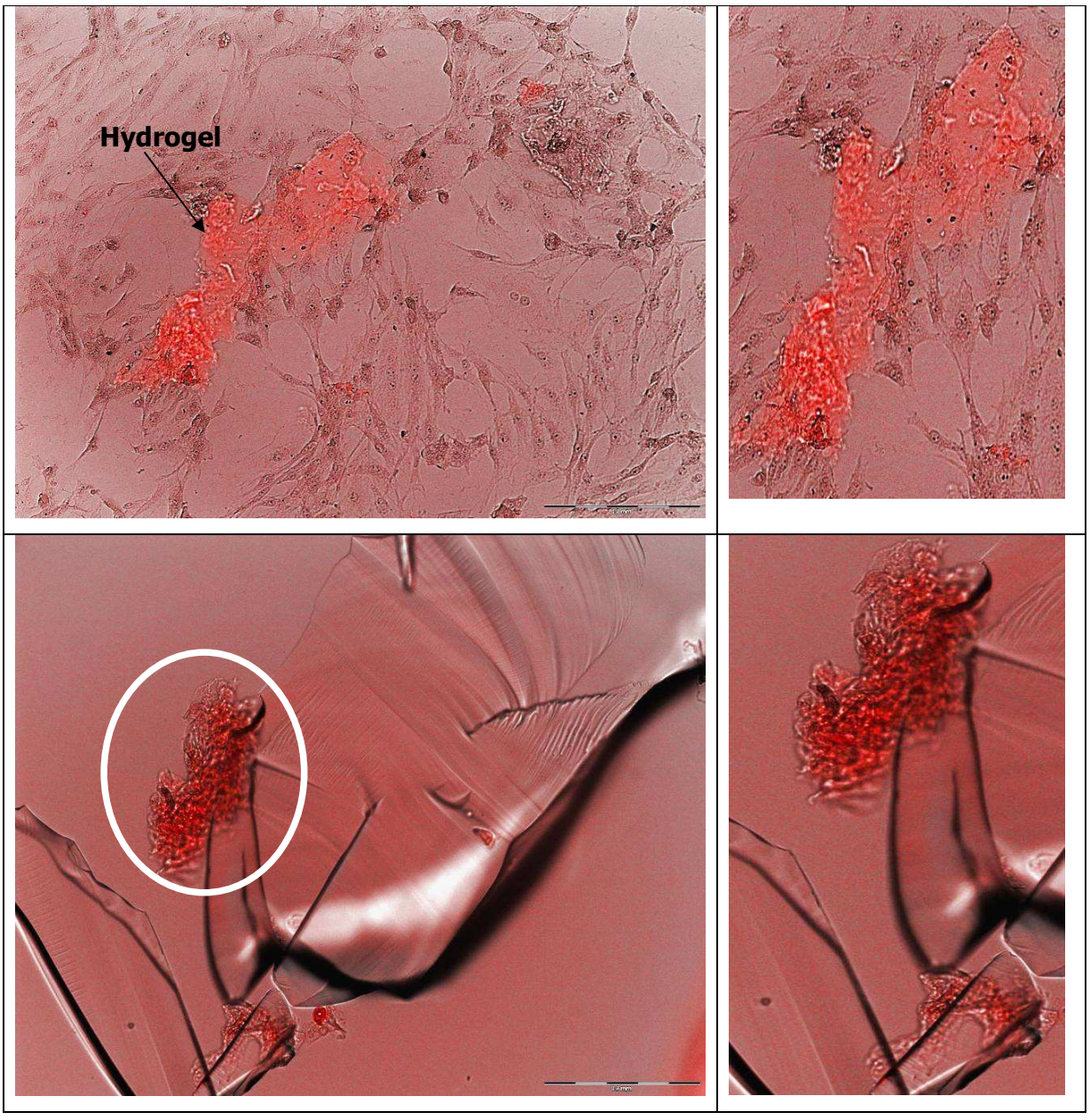

Image 6-2: Images of PVP-DIAC PEG hydrogel in presence H9c2 myoblast cells Optical Microscopy overlaid with Fluorescence Microscopy

In image 6-3 the red circles indicate the presence of cells that appear to be imbedded in the PVP-DIAC PEG hydrogel.

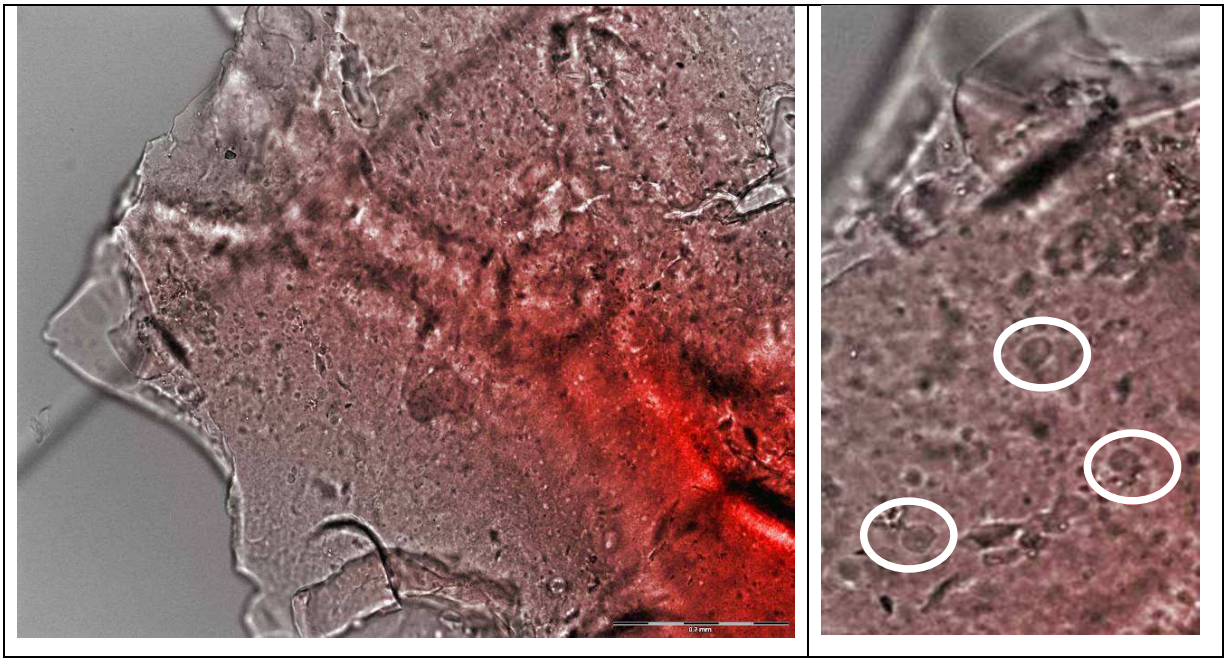

Image 6-3 Images of PVP-DIAC PEG hydrogel in the presence of H9c2 myoblast cells Optical Microscopy overlaid with Fluorescence Microscopy

6.3 Conclusion

It appears that PVP based hydrogels with covalent bonds through either Schiff base formation or Michael addition reaction both have very positive cell viability results. In the case of PVP-DIAC PEG hydrogel, cells seem to be experiencing stimulatory effects due to the presence of the hydrogel. This effect was shown to be independent of the presence of fetal calf serum in the nutrient medium[1] for PVP hydrogels. Cell migration away from the hydrogels was not observed in either PVP-DIAC PEG or PVP-BSA hydrogels and in fact it appears as if cells adhere to the hydrogels see *image 6.1 ; 6.2; 6.3* and migrate into the porous structure of both the hydrogels systems. To prove these initial observations beyond dispute it is advised that in future work multiple fluorescent staining experiments of the cellular DNA and xyz imaging of cellular mobility over time in the presence of treatments be performed.

References

1. Smith, L. E.; Rimmer, S.; MacNeil, S., Examination of the effects of poly(*N*-vinylpyrrolidinone) hydrogels in direct and indirect contact with cells. *Biomaterial* **2006,** 27, 2806-2812.

2. Vijayasekaran, S.; Chirila, T. V.; Hong, Y.; Tahija, S. G.; Dalton, P. D.; Constable, I. J.; McAllister, I. L., Poly(1-vinyl-2-pyrrolidinone) hydrogels as vitreous substitutes: Histopathological evaluation in the animal eye. *J. Biomater. Sci., Polym. Ed.* **1996,** 7, 685-696

3. Lopes, C. M. A.; Felisberti, M. I., Mechanical behaviour and biocompatibility of poly(1-vinyl-2-pyrrolidinone)-gelatin IPN hydrogels. *Biomaterials* **2003,** 24, 1279-1284.

4. Hong , Y.; Chirila, T. V.; Fitton, J. H.; Ziegelaar, B. W.; Constable, I. J., Effect of crosslinked poly(1-vinyl-2-pyrrolidinone) gels on cell growth in static cell cultures. *Bio-Med. Mater. Eng.* **1997,** 7, 35-47.

5. Harvey, D., *Modern analytical chemistry*. 1st ed.; McGraw-Hill: Dubuque: 2000.

7. Alternative Polymerization Methods

The controlled polymerization of *N*-vinyl pyrrolidone (NVP) via reversible addition fragmentation chain transfer (RAFT) mediated polymerization has been reported in the literature[1-4]. However the possibility for this monomer to undergo various side reactions is known[5]. Such side reactions caused by the reaction conditions of conventional RAFT polymerization can contribute to the loss of chain end functionality. To investigate alternative methods for a possible enhancement of the chain-end functionalization low temperature polymerization was investigated, namely photoinitiated polymerization at ambient temperature.

Photoinitiators used in free radical polymerization are divided into two classes: unimolecular and bimolecular photoinitiators. Unimolecular photoinitiators form the active radicals through a photoinduced α-cleavage process. Bimolecular photoinitiators abstract a hydrogen atom from a suitable co-initiator compound producing an initiating radical[6].

Organic compounds containing a thiol functionality have been shown to act irreversible chain transfer agents (CTA). An equilibrium state may occur between the triplet activated state of the activated dye photo initiator and the pseudo-CTA (thiol compound), resulting in increased control over the molar masses[7]. For the requirements of the project this was not enough as telechelic molecules with multiple topologies were desired.

To include the prerequisites of control over molar mass distribution, targetable molar mass and variable topology various xanthate type RAFT agents were added to a bimolecular photo initiated system. Xanthate RAFT agents may loose efficacy and stability when exposed to wavelengths in the UV and near UV ranges[8], thus visible light alone was investigated.

7.1 Material & Methods

7.1.1 Reagents

Benzophenone (for synthesis, Merck), 4-dimethylaminopyridine (DMAP) (for synthesis, Merck), triethylamine (≥98 %, Fluka), Rhodamine B (standard grade, Fluka), bromoanisole (reagent grade, Sigma Aldrich) and potassium *O*-ethyl xanthogenate (96 %, Fluka) were used without further purification. AIBN was recrystallized from ethanol (standard grade, KIMIX). *N*-vinylpyrrolidinone (>=99 %, Sigma Aldrich) was distilled under reduced pressure at 64˚C

7.1.2 Instrumentation

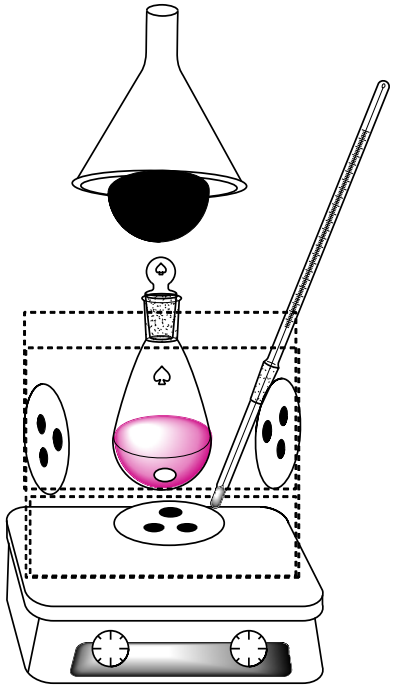

Figure 7-1: Schematic of the photopolymerization experiment setup, with three LED touch lights and one conventional 60 Watt desk lamp.

7.1.3 Procedure

The ratio of initiator to co-initiator was chosen according to experimental systems previously reported in the literature[9,10]. The choice of DMAP as a co-initiator was inspired by Xiao et al.[10] and was chosen as it is a common catalyst used in organic chemistry.

A typical polymerization was as follows: in a typical benzophenone system, (table 7.1, BP1) NVP (10.40 g, 9.36×10^{-2} mol), benzophenone (0.52 g, 2.87×10^{-3} mol) and DMAP (0.70 g, 5.69×10^{-3} mol), were placed in a pear shaped 50 mL Schlenk flask and purged via 4 consecutive freeze pump thaw cycles. In a typical Rhodamine B system (table 7.1, RP7), NVP (10.40 g, 9.36×10^{-2} mol), Rhodamine B (0.02 g, 4.13×10^{-5} mol) and DMAP (0.16 g, 1.31×10^{-3} mol), AIBN (0.06 g, 3.82×10^{-4} mol) were placed in a pear shaped 50 mL Schlenk flask and purged via 4 consecutive freeze pump thaw cycles. The vessel was filled with ultra high purity argon. The flask was then placed inside the setup presented in figure 7.1, the lights were turned on, the entire setup was insulated with tin foil to concentrate the light and the temperature around the vessel kept at 29 °C ±2 (see table 7.1). The photopolymerization reactions were carried out for 72 h (benzophenone) and 16 h (Rhodamine B) respectively. The mixture was precipitated into diethyl ether, dried under reduced pressure and analyzed.

7.1.4 Results

The experimental molar ratios and results of the photo initiated polymerizations are summarized in table 7.1, in every polymerization 10 mL, $9.36x10^{-2}$ mol of NVP was used.

Table 7-1: Experimental data summary of the photo initiated polymerization experiments

Exp reference	Reagent	n (mol)	Mol%	Wt%	Conv %	$M_{n\ GPC\ DMF}$ (g/mol)	PDI
BP1	benzophenone	$2.87x10^{-3}$	3.06	5.02	16	4944	1.3
	DMAP	$5.69x10^{-3}$	6.08	6.68			
BP2	benzophenone	$2.91x10^{-3}$	3.11	5.10	35	1649	1.2
	DMAP	$5.55x10^{-3}$	5.93	6.52			
	bromoanisole	$2.85x10^{-3}$	3.05	5.13			
BP3	benzophenone	$9.81x10^{-4}$	1.05	1.72	1	4852	1.2
	DMAP	$1.78x10^{-3}$	1.90	2.09			
	AIBN	$2.01x10^{-4}$	0.21	0.32			
	X_{L2}	$9.84x10^{-4}$	1.05	2.14			
FP4	DMAP	$2.05x10^{-2}$	21.9	24.0	0	/	/
	AIBN	$2.14x10^{-3}$	2.3	3.4			
	bromoanisole	$1.07x10^{-2}$	11.4	19.2			
FP5	DMAP	$2.62x10^{-3}$	2.8	3.1	0	/	/
	AIBN	$1.70x10^{-3}$	1.8	2.7			
	X_{L2}	$5.37x10^{-3}$	5.7	11.7			
	bromoanisole	$1.07x10^{-3}$	1.1	1.9			
RP6	Rhodamine B	$4.18x10^{-5}$	0.04	0.2	34	2686	1.2
	DMAP	$9.79x10^{-4}$	1.0	1.2			
	AIBN	$3.66x10^{-4}$	0.4	0.6			
	bromoanisole	$1.07x10^{-3}$	1.1	1.9			
RP7	Rhodamine B	$4.13x10^{-5}$	0.04	0.2	86	14012[2]	9.0
	DMAP	$1.31x10^{-3}$	1.4	1.5			
	AIBN	$3.82x10^{-4}$	0.4	0.6			
RP8	dye	$4.18x10^{-5}$	0.04	0.2	9	6885♥	1.9
	DMAP	$9.84x10^{-4}$	1.1	1.2			
	AIBN	$3.69x10^{-4}$	0.4	0.6			
	X_{L2}	$1.77x10^{-4}$	0.2	0.4			
	bromoanisole	$1.07x10^{-3}$	1.1	1.9			

[2] ♥$M_{n\ GPC\ DMAc}$

Observations from Table 7.1:

Polymer was only obtained from systems that contained either benzophenone or Rhodamine B, proving that these compounds were acting as radicals source for the polymerization of NVP, from excitation by visible light.

The polymerization appeared to be tolerant towards the functionalities of the initiators[5]. The carboxylic group on Rhodamine B (C(O)OH) was expected to act as a contaminant that would result in dimerization of NVP. However, this was not observed. We attribute this to the extremely low concentrations of this reactant.

The bromoanisole was added as a template alkyl halide contaminant, alkyl halides are common contaminants during RAFT polymerizations as they are usually used during RAFT agent synthesis. The addition of bromoanisole to the conventional photoinitiated system without any RAFT agent resulted in a lowered molar mass (14, 000 g/mol to 2690 g/mol) and gravimetric conversion of monomer to polymer from 86% to 34% (RP7 *vs.* RP6).

In RP8, the molar ratios were kept the same as in RP7 except for the addition of a RAFT agent. The PDI was lowered from 9.0 (14, 000 g/mol) to 1.9 (6900 g/mol) under the same SEC conditions.

In RP8, xanthate chain ends were observed at 4.6 ppm (2H, C(S)O*C*$\underline{H_2}$), but at a concentration of 1.1 % (4.6 ppm ^{1}H NMR) relative to 100 % (4.0 - 3.5 ppm ^{1}H NMR) polymer integration. If all the chains were functionalized a concentration of 3 % xanthate chain ends would be expected. After hydrolysis and heating steps (method as described in Section 4.1.3) no aldehyde peaks were observed. The aldehyde concentration was possibly so low that it could not be detected by this method.

7.2 Conclusions

Positively very low dimerization products and loss of chain ends due to unsaturation were observed in the ^{1}H NMR during photo-initiated polymerization. It must be noted however that degree of chain end functionalization with the xanthate mediating RAFT agent is thus far inconclusive.

It was concluded that under our experimental conditions, this method would need further experiments to optimize conditions for the effective synthesis of xanthate endfunctional PVP at room temperature. This method might however be of industrial interest for the production of tuneable molar mass PVP with relatively little energy requirements.

References

1. Wan, D.; Satoh, K.; Kamigaito, M.; Okamoto, Y., Xanthate-Mediated Radical Polymerization of *N*-Vinylpyrrolidone in Fluoroalcohols for Simultaneous Control of Molecular Weight and Tacticity. *Macromolecules* **2005,** 38, 10397-10405.

2. Devasia, R.; L Bindu, R.; Mougin, N.; Gnanou, Y., Controlled Radical Polymerization of N-vinylpyrrolidone by Reversible Addition Fragmentation Chain Transfer (RAFT) and the Synthesis of its Block Copolymers. *Polymer Preprints* **2005,** 46, 195-196.

3. McDowall, L.; Chen, G.; Stenzel, M. H., Synthesis of Seven-Arm Poly(vinyl pyrrolidone) Star Polymers with Lysozyme Core Prepared by MADIX/RAFT Polymerization. *Macromol. Rapid Commun.* **2008,** 29, 1666-1671.

4. Gargallo, L.; Pérez-Cotapos, J.; Santos, J. G.; Radić, D., Active Centers and Polymeric Effect in Poly(N-vinyl-2-pyrrolidone)-MonoalkylXanthate Systems. *Langmuir* **1994,** 10, 1624-1626.

5. Pound, G.; Eksteen, Z.; Pfukwa, R.; McKenzie, J. M.; Lange, R. F. M.; Klumperman, B., Unexpected reactions associated with the xanthate-mediated polymerization of N-vinylpyrrolidone. *J. Polym. Sci., Part A: Polym. Chem.* **2008,** 46, 6575-6593.

6. Popielarz, R.; Vogt, O., Effect of Coinitiator Type on Initiation Efficiency of Two-Component Photoinitiator Systes Based on Eosin. *J. Polym. Sci., Part A: Polym. Chem* **2008,** 46, 3519-3532.

7. Valdebenito, A.; Encinas, M. V., Chain transfer agents in vinyl polymerizations photoinduced by bimolecular photoinitiators. *J. Photochem. Photobiol., A* **2008,** 194, 206-211.

8. Lu, L.; Zhang, H.; Yang, N.; Cai, Y., Toward Rapid and Well-Controlled Ambient Temperature RAFT Polymerization under UVâˆ'Vis Radiation: Effect of Radiation Wave Range. *Macromolecules* **2006,** 39, 3770-3776.

9. Xiao, P.; Wang, Y.; Dai, M.; Shi, S.; Wu, G.; Nie, J., Synthesis and Photopolymerization Kinetics of Polymeric One-Component Type II Photoinitiator Containing Benzophenone Moiety and Teriary Amine. *Polym. Eng. Sci.* **2008**, 884-888.

10. Xiao, P.; Dai, M.; Nie, J., Synthesis and Photopolymerization Characterization of a Novel Difunctional Photoinitiator. *J. Appl. Polym. Sci.* **2008,** 108, 665-670.

8. Conclusions

RAFT agents and PVP of various topologies were synthesized successfully with high purity and analyzed in detail.

Xanthate chain-end functional PVP of di functional, tetra functional star and multifunctional star topologies were successfully modified into both thiol and aldehyde chain-end functionalities. The functionalized PVP molecules were analyzed by ^{1}H NMR, HPLC, HPLC MS and IR.

Functionalized PVPs of varying topologies were crosslinked with various commercially available or synthesized crosslinkers. The effect of the stoichiometric ratio of PVP to crosslinker on the crosslinking reaction rates and end properties of the hydrogel were investigated. The pH of the crosslinking medium was varied to investigate the influence of pH on the reaction rate.

In PVPALD, systems that produced hydrogels had a fraction of functional chain ends value of at least 0.88 for difunctional and 0.50 for tetrafunctional topologies. Crosslinkers with a higher degree of functionalities (60 for BSA) outperformed crosslinkers of low degree of functionality (2 for *bis*-(2-amino ethyl)amine), irrelevant of which PVPALD was used. The optimal pH range for covalent bond formation was 5.4-6.4. The molar ratio played an important role in gelling efficacy. Between aldehyde and amine moieties the optimum molar ratio range of 0.7-1.0 was observed.

Non-reduced hydrogels, consisting of imine crosslinking points degraded significantly faster than reduced hydrogels with secondary amine crosslinking points. Also, PVP-BSA unreduced hydrogels with a lower stoichiometric ratio of aldehyde: amine, were observed to degrade faster.

The $PVP(SH)_4$ systems that produced hydrogels via Michael addition had an initial degree of conversion of xanthate to thiol of larger than 40% according to Ellman's Test. The molar ratios of reagents and the chain length of the arms influenced the material properties of the hydrogel.

Hydrogels of tuneable material characteristics were synthesized through varying stoichiometric ratios.

From kinetic studies it was concluded that when using the core first RAFT method, the cross-linker molecule *e.g.* ethyl acrylate must have a functionality of larger than two to compensate for the inevitable loss of functionalizable polymer arms during the core first RAFT mediated polymerization.. From this study it was conclude that PVP SH Michael addition acceptors can be arranged with increasing reactivity vinyl acetate<<ethyl acrylate<maleimides.

Competing reactions of the thiol moieties have to be taken into account during the synthesis of hydrogels via the Michael addition reaction. Disulphide bridges were observed in our hydrogels via non ideal swelling ratios, indicating that the properties of the formed hydrogels were affected by these random factors. From a macromolecular design perspective, this is not ideal as it is not predictable. I would suggest the careful selection of a suitable reducing agent (not DTT[1] as it could act as a competing thiol nucleophile) and a stable protecting group *e.g.* thioacetate[2]

PVP based hydrogels with covalent bonds through either Schiff base formation or through the Michael addition reaction both have very positive cell viability results. In the case of PEG-PVP hydrogels, cells even seem to be experiencing stimulatory effects due to the presence of hydrogel.

Alternative polymerization conditions were investigated in an attempt to reduce side reactions due to thermal effects by performing photo-initiated polymerization. No dimerization or loss of chain ends due to unsaturation

were observed in photo-initiated polymerization. The xanthate functionality of the RAFT agent was quantitatively attached to PVP chain ends. It was concluded that this method has great potential for the synthesis of complex architectures required for the synthesis of PVP-based hydrogels.

References

1. Metters, A.; Hubbell, J., Network Formation and Degradation Behavior of Hydrogels Formed by Michael-Type Addition Reactions. *Biomacromolecules* **2005,** 6, 290-301.

2. Goessl, A.; Tirelli, N.; Hubbell, J., A hydrogel system for stimulusresponsive, oxygen-sensitive in situ gelation. *J. Biomater. Sci., Polym. Ed.* **2004,** 15, 895–904.